



Contents

Preface	iv
Acknowledgments	vi
1 INTRODUCTION	1-1
1.1 Background and origin	1-1
1.2 Space and time scales	1-3
1.3 References	1-4
2 THE WATER TRANSPORT MODULE	2-1
2.1 The soil water flow equation	2-1
2.2 The soil hydraulic properties	2-2
2.2.1 The soil moisture retention characteristic	2-2
2.2.2 The hydraulic conductivity relationship	2-7
2.3 Numerical solution of the water flow equation	2-9
2.3.1 The solution procedure	2-9
2.3.2 Definition of the upper boundary condition	2-15
2.3.3 Definition of the bottom boundary condition	2-18
2.4 Modelling of the water transport in cropped soils	2-22
2.4.1 Introduction	2-22
2.4.2 Crop interception	2-23
2.4.3 Calculation of the potential evapotranspiration of a crop	2-23
2.4.4 Estimation of the potential transpiration and evaporation	2-29
2.4.5 Description of the root water uptake	2-29
2.5 References	2-33
3 THE SOLUTE TRANSPORT MODULE	3-1
3.1 Introduction	3-1
3.2 The soil solute transport equation	3-2
3.3 Numerical solution of the solute transport equation	3-7
3.3.1 The solution procedure	3-7
3.3.2 Definition of the upper boundary condition	3-11
3.3.3 Definition of the lower boundary condition	3-12
3.4 References	3-13
4 THE HEAT TRANSPORT MODULE	4-1
4.1 Introduction	4-1
4.2 The soil heat flow equation	4-1
4.3 Numerical solution of the heat flow equation	4-2
4.3.1 The solution procedure	4-2
4.3.2 Definition of the upper boundary condition	4-2
4.3.3 Definition of the lower boundary condition	4-3
4.4 References	4-3
5 THE CROP GROWTH MODULE	5-1
5.1 Introduction	5-1
5.2 Calculation of the plant development rate	5-2



5.3	Calculation of the daily crop assimilation rate	5-4
5.3.1	Photosynthetic response of individual leaves	5-4
5.3.2	Global, direct and diffuse irradiance at the top of the crop canopy	5-9
5.3.3	Crop canopy reflection	5-10
5.3.4	Penetration of the downward radiation flux in the crop canopy	5-11
5.3.5	Calculation of the daily rates of the light absorption- and CO ₂ -assimilation	5-12
5.4	Calculation of the dry matter growth rate of the different plant components	5-14
5.5	Leaf area development	5-20
5.6	Rooting depth and root density development	5-24
5.7	References	5-26
6	THE NITROGEN FATE MODULE	6-1
6.1	Introduction	6-1
6.2	Modelling of nitrogen transformations in soils	6-2
6.2.1	Mineralization of the soil organic nitrogen	6-2
6.2.2	Denitrification	6-9
6.2.3	Volatilization	6-9
6.3.4	Nitrification	6-10
6.2.5	Hydrolysis of urea	6-10
6.2.6	Uptake of ammonia and nitrate	6-10
6.3	References	6-13
7	DESCRIPTION OF THE MODEL INPUT AND OUTPUT	7-1
7.1	Introduction	7-1
7.2	The input	7-1
7.2.1	Definition of the input syntax	7-1
7.2.2	Verification of the input	7-3
7.2.3	Input files used by the WAVE-programme * GENDATA.IN * CLIMDATA.IN * WATDATA.IN * SOLDATA.IN * NITDATA.IN * CROPDATA.IN * TEMPDATA.IN	7-4 7-5 7-7 7-8 7-14 7-17 7-19 7-24 7-25
7.3	The output	7-25
8	DESCRIPTION OF THE COMPUTER PROGRAMME	8-1
8.1	General considerations	8-1
8.1.1	Limiting variable visibility	8-1
8.1.2	The 'uses'-relationship	8-1
8.1.3	Abstractions	8-2
8.2	The structure of the WAVE-programme	8-2
8.2.1	General structure of the programme	8-2
8.2.2	The structure of each module * The input module * The output module * The module with general and climate information * The module for calculating the water balance	8-3 8-4 8-5 8-5 8-6



* The module for calculating the solute balance	8-7
* The module for calculating the nitrogen balance	8-7
* The module for calculating the heat balance	8-8
* The module for calculating crop growth	8-9
8.3 Variables of the programme	8-9
8.3.1 GEN.COM: general information	8-9
8.3.2 CLIM.COM: climate information	8-10
8.3.3 WAT.COM: variables used in the water balance module	8-11
8.3.4 SOL.COM: variables used in the solute transport module	8-14
8.3.5 NIT.COM: variables used in the nitrogen balance module	8-17
8.3.6 TEMP.COM: variables used in the heat balance module	8-21
8.3.7 CROP.COM: variables used in the crop growth module	8-21



PREFACE

The need for more careful management of our planet's land and water resources is quickening. This results from two clashing realities: the growing numbers of fellow humans with their increasing expectations for a more bountiful life, and the limitations of the planet's natural resources and ability to absorb environmental abuse.

Excessive use of agrochemicals in many industrialized countries endanger the quality of land and water resources and will do so if no drastic measures are taken. In Europe for example the drinking water quality standard of 50 ppm nitrates is exceeded at several locations. Legislation measures for controlling fertilizer, pesticide and herbicide applications are currently considered at regional, national and transnational levels. Several authorities have already enacted different measures to reduce nitrate pollution. Most of these measures are based on rough estimations of nitrogen leaching risk, which not always consider the interaction between climate, crop, soil and geo-hydrology. Even if these effects are considered, it is not clear what the long term effect of regulative measures will be. Both the developments of regulations and the assessment of their long term effects would be substantially simplified by the availability of comprehensive and tested simulation models. Such models can help the decision makers to define about when, where and how much fertilizer or pesticide to apply on agricultural land to ensure that the soil, surface and groundwater resource system are least effected.

The foregoing requires good understanding of the transfer and transformation processes of solutes as they migrate through the soil, and as such requires a good knowledge of the physical, chemical and biological laws governing the changes in the atmosphere-plant-soil continuum. Although considerable expertise has been gained in each of these domains, only recently due to the development of simulation models the interactions of the different processes effecting the fate of chemicals in the vadose environment are studied. As a result, a tremendous interest in system studies, using mathematical modelling, has emerged the last decade. Mathematical modelling is increasingly applied in environmental studies because it enables to get a better insight in processes, integrate knowledge of different disciplines, analyse complex problems in a holistic way, and predict short and long-term impacts of changes in climate and farming on the environment.

The major purpose of this reference and user's manual is to convey a modular modelling system for studying the transport and transformations of matter and energy in the soil, crop and vadose environment. The version of the WAVE-model, presented herein, is based on the SWATRER (the extended and revised version of the Soil Water and Actual Transpiration Rate model of Feddes et al., 1978 (Dierckx et al., 1986)). After 1986, this version was regularly upgraded and extended within the frame of different doctoral research projects of the Institute for Land and Water Management of the K.U.Leuven. This resulted in several upgrades of the SWATRER programme and the development of models like SWATNIT (Vereecken et al., 1989). The latter is a programme for modelling the behaviour of nitrogen species in the soil-plant continuum. However, due to the different upgrading and adding of new sections the programme became rather complex and difficult to manipulate. Therefore, it was decided to completely restructure and



rewrite the code of the programme to improve its transparency and user friendliness. The programme has been structured so that it will be easy to add new modules if knowledge of other soil processes than those already present in the programme, and relevant for the analysis of the fate and transfer of chemicals in soils, becomes available. The new programme code was given the name WAVE, which stands for simulation of the substances Water and Agrochemicals in the soil, crop and Vadose Environment.

To simplify the use of the reference and user manual, the chapters are presented in the sequence the WAVE-model describes the different processes. Furthermore, most of the analytical material is presented in a brief form with limited attention given to the derivation of the equations presented. This has been done to focus on the synthesis of the entire process rather than concentration on the analysis of the individual steps along the way. Throughout the different sections of the reference manual special emphasis is given to different parametric models for the description of model parameters. In addition, the manual contains extensive tables with published values of difficult to measure parameters and factors. In this way the manual serves also the objective of providing a comprehensive literature review of parametric models used to describe certain model parameters and value ranges for model parameters. Besides a description of the main transport modules (water, solutes and energy), the crop growth and the nitrogen fate module, the reference and user's manual devotes quite some attention to the model 'input' and 'output', and the description of the structure of the programme code and the variables used.

First and foremost, this is a reference and user's manual for both teachers, researchers and students. Its objective is to present and convey the state-of-the-art in the field of modelling some physical, chemical and biological processes in the vadose environment, which control the fate and transfer of agrochemicals. Therefore, the emphasis is on approaches for conceptualizing, applying, and synthesizing basic underlying concepts. For the convenience of engineers there is an extensive section on how to use the programme code, and in rewriting the code considerable attention is given in adding special check routines for controlling the consistency of the model input.

The reference and user's manual is written from the perspective of authors with scientific background in soil physics, agronomy and computer science and skill in the measurement of static and dynamic soil properties, and the monitoring of complex laboratory and field experiments. In addition, the authors are experienced in fields such as model calibration and validation, and in quantifying the effect of poor concept formulation and random input uncertainty on model output. Furthermore, they have gone through several exercises of using the WAVE-model for engineering purposes. The manual integrates the efforts of the Institute for Land and Water Management on grappling during 20 years of how best to understand and model some dominant processes in the vadose environment. Since continuous developments and research findings will become available, the authors are convinced that this reference and user's manual in future will be replaced by new updates.

Professor Jan FEYEN
Head of the Institute for Land and Water Management
Katholieke Universiteit Leuven



ACKNOWLEDGMENTS

The authors like to express their appreciation to the different doctoral students that have been working at the Institute for Land and Water Management (formerly called the Laboratory of Soil and Water Engineering) over the past 16 years on aspects of the field water balance and the modelling of the behaviour of water and agrochemicals in soils and shallow aquifers. We are aware that the information on modelling and model input and parameters provided in this reference and user's manual are the result of the material published in 12 dissertations, in the period 1979-1994 [Belmans, 1979; Ragab, 1982; Raes, 1982; Badji, 1984; Michels, 1984; Farshi, 1986; Vereecken, 1988; Kihupi, 1990; Singh, 1990; Xevi, 1992; Kim, 1992; and Diels, 1994]. The authors, of course, also recognize the contribution of the present generation of doctoral students [Christiaens, Hubrechts, Mallants, Gonzalez, Meddahi, Mulonga, Sewnandan, and Vanderborght] exploring new numerical and experimental facets of the processes controlling the transfer and transformation of agrochemicals in the vadose environment. Those days, the PhD-staff of the Institute pays particular emphasis to the mathematical description of the soil heterogeneity, the macropore structure in soils, the transport through macropores and cracks, chemical and biological processes, and aspects related to methods for estimating the value of parameters at different scales, model calibration and validation procedures.

We are also grateful for having had the opportunity of working with the many dedicated and enthusiastic undergraduate students of the Institute who have given so much of their time and talents in exploring and testing the present programme code of the WAVE-model.

The authors are especially grateful to the Institute for Land and Water Management for promoting this project and making this publication possible by defraying the costs of its development. Special appreciation goes to the Belgian Institute for Encouragement of Scientific Research in Agriculture and Industry (I.W.O.N.L.) and the Directorates General VI (DG for Agriculture) and XII (DG for Science, Research and Development) of the European Union for making available the funds to conduct research in this domain, and making it possible to collaborate with the international scientific community.

Marnik VANCLOOSTER
Peter VIAENE
Jan DIELS
Karen CHRISTIAENS

INTRODUCTION



1 INTRODUCTION

1.1 BACKGROUND AND ORIGIN

Expansion of human activities causes dispersion of pollutants in the subsurface environment. Today, acid rain, hazardous chemical wastes, fertilisers, pesticides, heavy metals, nuclear deposits, solvents and sewage sludge are amongst other things, a serious threat to soil and groundwater quality. Therefore, existing groundwater and soil conservation policies and strategies are reconsidered, while new are developed. For the development of adequate and durable measures the system analytic approach offers many interesting features. A system approach, encompassing the development and validation of simulation models, can help decision makers and scientists to get better insights in the complexity and the interaction of the different processes affecting the fate of chemicals in the dynamic soil-crop environment. As a result, a tremendous interest in system studies, especially through mathematical modelling, has emerged the last decade. Mathematical modelling is an important part of many current environmental studies and it is believed that there is still a lot of scope for model development as long as new insights in processes will emerge and computing facilities improve.

The WAVE-model (Water and Agrochemicals in soil, crop and Vadose Environment), is an example of such a mathematical tool. The model describes the transport and transformations of matter and energy in the soil, crop and vadose environment. The model is mainly process-based, since physical, chemical and biological laws were considered when developing the model. The model is deterministic, by which is meant that one set of input data always yields the same model output values. The model is numerical, since finite difference techniques were used for the solution of the differential equations describing matter and energy transport in the soil-crop continuum. The model is holistic, which means that an attempt was made to integrate the different sub-processes (and hence sub-models) ruling the transfer and fate of different state variables in the complex soil-crop environment. The model is one-dimensional, because it is assumed that governing transport processes of matter and energy in the soil sub-system occur essentially in the vertical direction. The model is an explanatory model because it helps to understand the different processes and process interactions governing e.g. pollutants in the soil. However, results from these explanatory studies can always be used in extrapolation or prediction studies for decision making. Hence, the current model is one of the ad-hoc tools available to improve current management of the soil-crop environment. It is a unique tool for the better understanding of the processes controlling the transfer and fate of chemicals in soils, the evaluation of experimental field data, the prediction of short and long-term impact of farming strategies on the quality of soil and the groundwater and the development of soil specific environmental measures for the application of fertilisers.



The present WAVE-model is the output of different research projects which aimed at the development, calibration and validation of mathematical models for the quantitative description of matter and energy in soils and environment. These projects were funded by the Institute for the Encouragement of Scientific Research in Agriculture and Industry, Belgium (I.W.O.N.L.) and the Directorates General VI and XII of the European Union. The projects output is, amongst other things, a model consisting of different modules simulating respectively the fate of water, solute, heat, or nitrogen in the soil environment and crop growth. The model is structured in a modular way, enabling the user to use only those modules required to analyse his problem. This allows also the extension of the present model with other modules without the need to adapt the model structure or existing input files of the model. It offers the possibility to exchange modules when new concepts and insights of certain processes becomes available. Fig. 1-1 present the different modules and the arrows indicate the 'uses-relationships' among them. For example, the solution of the solute flow equation needs to be proceeded by the solution of the water flow equation. Hence the solute module 'uses' the water flow module, which is indicated by the direction of the arrow.

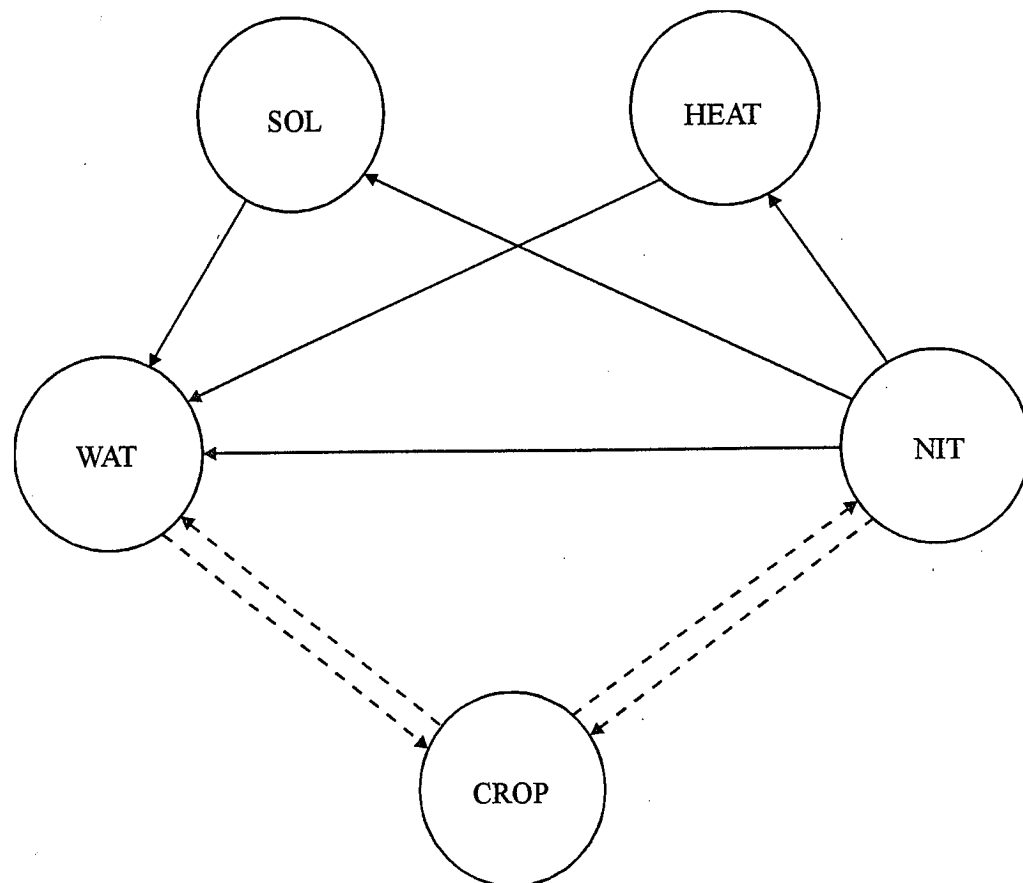


Fig. 1-1: Schematic presentation of the modules in WAVE (release 2.0). Full line arrows represents obligatory 'uses-relations', dashed lines are optional



The WAVE-model is a software package developed by the Institute for Land and Water Management of the K.U.Leuven, Belgium. The present version of the model integrates earlier models and packages developed by the Institute or developed and published by other scientific institutes. The model is a revised version of the SWATNIT-model (Vereecken et al., 1990; 1991), which integrates the SWATRER-model (Feddes et al., 1978; Belmans et al., 1983; Dierckx et al., 1986), a nitrogen model based on the SOILN-model (Bergström et al., 1991), a heat and solute transport model based on the LEACHN-model (Wagenet and Hutson, 1989) and the universal crop growth model SUCROS (van Keulen et al., 1982; Spitters et al., 1988). New modules, considering macroporous flow, pesticide flow, amongst other things are in current development, and will be added after extensive validation. The WAVE-model is written in MS-FORTRAN 5.10 and can be run either under UNIX or MS-DOS.

The user's manual is a revised form of the report of Vanclooster et al. (1993). In the user's manual an attempt is made to describe in detail all the process formulations. Special emphasis is given to the quotation of recent and relevant literature and to the listing of default values for model parameters and constants. This information together with the integration of automatic data quality control checks in the input files and the use of menus will certainly facilitate the use of the WAVE-model.

1.2 SPACE AND TIME SCALES

WAVE is essentially a 1-D model for the description of matter and energy flow in the soil and crop system. Mass and energy fluxes in the soil system are known to be strong non-linear processes. The numerical solution of the 3-D transport problem for unsteady state boundary conditions is, from a computational point of view, still an arduous task. Hence the model is conceived to describe flow only in 1-D systems, as in soil laboratory columns or field lysimeters. The model can also be used to describe transport at the field scale (or a small pedon) if transport is mainly vertical and if effective (1-D) parameters are used. If not, the model describes only flow for a horizontally isolated pedestals.

In the vertical direction, the model considers the existence of heterogeneity in the form of soil layers within a soil profile (Fig. 1-2). The soil layers are subdivided in space intervals called the soil compartments. Halfway each soil compartment a node is identified, for which state variable values are calculated using finite difference techniques. All soil compartments have the same thickness and the user can specify the thickness depending on the desired accuracy. Increasing the compartment thickness will decrease the calculation time but also the numerical accuracy.

The WAVE-model uses a time step smaller than a day to calculate the different system state variables, for processes which are strongly dynamic (water



transport, heat transport, solute transport, solute transformations). The time step is variable, and is chosen as to limit mass balance errors induced by solving the water flow equation. However, the time step size criterion can be input to change the model's robustness. For less dynamic processes (crop growth) a fixed daily time step is used. The model input is specified on a daily basis and flux type boundary conditions, are assumed constant within the time span of a day. This means, for example, that the daily precipitation is distributed equally within the day. State variables are integrated after each day to yield daily output. The simulation period should not exceed one single year. The simulation starts at midnight of the specified starting date and ends at midnight of the specified ending date.

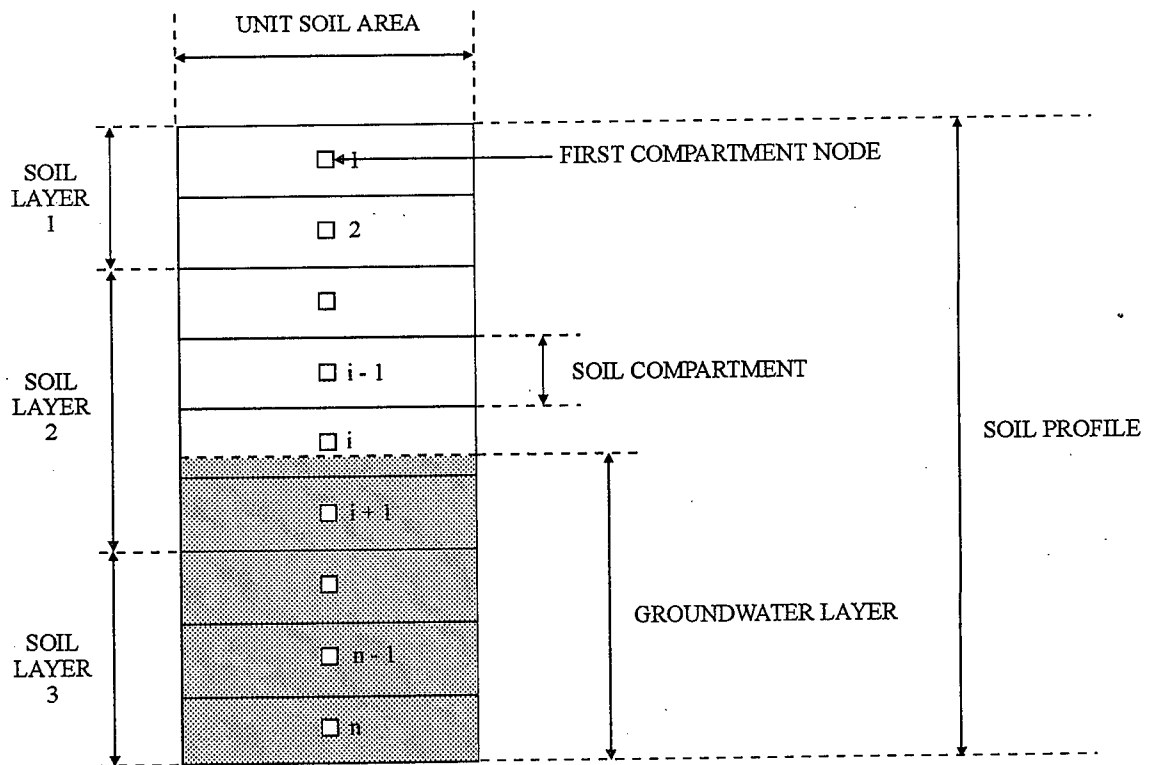


Fig. 1-2: Concept of the vertical space scale

1.3 REFERENCES

- Belmans, C., J.G. Wesseling and R.A. Feddes, 1983. Simulation of the water balance of a cropped soil: SWATRE. *J. of Hydrol.*, 63:271-286.
- Bergström, L., H. Johnsson and G. Tortensson, 1991. Simulation of nitrogen dynamics using the SOILN model. *Fert. Res.*, 27:181-188.



Dierckx, J., C. Belmans and P. Pauwels, 1986. SWATRER, a computer package for modelling the field water balance. Reference manual. Soil and Water Engng. Lab., K.U.Leuven, Belgium, 114 pp.

Feddes, R.A. , P.J. Kowalik and H. Zaradny, 1978. Simulation of field water use and crop yield. Simulation Monographs, PUDOC, Wageningen., The Netherlands. 189 pp.

Spitters, C.J.T, H. Van Keulen and D.W.G. Van Krailingen, 1988. A simple but universal crop growth simulation model, SUCROS87. In: R. Rabbinge, H. Van Laar and S. Ward (eds.). Simulation and systems management in crop protection. Simulation Monographs, PUDOC, Wageningen, The Netherlands.

Van Keulen, H., F.W.T. Penning de Vries and E.M. Drees, 1982. A summary model for crop growth. In: F.W.T. Penning de Vries and H.H. van Laar (eds.) Simulation of crop growth and crop production. PUDOC, Wageningen, 87-98.

Vanclooster, M., J. Diels, P. Viaene and J. Feyen, 1993. The SWAT-modules: Theory and input requirement. Internal Report 10. Institute for Land and Water Management, K.U.Leuven, 86 pp.

Vereecken, H., M. Vanclooster and M. Swerts, 1990. A simulation model for the estimation of nitrogen leaching with regional applicability. In: R. Merckx and H. Vereecken (eds.). Fertilization and the environment. Leuven Academic Press, Belgium, 250-263.

Vereecken, H., M. Vanclooster, M. Swerts and J. Diels, 1991. Simulating water and nitrogen behavior in soil cropped with winter wheat. Fert. Res., 27: 233-243.

Wagenet, R.J. and J. Hutson, 1989. LEACHN, a process-based model of water and solute movement, transformations, plant uptake and chemical reactions in the unsaturated zone. Centre for Environ. Res., Cornell University, Ithaca, NY, 147 pp.

THE WATER TRANSPORT MODULE



2 THE WATER TRANSPORT MODULE

2.1 THE SOIL WATER FLOW EQUATION

In the absence of plants, the soil field water balance can simply be written as:

$$\Delta W = (P + I + U) - (R + E + D) \quad (2-1)$$

where ΔW is the change in water content (mm) in the soil volume (set equal to the soil profile volume), P the precipitation (mm), I the irrigation depth applied (mm), U the upward capillary flow into the soil profile (mm), R the water depth lost by runoff (mm), E the actual evaporation (mm) and D the percolation or drainage depth. Generally, P and I are known system input, while U , R , E and D are unknown terms of the water balance. In order to quantify the unknown terms of the water balance, the soil water flow equation is solved.

For homogeneous isotropic isothermal rigid porous media one-dimensional water transport in an infinitesimal small soil element can be described using the Richards equation (Jury et al., 1991):

$$\frac{\partial \theta}{\partial t} = \frac{\partial}{\partial z} \left[K(\theta) \left(\frac{\partial h}{\partial z} + 1 \right) \right] \quad (2-2)$$

where θ is the volumetric water content ($m^3 m^{-3}$); z is the vertical co-ordinate (cm) defined as positive upward; t is the time (day); $K(\theta)$ is the hydraulic conductivity ($cm day^{-1}$); h is the soil water pressure head (cm).

Equation (2-2) combines the Darcian water flow equation with the water mass conservation law. By introducing the differential water capacity $C(h) = \partial \theta / \partial h$, which represents the slope of the water retention curve, and by expressing the hydraulic conductivity as a function of the pressure head one can convert Eq. (2-2) to a differential equation with only one unknown h :

$$C(h) \frac{\partial h}{\partial t} = \frac{\partial}{\partial z} \left[K(h) \left(\frac{\partial h}{\partial z} + 1 \right) \right] \quad (2-3)$$

Equation (2-3) is applicable for both unsaturated and saturated flow conditions. In the first case this equation is parabolic, whereas in the second case ($C(h)=0$) it reduces to an elliptic differential equation. Because both the hydraulic conductivity and the differential water capacity are non linear functions of h , Eq.(2-3) is non-linear. Analytical solutions of Eq.(2-3) only exist for specific boundary conditions (see Philip et al., 1957; amongst others). To handle more general flow situations, a numerical solution is applied in the WAVE-model to solve the soil water flow equation.



2.2 THE SOIL HYDRAULIC PROPERTIES

2.2.1 THE SOIL MOISTURE RETENTION CHARACTERISTIC

To solve the flow equation Eq. (2-3), the moisture retention ($MRC = \theta(h)$) and hydraulic conductivity ($HCC = K(\theta)$ or $K(h)$) functions need to be specified. A parametric model is available to describe the shape of the MRC. In addition to the widely used non-hysteretic retention models, some parametric hysteresis models are available in WAVE. Since the beginning of the century (Haines, 1930), it is known that the MRC of a soil is hysteretic i.e. the moisture content corresponding to a certain pressure head depends on the drying or wetting history. Hysteresis is caused by the irregular geometry of a pore, air inclusions in the soil matrix, shrinking and swelling characteristics (Childs, 1969). It has been observed that the occurrence of hysteresis substantial influence the calculated water fluxes (Russo et al., 1990; Jones et al., 1990).

When no hysteresis is assumed, moisture retention in the WAVE-model is described using the power function model of van Genuchten (van Genuchten, 1980; van Genuchten and Nielsen, 1985):

$$\theta(h) = \theta_r + \frac{\theta_s - \theta_r}{(1 + (\alpha|h|)^n)^m} \quad (2-4)$$

where θ_s is the saturated volumetric soil water content ($m^3 m^{-3}$); θ_r is the residual volumetric soil water content ($m^3 m^{-3}$); α is the inverse of the air entry value (m^{-1}); and n, m are shape parameters (-). Fig. 2-1 illustrates a physical interpretation of the parameters of Eq.(2-4) with exception of the m parameter which characterises the asymmetry.

When modelling the water balance of a field soil, the correct definition of the parameters of the MRC is crucial. If simultaneously measured moisture content and pressure head data are available, one can use these measurements to fit the parameters of Eq.(2-4) using non-linear optimisation techniques. Therefore, one can develop his own programmes using e.g. statistical software or spreadsheet programmes. Alternatively, one can use special softwares (e.g. van Genuchten, 1991).

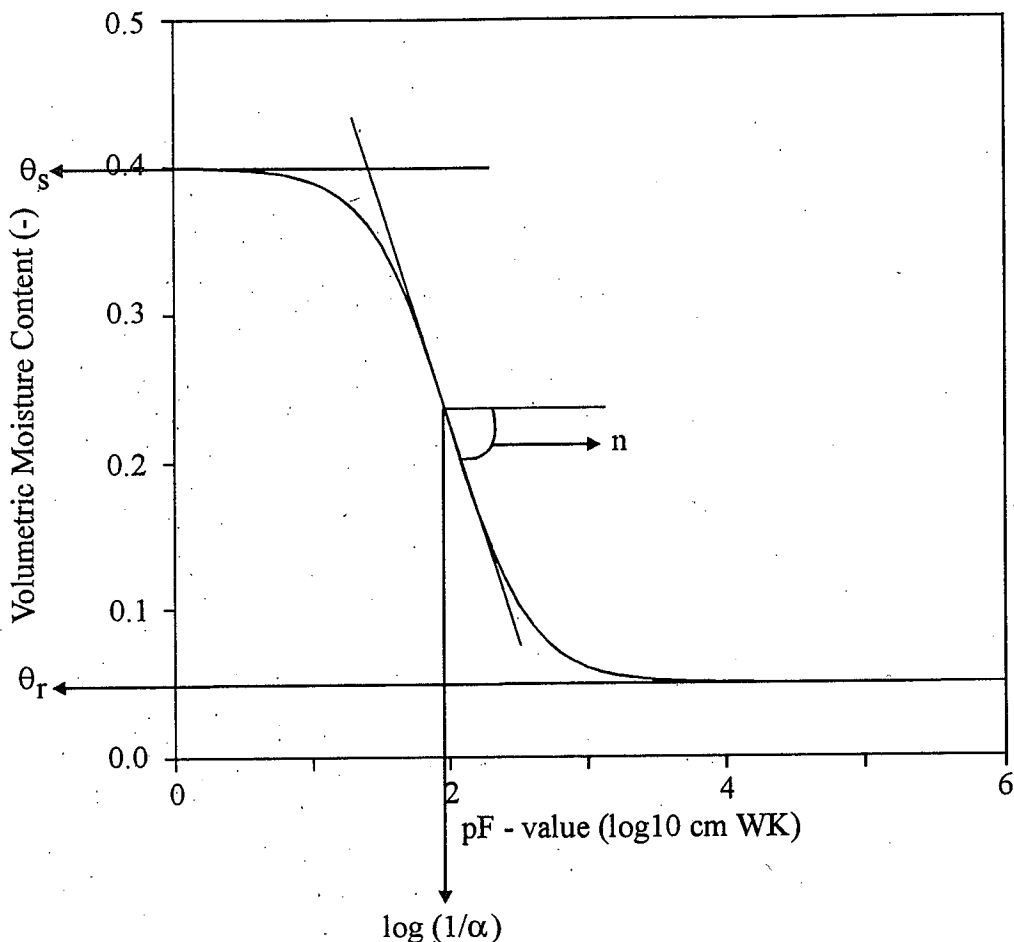


Fig. 2-1: Moisture retention characteristic as described by the van Genuchten model

In many cases, no measurement data of the MRC are available and so one needs an indirect estimate of the MRC parameters. For a range of soils, Vereecken et al. (1989) found that the MRC can reasonably well be estimated by assuming a symmetrical moisture retention characteristic (or $m=1$). Pedo-transfer functions, relating the remaining parameters of Eq.(2-4) to basic soil properties such as texture, soil organic carbon and others, were developed and validated (Vereecken et al., 1989; Vereecken et al., 1992; Tietje and Tapkenhinrichs, 1993). The following multiple regression pedo-transfer functions, taken from Vereecken et al., (1989) can be used to estimate the parameters of Eq.(2-4):

$$\begin{aligned}
 \theta_s &= 0.81 - 0.283(\text{Bd}) + 0.001(\text{Cl}) \\
 \theta_r &= 0.015 + 0.005(\text{Cl}) + 0.014(\text{C}) \quad L. 617 \\
 \ln(\alpha) &= -2.486 + 0.025(\text{Sa}) - 0.351(\text{C}) - 0.2647(\text{Bd}) - 0.023(\text{Cl}) \\
 \ln(n) &= 0.053 - 0.009(\text{Sa}) - 0.013(\text{Cl}) + 0.00015(\text{Sa})^2
 \end{aligned} \tag{2-5}$$



where B_d is the soil bulk density (g cm^{-3}); C = the carbon content (%); S_a = the sand content (fraction $50\text{-}2000\mu$ in %); C_l = the clay content (fraction $\leq 2\mu$ in %).

When hysteresis of the MRC is considered, four types of relations should be distinguished. If desorption starts from saturation, the main drying branch of the MRC (θ^d) is obtained. Branching from this curve results in a primary wetting curve (θ_1^w) which in turn leads to a secondary drying curve (θ_2^d) upon drying. All curves that once originated from the main drying curve are either uneven order wetting curves (θ_n^w , with $n=1,3,\dots$) or even order drying curves (θ_n^d , with $n=2,4,\dots$). In the same way, branching from the main wetting curve (θ^w) can only result in uneven drying curves (θ_n^d , with $n=1,3,\dots$), or even wetting curves (θ_n^w , with $n=2,4,\dots$).

In the WAVE-model, the second model reported by Mualem (1974) is included to describe the MRC. This model was found to be one of the most accurate in a comparative study of hysteresis models (Viaene et al., 1994). Mualem's model is a two branch, conceptual model. The conceptual foundation for the model is the independent domain theory of hysteresis (Néel, 1942-1943). As a two branch model, the model describes the moisture content on a curve of the MRC as a function of the moisture content on the two main curves. In the comparative study of hysteresis models, it was found that the main loop can be considered as a primary wetting loop without significant loss of accuracy. This implies that only two groups of scanning curves need to be considered: uneven order wetting curves and even order drying curves. For an uneven order wetting scanning curve branching from a drying curve at $\theta_{n-1}(h_\Delta)$, the moisture content $\theta_n^w(h)$ can be calculated as:

$$\theta_n^w(h) = \theta_{n-1}^d(h_\Delta) + (\theta^w(h) - \theta^w(h_\Delta)) \left(\frac{\theta_s - \theta^d(h_\Delta)}{\theta_s - \theta^w(h_\Delta)} \right) \quad (2-6)$$

where $\theta_{n-1}^d(h_\Delta)$ and h_Δ are respectively the water content and pressure head at the transition from the previous drying curve to the present wetting curve; $\theta^w(h)$ is the main wetting curve; $\theta^d(h)$ is the main drying curve; and θ_s , the saturated moisture content. Similarly, an even order drying scanning curve branching from a wetting curve at $\theta_{n-1}^w(h_\Delta)$ can be calculated as:

$$\theta_n^d(h) = \theta_{n-1}^w(h_\Delta) - (\theta^w(h_\Delta) - \theta^w(h)) \left(\frac{\theta_s - \theta^d(h)}{\theta_s - \theta^w(h)} \right) \quad (2-7)$$

where $\theta_{n-1}^w(h_\Delta)$ and h_Δ are respectively the water content and the pressure head at the transition from the previous wetting curve to the present drying curve; and $\theta_{n-1}^w(h)$ is the previous wetting curve.

The $\theta^d(h)$ and $\theta^w(h)$ relationships are described with the van Genuchten model (Eq.(2-4)). Assuming a closed main loop implies the same residual and saturated



moisture content for the main drying and wetting curve. Practical application of the model revealed that a different choice of n and m for the main curves results in numerical errors. Therefore the n and m parameters are default equal for both main retention curves. A hysteresis model needs to be combined with a K(θ) model since the K(h) relationship is also hysteretic. A common choice is the use of Mualem's conductivity model (cf. infra). For the use of this model, and hence for the use of Mualem's hysteretic retention model, the m parameter is restricted to $m = 1 - 1/n$. So, the only parameter differing between the main wetting and drying curve is α . For the main drying curve, α^d is the inverse of the air entry point, while for the main wetting curve α^w is the inverse for the water entry point. If Mualem's two branch model is used, one needs to input α^w as additional parameter to the parameters of Eq.(2-4). In Fig.2-2 the effect of different values of n, m, α^w and α^d are illustrated for the main loop and a small primary wetting - secondary drying loop. Notice the increase of the main loop area when a large α^w/α^d and large n, m are selected.

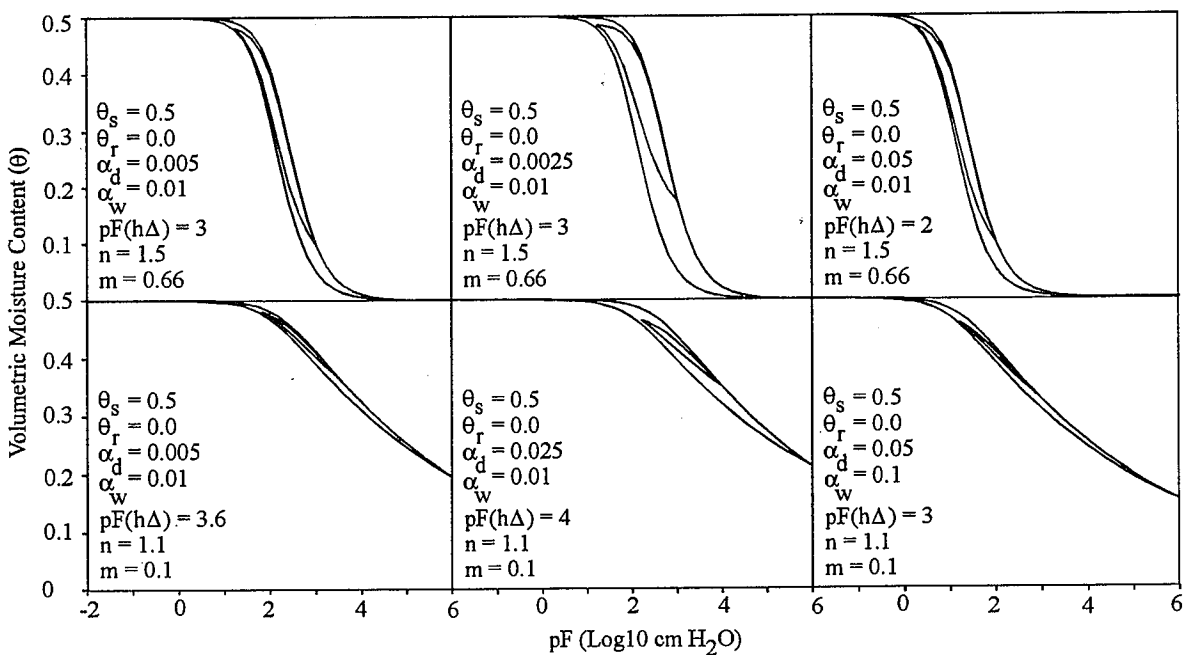


Fig. 2-2: Examples of hysteretic moisture retention characteristic, for a range of α_d , α_w and n, m values

In many situations only the main drying curve of the MRC is determined. In those cases the rule of thumb $\alpha^w/\alpha^d = 2$ can be used (Kool and Parker, 1987). Alternatively, one can use Mualem's universal hysteresis model to estimate the main drying loop from the main wetting (Mualem, 1977):



$$\theta_d(h) = (2\theta_s - \theta_w(h) - \theta_r) \left(\frac{\theta_w(h) - \theta_r}{\theta_s - \theta_r} \right) + \theta_r \quad (2-8)$$

This model is available in the WAVE-model. As input for this MRC model, the user specifies the parameters of Eq.(2-4) for the main wetting curve.

When applying Eq.(2-4), it is assumed that the pore-size distribution of the soil matrix follows a mono-modal distribution. Multi-porosity systems, assuming that the matrix system is the combination of different mono-modal systems, are more flexible in describing accelerated flow phenomena (preferential flow) in soils (Gerke and van Genuchten, 1993; Durner, 1994). The multi-porosity model available in the WAVE-model, assumes that the complete MRC curve in a multi-porous system can be described by the sum of separate mono-modal MRC's, similar to Eq.(2-4):

$$Se = \sum_i^n \frac{w_i}{\left(1 + (\alpha_i h)^{n_i}\right)^{m_i}} = \sum_i^n w_i S_i \quad (2-9)$$

where w_i are the weights of the individual partial MRC's S_i , with $\sum w_i = 1$. The saturation degree is a dimensionless moisture content and is defined as:

$$Se = \frac{\theta - \theta_r}{\theta_s - \theta_r} \quad (2-10)$$

An example of a multi-porous MRC is given in the Fig.2-3. When using the multi-porous MRC, α_i , n_i , m_i and w_i parameter need to be specified for each partial MRC, while θ_r and θ_s are needed to rescale Se back to volumetric moisture contents θ .

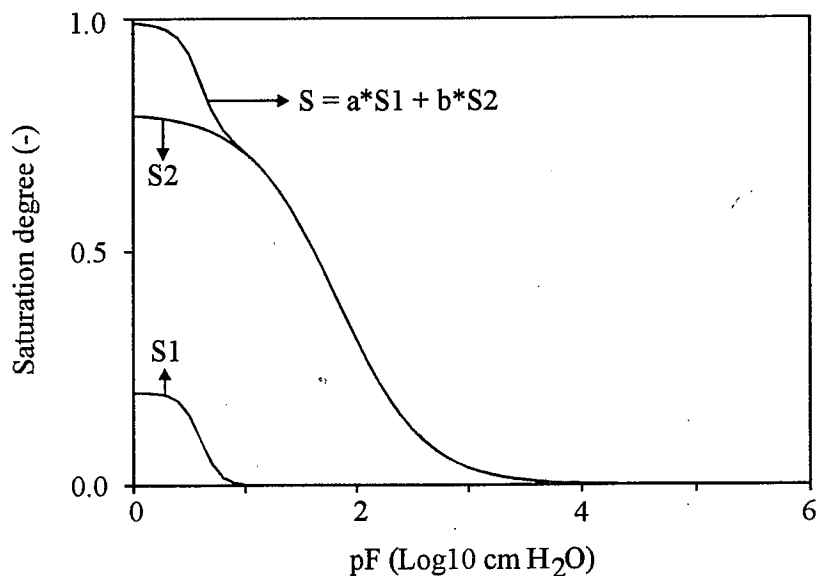


Fig.2-3: Bi-modal moisture retention characteristic as described with the sum of two van Genuchten equations



2.2.2 THE HYDRAULIC CONDUCTIVITY RELATIONSHIP

Just like for the MRC, conceptual, empirical or hybrid parametric models have been cited in literature to describe the hydraulic conductivity curve (HCC) of soils. The HCC can be expressed in terms of pressure head (h), volumetric moisture content (θ) or effective saturation (Se). The different mono-modal models for the HCC which are available in the WAVE-model are listed in Table 2-1.

Table 2-1: Hydraulic conductivity models available in the WAVE-model

Model Equation	Parameter	References
$K(h) = \frac{K_{sat}}{1 + (b h)^N}$ (2-11)	K_{sat}^{\dagger}, b, N	Gardner (1958)
$K(h) = K_{sat} * e^{\alpha h}$ (2-12)	$K_{sat}^{\dagger}, \alpha$	Gardner (1958)
$K(\theta) = K_{sat} * \theta^c$ (2-13)	K_{sat}^{\dagger}, c	Gilham et al. (1976)
$K(Se) = K_{sat} * Se^{\left(\frac{2+3l}{l}\right)}$ (2-14)	K_{sat}^{\dagger}, l	Brooks and Corey (1964)
$K(Se) = K_{sat} * Se^{\lambda} \left(1 - (1 - Se^{1/m})^m\right)^2$ (2-15)	$K_{sat}^{\dagger}, \lambda^{\dagger}, m^{\ddagger}$	van Genuchten (1980), Mualem (1976)

Legend: (\dagger): the saturated hydraulic conductivity(cm day^{-1}); (\dagger): the pore connectivity parameter; (\ddagger): the m parameter of the moisture retention characteristic with $m=1-1/n$.

The parameters of the HCC again can be fitted using optimisation techniques if measurements of the HCC at different moisture contents (or h or Se) are available. Different field and laboratory techniques are at hand to measure discrete points of the HCC, though still no standardised technique is available to yield an effective HCC. All parametric models use K_{sat} (the saturated hydraulic conductivity value) as first point of the hydraulic conductivity curve. The definition of an effective saturated conductivity is a tedious task. K_{sat} is strongly influenced by structural phenomena resulting from e.g. worm activity, crop roots, etc. So, the K_{sat} is behaving as a random variable rather than a deterministic property within the field. Hence, measurements of K_{sat} are varying tremendously within a field. Therefore it is suggested to measure K_{sat} slightly below saturation to exclude wormholes or cracks. This value can be obtained from e.g. sorption infiltrometer data.

When comparing different conductivity models for the description of the HCC, Gardner's model (1958) turned out to perform well for Belgian conditions (Vereecken et al., 1990), though the exponential Gardner model is more widely used to describe the HCC of undisturbed soils. For the Gardner model (1958), the following pedo-transfer function can be used if no good measurement of K_{sat} is available:

$$\begin{aligned} \ln(K_{sat}, e) &= 20.62 - 0.96 * \ln(Cl) - 0.66 \ln(Sa) - 0.46 * \ln(C) - 8.43 * Bd \\ \ln(b) &= -0.73 - 0.01877 * Sa + 0.058 * Cl \\ \ln(N) &= 1.186 - 0.194 * \ln(Cl) - 0.0489 * \ln(Si) \end{aligned} \quad (2-16)$$



where $K_{sat,e}$ is the estimate of the saturated hydraulic conductivity (cm day^{-1}), C_l , S_a and S_i the clay ($<2\mu$), sand (50-2000 μ) and silt (2-50 μ) content (%), B_d the soil bulk density (g cm^{-3}) and C the organic carbon content (%). The explanation of the pedo-transfer function of the observed variation increases if a measurement of the saturated hydraulic conductivity is included as predictor variable. In this case the following equations can be used to estimate Gardner's parameters:

$$\begin{aligned}\ln(K_{sat,e}) &= \ln(K_{sat,m}) \\ \ln(b) &= -2.640 - 0.019 * S_a + 0.05 * C_l + 0.506 * \ln(K_{sat,m}) \\ \ln(N) &= 1.186 - 0.194 * \ln(C_l) - 0.0489 * \ln(S_i)\end{aligned}\quad (2-17)$$

where $K_{sat,m}$ is the measurement of the saturated hydraulic conductivity curve (cm day^{-1}).

The theoretical HCC model of van Genuchten (1980) is a particular solution of the general statistical pore size distributed conductivity model of Mualem (1976). It uses the same parameters as for the MRC, though with the restriction that m must be equal to $1-1/n$. This HCC model is theoretically well elaborated. In practice, however, the resulting $K(\theta)$ -curve is very susceptible to the K_{sat} value. If only K_{sat} is measured, the typical difficulties with K_{sat} measurements (effect of sample size, high short-range variation, continuous cracks/pores through samples) can yield unrealistic $K(\theta)$ -curves. So one should be tremendously careful when using this indirect estimation model to estimate the HCC.

When modelling the field water balance with a multi-porosity system, the closed form expression of the van Genuchten-Mualem HCC needs to be replaced by the general Mualem model (Mualem, 1976):

$$K(h) = K_{sat} * S_e^\lambda \left(\frac{\int_0^{S_e} \frac{1}{h(S_e)} dS_e}{\int_0^h \frac{1}{h(S_e)} dS_e} \right)^2 \quad (2-18)$$

where the $h(S_e)$ curve is the inverse of the MRC curve. When a multi-modal MRC is assumed, the inverse of the MRC, $h(S_e)$, cannot be calculated directly. Therefore, the integrals in Eq.(2-18) need to be solved numerically. Substituting Eq. (2-9) in the denominators of Eq.(2-18) yields:

$$\begin{aligned}\int_0^{S_e} \frac{1}{h(S_e)} dS_e &= \int_{-\infty}^h \frac{1}{h(S_e)} \frac{\partial S_e}{\partial h} dh \\ &= \int_{-\infty}^h \frac{1}{h(S_e)} \left(\sum w_i \frac{\partial S_i}{\partial h} \right) dh = \sum w_i \int_{-\infty}^h \frac{1}{h(S_e)} \left(\frac{\partial S_i}{\partial h} \right) dh = \sum w_i \int_0^{S_i} \frac{1}{h(S_e)} dS_i\end{aligned}\quad (2-19)$$



or the integral of the multi-porous 1/h curve is the weighed sum of integrals of the partial 1/h curves. The integral of the partial 1/h curve can be solved by inversion (van Genuchten and Nielsen, 1985):

$$\int_0^{S_i} \frac{1}{h(S_e)} dS_i = \int_0^{S_i} \left(\frac{x^{1/m}}{1-x^{1/m}} \right)^{1/n} dx \quad (2-20)$$

The substitution $x=y^m$ reduces Eq.(2-20) to:

$$\int_0^{S_i} \frac{1}{h(S_e)} dS_i = m \int_0^{S_i^{1/m}} y^{m-1+1/n} (1-y)^{-1/n} dy = m * I_\zeta(p, q) * B(p, q) \quad (2-21)$$

where $I_\zeta(p, q)$ is the Incomplete Beta function and $B(p, q)$ is the Complete Beta function, and $\zeta=S_e(1/m)$, $p=m+1/n$ and $q=(1-1/n)$. The Incomplete Beta function in the WAVE-model is evaluated numerically using continued fractions (see e.g. van Genuchten, 1991):

$$I_\zeta(p, q) = \frac{\zeta^p (1-\zeta)^q}{pB(p, q)} \left(\frac{1}{1+} \frac{d_1}{1+} \frac{d_2}{1+} \right) \quad (2-22)$$

where

$$d_{2m+1} = \frac{-(p+q)(p+q+m)}{(p+2m)(p+2m+1)} \zeta \quad (2-23)$$

$$d_{2m} = \frac{m(q-m)}{(p+2m-1)(p+2m)} \zeta \quad (2-24)$$

2.3 NUMERICAL SOLUTION OF THE WATER FLOW EQUATION

2.3.1 THE SOLUTION PROCEDURE

In order to solve Eq.(2-3) numerically, the soil profile is discretised into a number of compartments and the total time period into discrete time increments (time steps) of unequal lengths. The soil compartments are grouped in different pedological layers (cf. Fig. 1-3). For each soil layer, the parameters of the MRC and HCC are specified. In this way, the partial derivatives of Eq.(2-3) can be approximated as ratio's of finite differences. An implicit discretisation scheme with explicit linearisation of the conductivity and the differential moisture capacity is used. In a comparative study of 6 different discretization methods, Haverkamp et al. (1977) found that the implicit schemes are superior in terms of applicability and efficiency. Furthermore Huwe and van der Ploeg (1988) observed that the explicit methods fail in case of saturated conditions. With this implicit difference scheme Eq.(2-3) can be approximated as:



$$C_i^j \frac{h_i^{j+1} - h_i^j}{\Delta t} = \frac{K_{i-1/2}^j \left[\frac{h_{i-1}^{j+1} - h_i^{j+1}}{\Delta z_i^*} + 1 \right] - K_{i+1/2}^j \left[\frac{h_i^{j+1} - h_{i+1}^{j+1}}{\Delta z_{i+1}^*} + 1 \right]}{\Delta z_i} \quad (2-25)$$

where :

$$\Delta z_i = z_{i-1/2} - z_{i+1/2} \quad (2-26)$$

is the thickness of the i-th compartment (mm);

$$\Delta z_i^* = z_{i-1} - z_i \quad (2-27)$$

is the distance between the nodes (mm); and

$$\Delta t = t^{j+1} - t^j \quad (2-28)$$

is the length of the time step (day).

Pressure heads are considered only at specific nodes in the time-depth space. The subscript i refers to the depth position, whereas j refers to the position on the time axis. The position of the variables h, K, and C in the numerical solution grid is illustrated in Fig. 2-4. Nodal points are situated in the middle of the compartments.

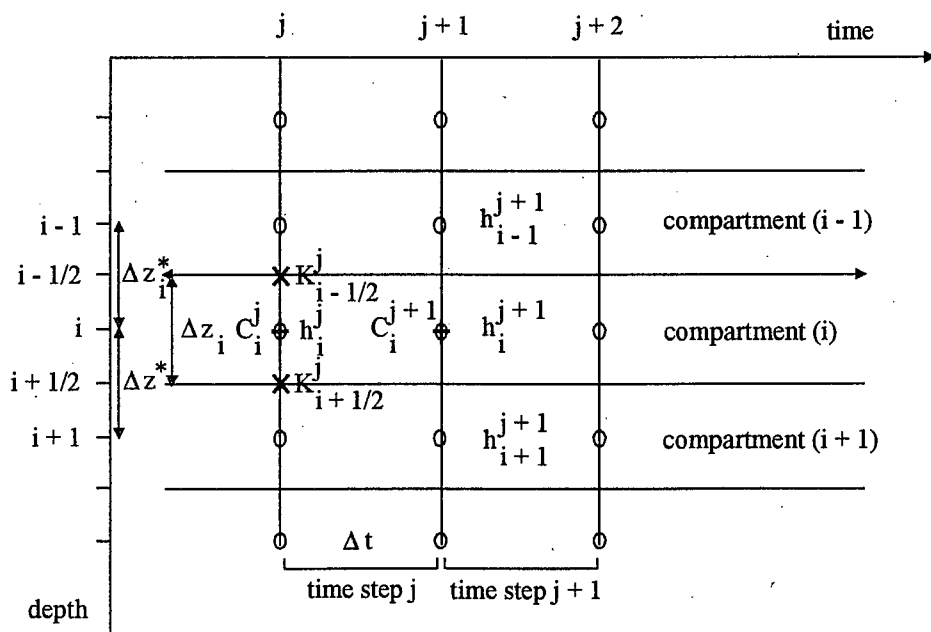


Fig. 2-4: Numerical grid, with location of pressure heads h (o), hydraulic conductivity K (x) and differential water capacity (+) as used in the finite difference equation (Eq. 2-25)



For the hydraulic conductivity between the nodal points, the geometric mean is taken as proposed by Vauclin et al. (1979).

$$\begin{aligned} K_{i-1/2}^j &= \sqrt{(K(h_{i-1}^j) * K(h_i^j))} \\ K_{i+1/2}^j &= \sqrt{(K(h_i^j) * K(h_{i+1}^j))} \end{aligned} \quad (2-29)$$

As can be seen in Eq. 2-25 and Fig. 2-4, the term $\partial h / \partial z$ is evaluated at the end of the time step (implicit discretisation), whereas K and C are set equal to their values at the beginning of the time step (explicit linearisation of K and C). This scheme implies that the equation, which can be written for node i , contains three unknowns (h_{i-1}^{j+1} , h_i^{j+1} and h_{i+1}^{j+1}). Rearranging Eq.(2-25) in terms of these unknowns, yields:

$$-d_i h_{i-1}^{j+1} + b_i h_i^{j+1} - a_i h_{i+1}^{j+1} = e_i \quad (2-30)$$

where:

$$\begin{aligned} a_i &= \frac{\Delta t}{\Delta z_i \Delta z_{i+1}^*} K_{i+1/2}^j \\ b_i &= C_i^j + \frac{\Delta t}{\Delta z_i \Delta z_{i+1}^*} K_{i+1/2}^j + \frac{\Delta t}{\Delta z_i \Delta z_{i+1}^*} K_{i-1/2}^j \\ d_i &= \frac{\Delta t}{\Delta z_i \Delta z_i^*} K_{i-1/2}^j \\ e_i &= C_i^j h_i^j - \frac{\Delta t}{\Delta z_i} K_{i+1/2}^j + \frac{\Delta t}{\Delta z_i} K_{i-1/2}^j \end{aligned} \quad (2-31)$$

Equation (2-30) is written for each node, except for the top and bottom one. As will be explained later, a similar equation can be developed for these boundary nodes. For the top node, Eq.(2-25) reduces to:

$$b_1 h_1^{j+1} - a_1 h_2^{j+1} = e_1 \quad (2-32)$$

where for the bottom node:

$$-d_n h_{n-1}^{j+1} + b_n h_n^{j+1} = e_n \quad (2-33)$$

In this way, the n pressure head values at the end of each time step (superscript $j+1$) are derived from the pressure head profile at the beginning of the time step and information of the boundary conditions, by solving a system of n equations having the following form:



$$\left[\begin{array}{cccccc} b_1 & -a_1 & 0 & . & . & 0 \\ -d_2 & b_2 & -a_2 & 0 & . & . \\ 0 & -d_3 & b_3 & -a_3 & 0 & . \\ . & 0 & . & . & . & * \\ . & -d_i & b_i & -a_i & . & h_i^{j+1} \\ . & 0 & . & 0 & . & e_i \\ . & -d_{n-1} & b_{n-1} & -a_{n-1} & . & h_{n-1}^{j+1} \\ 0 & . & 0 & -d_n & b_n & h_n^{j+1} \end{array} \right] = \left[\begin{array}{c} e_1 \\ e_2 \\ e_3 \\ . \\ . \\ . \\ e_{n-1} \\ e_n \end{array} \right] \quad (2-34)$$

To solve this tridiagonal system of linear equations, the Thomas algorithm which is a direct non-iterating solution technique is used (see e.g. Remson et al., 1971). Once the pressure head profile at the end of the time step is calculated, the corresponding water content profile is obtained by using the MRC. Next, the whole procedure is repeated for the next time step.

However, as a result of the explicit linearisation of the differential water capacity, mass balance errors occur, especially in case of large water content changes and nearly saturated moisture conditions. As stated before, the $\partial\theta/\partial t$ derivative in Eq.(2-2) has been replaced by $C(h)\partial h/\partial t$ (Eq.(2-3)), which in turn is approximated by its finite difference analog (Eq.(2-25)):

$$C(h) \frac{\partial h}{\partial t} \approx C_i^j \frac{h_i^{j+1} - h_i^j}{\Delta t} \quad (2-35)$$

Hence, a mass balance error resulting from this explicit linearisation of C is made which is equal to:

$$(e_i^{j+1} - e_i^j) - C_i^j (h_i^{j+1} - h_i^j) \quad (2-36)$$

In order to reduce these mass balance errors, the Newton-Raphson solution technique is used in the WAVE-model. The Newton-Raphson technique (see e.g. Carnahan et al., 1969) is an iterating solution method for a system of non-linear equations, and has the following form:

$$F_i(\bar{X}) = 0 \quad (2-37)$$

for $i=1,\dots,n$; with $\bar{X} = (x_1, \dots, x_n)$ the vector of unknowns. If the function values are known for a given vector $\bar{X}^t = (x_1^t, \dots, x_n^t)$, the function values F_1, \dots, F_n for a vector \bar{X}^{t+1} in the neighbourhood of the first one can be approximated by using a first order Taylor series expansion around \bar{X}^t :



$$F_i(\bar{X}^{\tau+1}) = F_i(\bar{X}^\tau) + \sum_{k=1}^n \frac{\partial F_i(\bar{X}^\tau)}{\partial x_k} (x_k^{\tau+1} - x_k^\tau) \quad (2-38)$$

If \bar{X}^τ is known as approximate solution of Eq.(2-25), an improvement can be obtained by solving $F_i(\bar{X}^{\tau+1})=0$, using the Taylor expansion given by Eq.(2-38). This means that successive improvements of the solution can be obtained by solving the following system of linear equations:

$$\begin{bmatrix} F_1(\bar{X}^\tau) \\ \vdots \\ F_n(\bar{X}^\tau) \end{bmatrix} + \begin{bmatrix} \frac{\partial F_1(\bar{X}^\tau)}{\partial x_1} & \cdots & \frac{\partial F_1(\bar{X}^\tau)}{\partial x_n} \\ \vdots & \ddots & \vdots \\ \frac{\partial F_n(\bar{X}^\tau)}{\partial x_1} & \cdots & \frac{\partial F_n(\bar{X}^\tau)}{\partial x_n} \end{bmatrix} * \begin{bmatrix} x_1^{\tau+1} - x_1^\tau \\ \vdots \\ x_n^{\tau+1} - x_n^\tau \end{bmatrix} = 0 \quad (2-39)$$

where $\bar{X}^{\tau+1} = (x_1^{\tau+1}, \dots, x_n^{\tau+1})$ being the unknowns.

Let's consider the θ -formulation of the water flow equation given by Eq.(2-2). The finite difference analog of this equation is similar to Eq.(2-25) and is rearranged in the form $F_i(H) = 0$ with $H = (h_i^{j+1}, \dots, h_n^{j+1})$ being the vector of unknown pressure heads:

$$F_i(\bar{H}) = \frac{\theta_i^{j+1} - \theta_i^j}{\Delta t} - \frac{K_{i-1/2}^j \left[\frac{h_{i-1}^{j+1} - h_i^{j+1}}{\Delta z_i^*} + 1 \right] - K_{i+1/2}^j \left[\frac{h_i^{j+1} - h_{i+1}^{j+1}}{\Delta z_{i+1}^*} + 1 \right]}{\Delta z_i} = 0 \quad (2-40)$$

This finite difference equation for node i is in fact the mass balance equation for compartment i . The solution of this system of equations yields an exact internal mass balance. Because θ_i^{j+1} is strongly dependent on the unknown h_{i+1}^{j+1} (non-linear $\theta(h)$); this equation is non-linear and the Newton-Raphson method offers the possibility to solve it in an iterative way. Assume $H^{j+1,\tau} = (h_1^{j+1,\tau}, \dots, h_n^{j+1,\tau})$ is the τ -th approximate solution of the systems of non-linear equations. A better solution is obtained by solving:

$$F_i(\bar{H}^\tau) + \sum_{k=1}^n \frac{\partial F_i(\bar{H}^\tau)}{\partial h_k} (h_k^{j+1,\tau+1} - h_k^{j+1,\tau}) = 0 \quad (2-41)$$



Equation (2-41) is obtained by combining Eq. (2-39) with (2-40). The partial derivatives can easily be derived from Eq.(2-40):

$$\begin{aligned}
 \frac{\partial F_i(\bar{H}^{j+1})}{\partial h_i^{j+1}} &= \frac{1}{\Delta t} \frac{\partial \theta_i^{j+1}}{\partial h_i^{j+1}} + \frac{K_{i-1/2}^j}{\Delta z_i \Delta z_i^*} + \frac{K_{i+1/2}^j}{\Delta z_i \Delta z_{i+1}^*} \\
 \frac{\partial F_i(\bar{H}^{j+1})}{\partial h_{i-1}^{j+1}} &= -\frac{K_{i-1/2}^j}{\Delta z_i \Delta z_i^*} \\
 \frac{\partial F_i(\bar{H}^{j+1})}{\partial h_{i+1}^{j+1}} &= -\frac{K_{i+1/2}^j}{\Delta z_i \Delta z_{i+1}^*} \\
 \frac{\partial F_i(\bar{H}^{j+1})}{\partial h_k^{j+1}} &= 0 \quad \text{for } k < i-1 \text{ or } k > i+1
 \end{aligned} \tag{2-42}$$

After replacing the partial derivatives in Eq.(2-41) and rearranging in terms of the unknowns $h_1^{j+1,\tau+1}, \dots, h_n^{j+1,\tau+1}$ one obtains an improved approximation by solving the following tridiagonal system of linear equations :

$$-d_i(h_{i-1}^{j+1})^{\tau+1} + b_i(h_i^{j+1})^{\tau+1} - a_i(h_{i+1}^{j+1})^{\tau+1} = e_i \quad \text{for } i = 2, \dots, n-1 \tag{2-43}$$

where:

$$\begin{aligned}
 a_i &= \frac{\Delta t}{\Delta z_i \Delta z_{i+1}^*} (K_{i+1/2}^{j+1})^\tau \\
 b_i &= (C_i^{j+1})^\tau + \frac{\Delta t}{\Delta z_i \Delta z_{i+1}^*} (K_{i+1/2}^{j+1})^\tau + \frac{\Delta t}{\Delta z_i \Delta z_{i+1}^*} (K_{i-1/2}^{j+1})^\tau \\
 d_i &= \frac{\Delta t}{\Delta z_i \Delta z_i^*} (K_{i-1/2}^{j+1})^\tau \\
 e_i &= (C_i^{j+1} h_i^j)^\tau - ((\theta_i^{j+1})^\tau - \theta_i^j) - \frac{\Delta t}{\Delta z_i} (K_{i+1/2}^{j+1})^\tau + \frac{\Delta t}{\Delta z_i} (K_{i-1/2}^{j+1})^\tau
 \end{aligned} \tag{2-44}$$

Equation (2-43) is very similar to Eq.(2-30), the only difference is the additional $(\theta_i^{j+1,\tau} - \theta_i^j)$ term in coefficient e_i , and the fact that C and K are now evaluated at time $j+1$. Again, two additional equations, similar to Eq.(2-32) and Eq.(2-33) are written for the top and bottom nodes. The resulting tridiagonal system consists of n linear equations with n unknowns which are solved directly by the same Thomas algorithm. The set of equations is solved for each iteration loop within the same time step. After each iteration, function values $F_i(H)$, which are in fact the mass balance errors for the different compartments ($m^3 m^{-3} day^{-1}$), can be calculated. The iteration procedure continues as long as one or more internal mass balance errors exceed a predefined threshold value ERR_{max} . The solution algorithm is summarized as follows:



- (1) Given H^j , the pressure head profile at the beginning of the time step, the first approximation $H^{j+1,1}$ is calculated by solving Eq.(2-25).
- (2) Repeat the following steps for $\tau = 1, \dots, NITER_{max}$.
 - (2.1) Calculate the internal mass balance errors $F_i(H^j)$.
If all $F_i(H^{j+1,\tau}) < ERR_{max}$, end iteration loop and go to the next time step;
else continue the iteration loop.
 - (2.2) Calculate an improved solution $H^{j+1,\tau+1}$ by solving the system of linear equations given by Eq.(2-43) and the additional equations for the top and bottom nodes.
- (3) If the desired accuracy is not reached within $NITER_{max}$ iterations, then halve the time step size and repeat the calculations starting from step 1.

2.3.2 DEFINITION OF THE UPPER BOUNDARY CONDITION

As stated before, it is necessary to construct an additional equation for the first compartment, which has a form given by Eq.(2-32). The flow situation at the soil surface is determined by the infiltration or the evaporative flux. As long as the flow conditions at the soil surface are not limiting, the flux through the soil surface Q_s equals:

$$Q_s = E_{pot} - \left(Rain + Irr + \frac{Pond - Intc}{\Delta t} \right) \quad (2-45)$$

where: Q_s is the potential flux through the soil surface, defined as positive upward ($cm\ day^{-1}$); E_{pot} is the potential soil evaporation rate ($cm\ day^{-1}$) as determined by weather conditions and soil cover; Rain is the precipitation rate ($cm\ day^{-1}$); Irr is the irrigation amount ($cm\ day^{-1}$); Pond is the ponding depth at the soil surface (cm) and Intc the storage capacity of the canopy (m).

Most of the time, the boundary condition at the top is a *flux condition* (Neuman condition), with the flux calculated from Eq.(2-3):

$$K(h) \left(\frac{\partial h}{\partial z} + 1 \right) = -Q_s(t) \quad \text{for } z = 0 \quad (2-46)$$

However, in case of high rainfall (or irrigation) intensities, the soil surface becomes saturated and the infiltration capacity (=Ksat.gradient) limits the infiltration rate. If no ponding is assumed, the excess water runs off immediately. In this case, the pressure head at the surface is put to zero. When ponding occurs, the pressure head at the soil surface increases until a maximal ponding depth, specified by the user, is reached. The maximal ponding depth reflects the surface micro-catchment when the soil surface roughness is high. When the maximal ponding depth is reached, the excess water runs off. In both cases, the flux type boundary condition switches to a



pressure head condition (Dirichlet) for the node at the surface ($h_s=0$ or h_s =ponding depth).

A similar phenomenon is encountered in case of prolonged soil evaporation without rewetting. In the beginning the upward flux is equal to the evaporative demand. At a given moment the top soil becomes so dry (low hydraulic conductivity) that the upward flux through the soil surface becomes smaller than the evaporative demand. This implies that the actual soil evaporation rate (E_{act}) becomes smaller than the potential rate (E_{pot}). Reduction of the potential evaporation is simulated by changing from a flux to a *pressure head condition*. When the pressure head at the surface tends to become more negative than a value h_{airdry} , corresponding with the potential of the air ($\approx -10^6$ cm), the pressure head is fixed ($h_s = h_{airdry}$). The value h_{airdry} is specified by the user.

With the above concept, the appropriate top boundary condition for each time step depends on the moisture condition in the top soil at the beginning of the time step and the value of the flux Q_s during that step. At the beginning of a time step, the program assumes the same condition as used in the foregoing time-step. After the soil moisture equation is solved accordingly, it is checked whether the choice was justified. In case of a *flux condition*, the pressure head at the surface is calculated using Darcy's equation:

$$h_s = h_1 + \Delta z_1^* \left(-\frac{Q_s}{K_0} - 1 \right) \quad (2-47)$$

where

$$K_0 = \frac{K(h_s) + K(h_1)}{2}$$

$$\Delta z_1^* = z_0 - z_1 = \text{distance (cm) from surface to node 1}$$

As long as the calculated h_s remains within the interval ($h_{airdry}, 0$), the choice for a flux condition is correct. If not, the calculations for the given time step are repeated with the appropriate pressure head condition.

If a *pressure head condition* is adopted, the flux through the surface is calculated using the Darcy equation and compared to the 'potential' flux Q_s . In case of run-off and ponding (h_s , fixed), the actual infiltration should always be smaller than the potential infiltration rate (actual flux $> Q_s$, both fluxes being negative). A similar criterion is used in the case of a reduction of the soil evaporation in dry conditions. In this case the actual soil evaporation should remain smaller (less positive) than the potential rate (actual flux $< Q_s$). If these conditions are not fulfilled, calculations are repeated with a flux condition.

With this algorithm, the soil moisture equation is solved with either a Dirichlet or a Neuman condition at the top. In case of a Dirichlet condition, the finite difference



equation for the first node is the same as for the other ones (Eq.(2-25)), with the exception that the node above the first node is located at the surface (at a distance of half the compartment size), and that its pressure head is known ($h_{i-1} = h_s$):

$$C_1^j \frac{h_1^{j+1} - h_1^j}{\Delta t} = \frac{K_0 \left(\frac{h_s^{j+1} - h_1^{j+1}}{\Delta z_1^*} + 1 \right) - K_{1+1/2}^j \left(\frac{h_1^{j+1} - h_2^{j+1}}{\Delta z_2^*} + 1 \right)}{\Delta z_1} \quad (2-48)$$

Rearranging in terms of the two unknowns, h_1^{j+1} and h_2^{j+1} , yields the following expressions:

$$b_1 h_1^{j+1} - a_1 h_2^{j+1} = e_1$$

where

$$a_1 = \frac{\Delta t}{\Delta z_1 \Delta z_2^*} K_{1+1/2}^j \quad (2-49)$$

$$b_1 = C_1^j + \frac{\Delta t}{\Delta z_1 \Delta z_2^*} K_{1+1/2}^j + \frac{\Delta t}{\Delta z_1 \Delta z_1^*} K_0^j$$

$$e_1 = C_1^j h_1^j - \frac{\Delta t}{\Delta z_1} K_{1+1/2}^j + \frac{\Delta t}{\Delta z_1} K_0^j + \frac{\Delta t}{\Delta z_1 \Delta z_1^*} K_0^j h_s^{j+1}$$

In case of a *flux condition*, the equation for node 1 is written as:

$$C_1^j \frac{h_1^{j+1} - h_1^j}{\Delta t} = \frac{-Q_s - K_{1+1/2}^j \left(\frac{h_1^{j+1} - h_2^{j+1}}{\Delta z_2^*} + 1 \right)}{\Delta z_1} \quad (2-50)$$

As for the Dirichlet condition, this equation again contains only two unknowns, and can be written in the form:

$$b_1 h_1^{j+1} - a_1 h_2^{j+1} = e_1$$

where

$$a_1 = \frac{\Delta t}{\Delta z_1 \Delta z_2^*} K_{1+1/2}^j \quad (2-51)$$

$$b_1 = C_1^j + \frac{\Delta t}{\Delta z_1 \Delta z_2^*} K_{1+1/2}^j$$

$$e_1 = C_1^j h_1^j - \frac{\Delta t}{\Delta z_1} K_{1+1/2}^j - \frac{\Delta t}{\Delta z_1} Q_s$$



2.3.3 DEFINITION OF THE BOTTOM BOUNDARY CONDITION

To solve the water flow equation for the n nodes of a soil profile, the flow at the bottom boundary needs to be quantified. It is evident that the flow at the bottom of the soil profile is controlled by the geo-hydrological conditions. In the WAVE-model the flow situation at the bottom of the flow domain can be specified in seven different ways. These seven options are divided into four groups:

1. A groundwater table is present:
 - the groundwater level is given as a function of time;
 - the flux through the bottom of the soil profile is given as a function of time, the groundwater level is calculated;
 - the flux through the bottom of the soil profile is calculated with a flux-groundwater level relationship; the groundwater level is calculated.
2. The pressure head at the bottom is known as a function of time.
3. The flux through the bottom is known at each time step:
 - assumption of free drainage at the bottom;
 - zero flux.
4. Lysimeter with free outflow at the bottom.

The bottom boundary options offer the possibility to simulate a wide variety of flow situations. Before describing the options in detail, the formulation of the bottom boundary conditions as a flux or pressure head condition is given.

If the flux at the bottom of the flow domain is known (*Neuman condition*), the boundary condition is given by:

$$K(h) \left(\frac{\partial h}{\partial z} + 1 \right) = -Q(t) \quad (2-52)$$

where $Q(t)$ represents the flux (cm day^{-1} , positive upward) at the bottom of the flow domain ($z=L$). When combining Richards equation with Eq.(2-52), the following implicit finite difference equation for the bottom node n is obtained:

$$C_n^j \frac{h_n^{j+1} - h_n^j}{\Delta t} = \frac{K_{n-1/2}^j \left(\frac{h_{n-1}^{j+1} - h_n^{j+1}}{\Delta z_n^*} + 1 \right) + Q_{n+1/2}^{j+1}}{\Delta z_n} \quad (2-53)$$

Figure 2-5 gives the location of the variables involved in the finite difference equation.

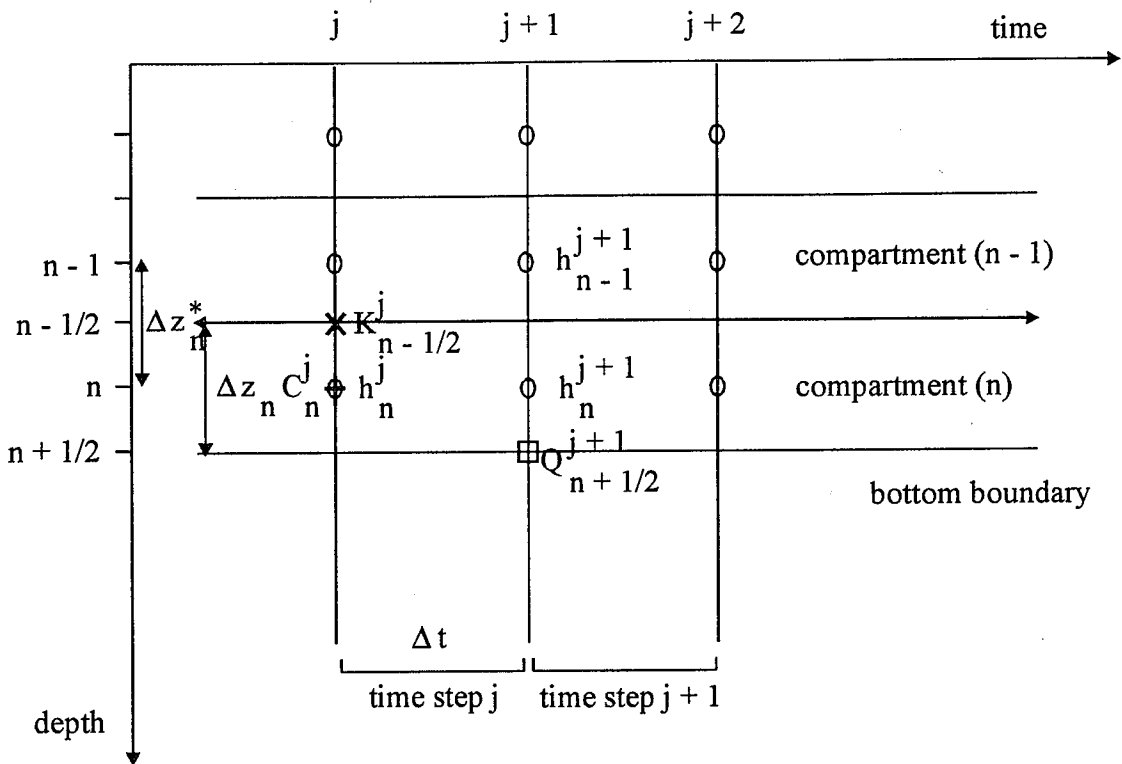


Fig. 2-5: Numerical grid, showing the location of the variables involved in the finite difference equation for the bottom compartment in case of a Neuman condition

Rearranging in terms of the unknowns h_{n-1}^{j+1} and h_n^{j+1} yields:

$$-d_n h_{n-1}^{j+1} + b_n h_n^{j+1} = e_n$$

where

$$b_n = C_n^j + \frac{\Delta t}{\Delta z_n \Delta z_n^*} K_{n-1/2}^j \quad (2-54)$$

$$d_n = \frac{\Delta t}{\Delta z_n \Delta z_n^*} K_{n-1/2}^j$$

$$e_n = C_n^j h_n^j + \frac{\Delta t}{\Delta z_n} Q_{n+1/2}^{j+1} + \frac{\Delta t}{\Delta z_n} K_{n-1/2}^j$$

In case of a *pressure head condition* at the bottom of the flow domain (*Dirichlet condition*), the finite difference equation for the bottom node n is identical to the equations for the other nodes:

$$C_n^j \frac{h_n^{j+1} - h_n^j}{\Delta t} = \frac{K_{n-1/2}^j \left(\frac{h_{n-1}^{j+1} - h_n^{j+1}}{\Delta z_n^*} + 1 \right) - K_{n+1/2}^j \left(\frac{h_n^{j+1} - h_{n+1/2}^{j+1}}{\Delta z_{i+1}^*} + 1 \right)}{\Delta z_i} \quad (2-55)$$



In this case the new pressure head at node $n+1$ is already known. Rearranging in terms of the two unknowns h_{n-1}^{j+1} and h_n^{j+1} yields:

$$-d_n h_{n-1}^{j+1} + b_n h_n^{j+1} = e_n$$

where

$$b_n = C_n^j + \frac{\Delta t}{\Delta z_n \Delta z_n^*} K_{n-1/2}^j \quad (2-56)$$

$$d_n = \frac{\Delta t}{\Delta z_n \Delta z_n^*} K_{n-1/2}^j$$

$$e_n = C_n^j h_n^j + \frac{\Delta t}{\Delta z_n \Delta z_{n+1}^*} K_{n+1/2}^j h_{n+1/2}^{j+1} - \frac{\Delta t}{\Delta z_i} K_{n+1/2}^j + \frac{\Delta t}{\Delta z_i} K_{n-1/2}^j$$

In the next section it will be shown how, for each of the seven bottom boundary options, the flow situation can be reduced to a flux or pressure head condition.

Option 1: A constant or time variant groundwater level is present and the water level depth (mm) is specified by the user as a function of time

When a groundwater level is given, the pressure head at the groundwater depth is exactly known ($h=0$) but no information is available regarding the flow conditions at the bottom of the soil profile. The characterisation of the bottom boundary condition proceeds as follows. Initially, the unsaturated node above the water level is considered as bottom node during the current day. Next, the pressure head at the underlaying (saturated) node ($n+1$) is calculated assuming equilibrium (zero hydraulic gradient) with the water level :

$$h_{n+1}^{j+1} = W^{j+1} - z_{n+1} \quad (2-57)$$

where W^{j+1} is the position of the groundwater level (cm) and z_{n+1} is the position of the first saturated node (cm) (z -axis is defined positive upward, $z=0$ at the surface). The foregoing means that the bottom of the unsaturated flow domain is determined by a *Dirichlet condition*. Further, the flow equation is solved for the unsaturated nodes (node 1 up to n). The error resulting from the assumption of zero gradient becomes negligible compared to the accuracy of the groundwater level data. Once the new pressure head profile and corresponding fluxes for the unsaturated zone have been calculated, the fluxes in the saturated compartments are calculated by assuming mass conservation for each saturated compartment. Finally, the (positive) pressure heads in the saturated zone are calculated by applying Darcy's equation, starting from node $n+1$.



Option 2: A groundwater table is present and the flux through the bottom compartment of the soil profile is given

In this case the user specifies the flux through the bottom of the soil profile for each day of the simulation period. This flux at the bottom of the soil profile is kept constant throughout a simulation day. The flow situation at the bottom of the soil profile is characterised by a *Neuman boundary condition* and the flow equation can be solved for all compartments in which the soil profile has been discretized. The new position of the water table is calculated from the pressure head profile at the end of each time step.

Option 3: A groundwater table is present and a flux-ground water level relationship is available

For the sandy soils in the eastern part of the Netherlands, the following relationship between the groundwater level and the discharge Q_b has been derived:

$$Q_b = a \cdot e^{b\phi} \quad (2-58)$$

where ϕ is the groundwater level (m) and a , b are regression coefficients. Examples of such measurements are given by Ernst and Feddes, (1979). Also for this case the flow situation at the bottom of the soil profile is determined by a *Neuman condition*.

Option 4: The pressure head at the bottom of the soil profile is given

In this case the pressure head is known for a nodal point outside the considered flow domain at the lower boundary of the soil profile (*Dirichlet condition*).

Option 5: Free drainage condition is assumed at the bottom of the soil profile

When free drainage occurs, the flux through the bottom of the soil profile is always negative (=downwards) and equal to the hydraulic conductivity of the bottom compartment:

$$Q_{n+1/2} = -K_n \quad (2-59)$$

According to this assumption the pressure head at the bottom of the soil profile is constant with depth and the flow of water is only controlled by gravity. This assumption is valid for conditions of a deep water table. Furthermore, the profile depth has to be chosen such that infiltration profiles never reach the bottom. Once again a *Neuman condition* exists at the bottom



of the soil profile. To estimate the first approximate solution of the water flow equation, the bottom flux yields:

$$Q_{n+1/2}^{j+1} = -K_n^j \quad (2-60)$$

For the successive Newton-Raphson iterations, the following expression holds:

$$Q_{n+1/2}^{j+1, \tau+1} = -K_n^{j, \tau} \quad (2-61)$$

Option 6: Zero flux through the bottom of the soil profile

This boundary condition needs no further comment because the situation at the bottom of the soil profile is a typical *Neuman condition*.

Option 7: Lysimeter bottom boundary condition

Lysimeters often have a drainage system or an outlet at the bottom, allowing free outflow when saturation occurs at the bottom. None of the foregoing conditions apply to this special case. When a small positive pressure is build up at the bottom, water will flow out. In this case the pressure head of the bottom node ($h_{n+1/2}$) is fixed to zero (*Dirichlet*), as if we had a water table at the bottom. The situation is however different from a water table, because upward flow can never occur in a free draining lysimeter. Therefore, every time step it is checked whether the flux through the bottom is still negative (downward). If not, the boundary condition is specified as a zero flux condition (*Neuman*) instead and this condition is maintained as long as $h_{n+1/2}$ remains negative.

2.4 MODELLING OF THE WATER TRANSPORT IN CROPPED SOILS

2.4.1 INTRODUCTION

When modelling the water balance of cropped soils crop transpiration and interception are part of the water balance. In the WAVE-model the interception capacity of the crop is input in the model. The potential transpiration rate is calculated as a fraction of the maximum potential evapotranspiration. The latter is obtained by multiplying the potential evapotranspiration of the reference crop or surface with a crop specific coefficient which varies as a function of the crop development stage (Doorenbos and Pruitt, 1977; Raes et al., 1986; Feddes, 1987). The fraction of the potential evapotranspiration allocated to the transpiration is calculated according to the leaf area index. Finally, the potential transpiration is reduced to an actual level, based on moisture conditions in the root zone.

There are two possibilities to specify crop development in the WAVE-model: (i) the leaf area and root development are specified as model input or (ii) leaf area and root growth are calculated using a crop growth model. Taking the first approach, only the



water uptake mechanism in the root zone is dynamically represented in the model. Other processes are not explicitly considered in the simulated system. Hence the leaf area and rooting depth are needed as input variables to the model. Yet, when also simulating the crop development and growth, the crop system and the soil water system are completely integrated, offering a framework with many more possibilities for including feed back mechanisms of soil moisture and nutrient availability on crop development. Before describing in detail the integrated crop growth model, the canopy interception model, the transpiration model, and the macroscopic root water uptake model will be discussed at length. These models assume that the crop root length, LAI and potential evapotranspiration are simulated/measured as a function of time.

2.4.2 CROP INTERCEPTION

Interception can be quite considerable. Yet, detailed data on the interception capacity as a function of development stage, for a range of crops and climate conditions are lacking. The interception capacity of water by the crop is not modelled in the WAVE-model, but specified as input. At a specified time step, the storage of water in the canopy, is calculated as the minimum of the sum of the potential precipitation and irrigation during that day and the specified potential interception capacity reduced with that water that is still stored from the previous time step. In calculating the actual transpiration (see later), the amount stored in the canopy is assumed to evaporate first. Hence, this amount is subtracted from the potential transpiration calculated with Eq. 2-62 (see infra).

2.4.3 CALCULATION OF THE POTENTIAL EVAPOTRANSPIRATION OF A CROP

The potential evapotranspiration of a disease free crop (ET_{crop}), grown under optimal soil water and fertility conditions is calculated in the WAVE-model by multiplying the potential evapotranspiration of a reference surface (ET_0) with a crop coefficient K_c . This procedure actually originates from irrigation science and is rather empirical. Since the rainfall surplus is one of the main driving mechanisms of transport in the soil, it is extremely important to try to correctly estimate the ET_{crop} . In this context, it should be noted that the K_c -factors used are the ones derived for a given calculation procedure of the potential evapotranspiration for a specific reference surface. The K_c -value varies throughout the growing season and its value depend on the crop development stage and the climatic conditions.

When the Penman equation is used to calculate potential evapotranspiration with grass as a reference surface, the K_c -factors of Doorenbos and Pruitt (1977) can be used to estimate ET_{crop} . In the approach of Doorenbos and Pruitt, the growing season is subdivided into 4 stages: the initial, the crop development, the mid-season and the late season stage (see Fig. 2-6). For bare soil conditions, or if the crop ground cover is less than 10 %, evapotranspiration is mainly controlled by the moisture content in the top soil. The soil evaporation decreases as the soil dries. This



effect is accounted for in the approach of Doorenbos and Pruitt by assuming a small value for K_c . Since the reduction of the evaporation is accounted for when solving the water flow equation, a K_c -factor of 1 should be used during the crop initial stages (from germination until the ground cover index is equal to 10%). During mid-season (from effective full ground cover until start of maturing) K_c -values as reported in Tables 2-2 and 2-3 are recommended to calculate the potential crop evapotranspiration, if grass is the reference surface. The value of the K_c -factor for the crop development phase (end of initial stage until attainment of effective full ground cover) is obtained by linear interpolation between the K_c -factor of the initial stage (which is mostly equal to 1.0) and the K_c -factor of the crop mid-season stage. The K_c -factor of the late-season stage (end of mid-season, until attainment of crop maturity) is obtained by linear interpolation between the mid-season and maturity K_c -value. The assumed K_c -development is given in Fig. 2-6.

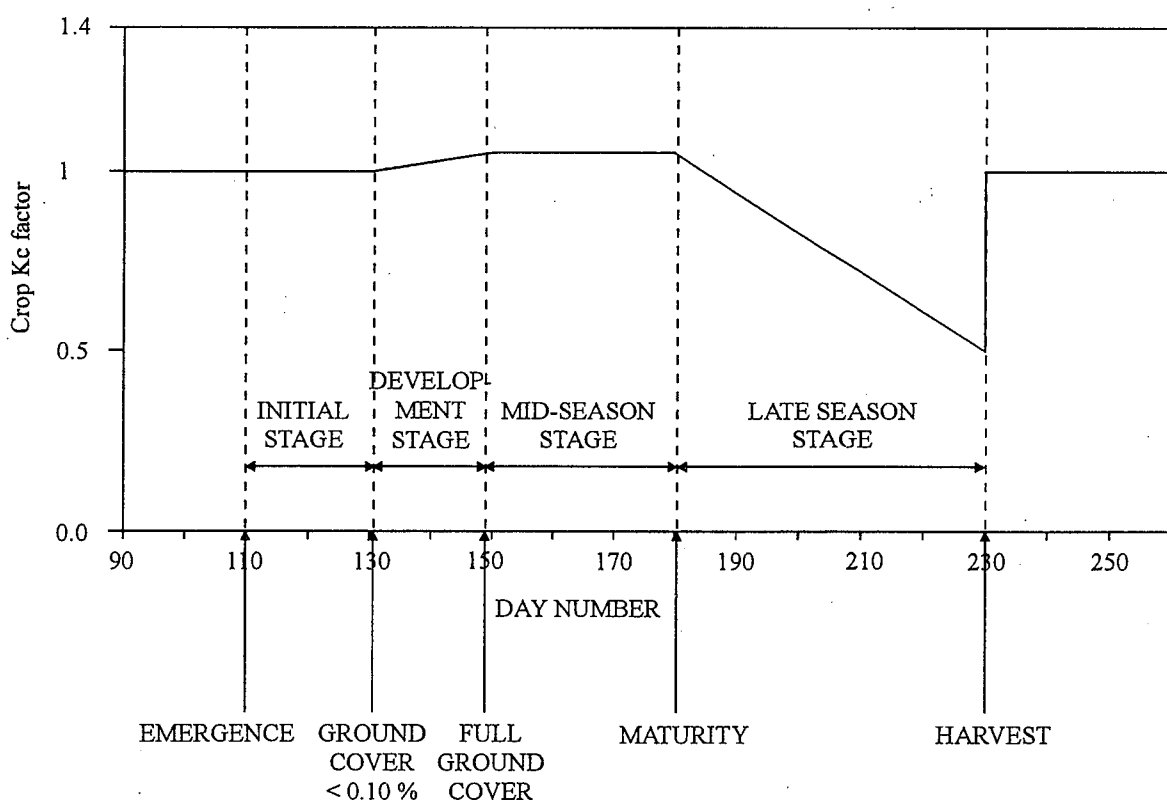


Fig. 2-6: Time course of the crop K_c -factor for WAVE in combination with the Doorenbos and Pruitt approach.



Table 2-2: K_c -factors during the mid-season stage for different crop and different prevailing climatic conditions according Doorenbos and Pruitt (1977). The value of the K_c -factor is related to ET_0 with grass as a reference surface

Crop	RH>70% Windspeed = 0-5 m s ⁻¹	RH>70% Windspeed = 5-8 m s ⁻¹	RH<20% Windspeed = 0-5 m s ⁻¹	RH<20% Windspeed = 5-8 m s ⁻¹
Artichokes	0.95	0.95	1.00	1.05
Barley	1.05	1.10	1.15	1.20
Beans (green)	0.95	0.95	1.00	1.05
Beans (dry), Pulses	1.05	1.10	1.15	1.20
Beets	1.00	1.00	1.05	1.10
Carrots	1.00	1.05	1.10	1.15
Castor beans	1.05	1.10	1.15	1.20
Celery	1.00	1.05	1.10	1.15
Corn (sweet)	1.05	1.10	1.15	1.20
Corn (grain)	1.05	1.15	1.15	1.20
Crucifers	0.95	1.00	1.05	1.10
Cucumber	0.90	0.90	0.95	1.00
Egg plant	0.95	1.00	1.05	1.10
Flax	1.00	1.05	1.10	1.15
Grain	1.05	1.10	1.15	1.20
Lentil	1.05	1.10	1.15	1.20
Lettuce	0.95	0.95	1.00	1.05
Melons	0.95	0.95	1.00	1.05
Millet	1.00	1.05	1.10	1.15
Oats	1.05	1.10	1.15	1.20
Onion (dry)	0.95	0.95	1.05	1.10
Onion (green)	0.95	0.95	1.00	1.05
Peanuts	0.95	1.00	1.05	1.10
Peas	1.05	1.10	1.15	1.20
Peppers	0.95	1.00	1.05	1.10
Potato	1.05	1.10	1.15	1.20
Radishes	0.80	0.80	0.85	0.90
Safflower	1.05	1.10	1.15	1.20
Sorghum	1.00	1.05	1.10	1.15
Soybeans	1.00	1.05	1.10	1.15
Spinach	0.95	0.95	1.00	1.05
Squash	0.90	0.90	0.95	1.00
Sugar beet	1.05	1.10	1.15	1.20
Sunflower	1.05	1.10	1.15	1.20
Tomato	1.05	1.10	1.20	1.25
Wheat	1.05	1.10	1.15	1.20



Table 2-3: K_c -factors at the end of the late-season stage for different crop and different prevailing climatic conditions according Doorenbos and Pruitt (1977). The values of the K_c -factor is related to ET_0 with grass as a reference surface

Crop	RH>70% Windspeed = 0-5 m s ⁻¹	RH>70% Windspeed = 5-8 m s ⁻¹	RH<20% Windspeed = 0-5 m s ⁻¹	RH<20% Windspeed = 5-8 m s ⁻¹
Artichokes	0.90	0.90	0.95	1.00
Barley	0.25	0.25	0.20	0.20
Beans (green)	0.85	0.85	0.90	0.90
Beans (dry), Pulses	0.30	0.30	0.25	0.25
Beets	0.90	0.90	0.90	1.00
Carrots	0.70	0.75	0.80	0.85
Castorbeans	0.50	0.50	0.50	0.50
Celery	0.90	0.95	1.00	1.05
Corn (sweet)	0.95	1.00	1.05	1.05
Corn (grain)	0.55	0.55	0.60	0.60
Crucifers	0.80	0.85	0.90	0.95
Cucumber				
Fresh market	0.70	0.70	0.75	0.80
Machine Harvest	0.85	0.85	0.95	1.00
Egg plant	0.80	0.85	0.85	0.90
Flax	0.25	0.25	0.20	0.20
Grain	0.30	0.30	0.25	0.25
Lentil	0.30	0.30	0.25	0.25
Lettuce	0.90	0.90	0.90	1.00
Melons	0.65	0.65	0.75	0.75
Millet	0.30	0.30	0.25	0.25
Oats	0.25	0.25	0.20	0.20
Onion (dry)	0.75	0.75	0.80	0.85
Onion (green)	0.95	0.95	1.00	1.05
Peanuts	0.55	0.55	0.60	0.60
Peas	0.95	1.00	1.05	1.10
Peppers	0.80	0.85	0.85	0.90
Potato	0.70	0.70	0.75	0.75
Radishes	0.75	0.75	0.80	0.85
Safflower	0.25	0.25	0.20	0.20
Sorghum	0.50	0.50	0.55	0.55
Soybeans	0.45	0.45	0.45	0.45
Spinach	0.90	0.90	0.95	1.00
Squash	0.70	0.70	0.75	0.80
Sugar beet	0.90	0.95	1.00	1.00
Sunflower	0.40	0.40	0.35	0.35
Tomato	0.60	0.60	0.65	0.65
Wheat	0.25	0.25	0.20	0.20



Table 2-4: Crop factors as related to the Penman open water evaporation equation, for different crops and different decades during the crop season (source: Feddes (1987))

	Ap 1	Ap 2	Ap 3	1	2	3	Ma 1	2	3	Ju 1	2	3	Jul 1	2	3	Au 1	2	3	Se 1	2	3
Grass	0.8	0.8	0.8	0.8	0.8	0.8	0.8	0.8	0.8	0.8	0.8	0.8	0.8	0.8	0.8	0.8	0.8	0.8	0.8	0.8	
Cereals	0.5	0.6	0.7	0.8	0.8	0.8	0.9	0.9	0.9	0.7	0.6	0.5	-	-	-	-	-	-	-	-	
Maize	-	-	-	0.4	0.5	0.6	0.7	0.8	0.9	1.0	1.0	1.0	1.0	1.0	1.0	1.0	1.0	1.0	1.0	1.0	
Potatoes	-	-	-	-	0.5	0.7	0.8	0.9	0.9	0.9	0.9	0.9	0.9	0.9	0.9	0.9	0.9	0.9	0.9	0.9	
Sugar beets	-	-	-	0.4	0.4	0.4	0.6	0.8	0.8	0.9	0.9	0.9	0.9	0.9	0.9	0.9	0.9	0.9	0.9	0.9	
Leguminous	-	0.4	0.5	0.6	0.7	0.8	0.9	0.9	0.9	0.8	0.8	0.8	0.8	0.8	0.8	0.8	0.8	0.8	0.8	0.8	
Plant-onions	0.4	0.5	0.5	0.6	0.6	0.7	0.8	0.8	0.8	0.8	0.8	0.8	0.8	0.8	0.8	0.8	0.8	0.8	0.8	0.8	
Sow-onions	-	0.3	0.4	0.4	0.5	0.5	0.6	0.6	0.7	0.7	0.8	0.8	0.8	0.8	0.8	0.8	0.8	0.8	0.8	0.8	
Chicory	-	-	-	-	-	-	-	0.4	0.4	0.4	0.4	0.4	0.4	0.4	0.4	0.4	0.4	0.4	0.4	0.4	
Winter carrots	-	-	-	-	-	-	-	0.4	0.4	0.4	0.4	0.4	0.4	0.4	0.4	0.4	0.4	0.4	0.4	0.4	
Celery	-	-	-	-	-	-	-	0.4	0.5	0.5	0.5	0.5	0.5	0.5	0.5	0.5	0.5	0.5	0.5	0.5	
Leek	-	-	-	-	-	-	-	0.4	0.4	0.4	0.4	0.4	0.4	0.4	0.4	0.4	0.4	0.4	0.4	0.4	
Bulb/tube crops	-	-	-	-	-	-	-	0.4	0.5	0.5	0.5	0.5	0.5	0.5	0.5	0.5	0.5	0.5	0.5	0.5	
Pome/stone fruit	0.8	0.8	0.8	1.1	1.1	1.1	1.2	1.2	1.2	1.3	1.3	1.3	1.3	1.3	1.3	1.3	1.3	1.3	1.3	1.3	



Table 2-5: Crop factors as related to the Makkink reference crop evapotranspiration for grass, for different crops and different decades during the crop season (source: Feddés (1987))

	Ap 1	Ap 2	Ap 3	1	2	3	Ma 1	2	3	Ju 1	2	3	Jul 1	2	3	Au 1	2	3	Se 1	2	3
Grass	1.0	1.0	1.0	1.0	1.0	1.0	1.0	1.0	1.0	1.0	1.0	1.0	1.0	1.0	1.0	1.0	1.0	1.0	0.9	0.9	0.9
Cereals	0.7	0.8	0.9	1.0	1.0	1.0	1.2	1.2	1.2	1.0	0.9	0.8	0.6	-	-	-	-	-	-	-	-
Maize	-	-	-	0.5	0.7	0.8	0.9	1.0	1.2	1.3	1.3	1.2	1.2	1.2	1.2	1.2	1.2	1.2	1.2	1.2	1.2
Potatoes	-	-	-	-	0.7	0.9	1.0	1.2	1.2	1.2	1.1	1.1	1.1	1.1	1.1	1.1	1.1	1.1	0.7	-	-
Sugar beets	-	-	-	0.5	0.5	0.5	0.8	1.0	1.0	1.2	1.1	1.1	1.1	1.2	1.2	1.2	1.2	1.2	1.1	1.1	1.1
Leguminous	-	0.5	0.7	0.8	0.9	1.0	1.2	1.2	1.2	1.0	0.8	-	-	-	-	-	-	-	-	-	-
Plant-onions	0.5	0.7	0.7	0.8	0.8	0.9	1.0	1.0	1.0	1.0	1.0	1.0	1.0	1.0	1.0	1.0	1.0	1.0	0.9	0.7	-
Sow-onions	-	0.4	0.5	0.5	0.7	0.7	0.8	0.9	0.9	1.0	1.0	1.0	1.0	1.0	1.0	1.0	1.0	1.0	1.0	1.0	1.0
Chicory	-	-	-	-	-	-	0.5	0.5	0.5	0.5	0.5	0.8	1.0	1.1	1.1	1.1	1.1	1.1	1.1	1.1	1.1
Winter carrots	-	-	-	-	-	-	0.5	0.5	0.5	0.5	0.5	0.8	1.0	1.1	1.1	1.1	1.1	1.1	1.1	1.1	1.1
Celery	-	-	-	-	-	-	0.5	0.7	0.7	0.7	0.7	0.8	0.9	1.0	1.1	1.1	1.1	1.1	1.1	1.1	-
Leek	-	-	-	-	-	-	0.5	0.5	0.5	0.5	0.7	0.7	0.8	0.8	0.8	0.8	0.8	0.9	0.9	0.9	0.9
Bulb/tube crops	-	-	-	-	-	-	0.5	0.7	0.7	0.9	1.2	1.2	1.2	1.2	1.2	1.2	1.2	1.2	1.2	1.2	1.2
Pome/stone fruit	1.0	1.0	1.0	1.4	1.4	1.4	1.6	1.6	1.6	1.7	1.7	1.7	1.7	1.7	1.7	1.7	1.7	1.7	1.2	1.2	1.2



As an alternative to the Doorenbos and Pruitt approach, one can also use tabular K_c -values. The tables 2-4 and 2-5 list monthly K_c -values for a few crops under Dutch conditions. Table 2-4 gives crop factors to be used in combination with open water evaporation (reference surface = water).

The aerodynamic term in the Penman formula is badly defined. Therefore, more simple but empirical approaches are often used (Makkink, 1957; Priestly and Taylor, 1972). When using the Makkink formula for calculating ET_0 of a grass reference surface, the K_c -factors as reported in Table 2-5 should be used.

2.4.4 ESTIMATION OF THE POTENTIAL TRANSPERSION AND EVAPORATION

The potential transpiration and evaporation are obtained by splitting the potential crop evapotranspiration, using the LAI as division parameter:

$$E_p = f \cdot e^{-c \cdot LAI} \cdot ET_{crop}$$

$$T_p = ET_{crop} - E_p - \frac{\text{CanStor}}{1\text{day}} \quad (2-62)$$

where E_p is the potential soil evaporation (mm day^{-1}); T_p is the potential crop transpiration (mm day^{-1}); ET_{crop} is the potential evapotranspiration (mm day^{-1}); CanStor, the amount of water which has been intercepted and is now released from the crop canopy (mm), and f , c are crop specific parameters (-). In the WAVE-model, the f is set fixed to 1 and c equal to 0.6. Eq. (2-62) implies that, if interception has occurred during the previous day, this water is allowed to evaporate fully during the current day. Furthermore, transpiration only starts after all intercepted water has been evaporated. The sum of soil evaporation, evaporated interception water and transpiration can of course not exceed the ET_{crop} .

2.4.5 DESCRIPTION OF THE ROOT WATER UPTAKE

Water uptake by roots is the result of a complex process which is controlled by soil, plant and atmospheric conditions. To simplify the description of the root water uptake, Feddes et al. (1978) introduced the maximal root water uptake rate as a function of depth $S_{max}(z)$ (day^{-1}). In the WAVE-model the relation $S_{max}(z)$ with depth is input. Note that this relation summarizes the influence of both crop and soil on root water uptake. A compilation of literature data for the $S_{max}(z)$ functions, for cereals and grass, is given by Diels (1994), and is depicted in the Figs. 2-7 and 2-8.

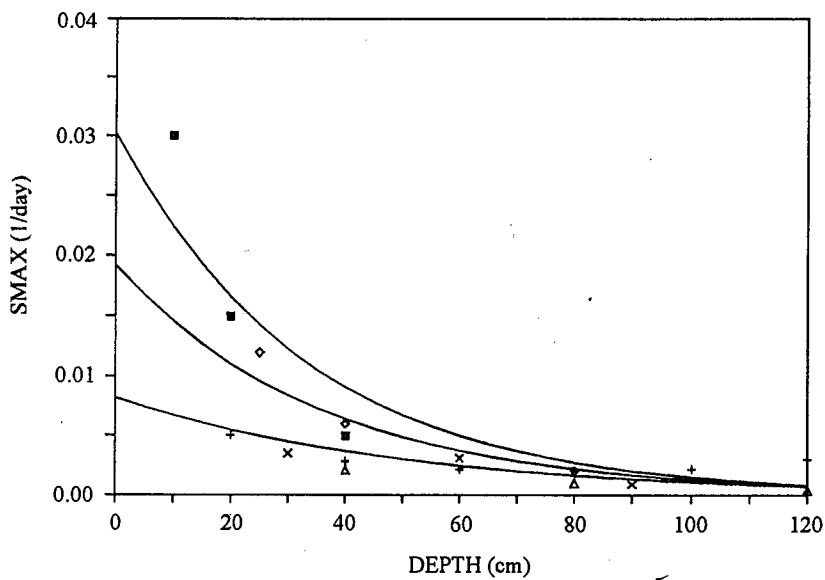


Fig.2-7: Maximum root extraction rates for cereals as a function of depth. The symbols represent literature data from field experiments with wheat (□ from Ehlers (1976); + from Gregory et al.(1978); ◇ from Strelbel(1978)) and barley (x from Maulé and Chanasyk (1986); Δ from McGowan et al.(1980)). The solid lines represent extreme curves and a reference curve halfway between both extreme curves

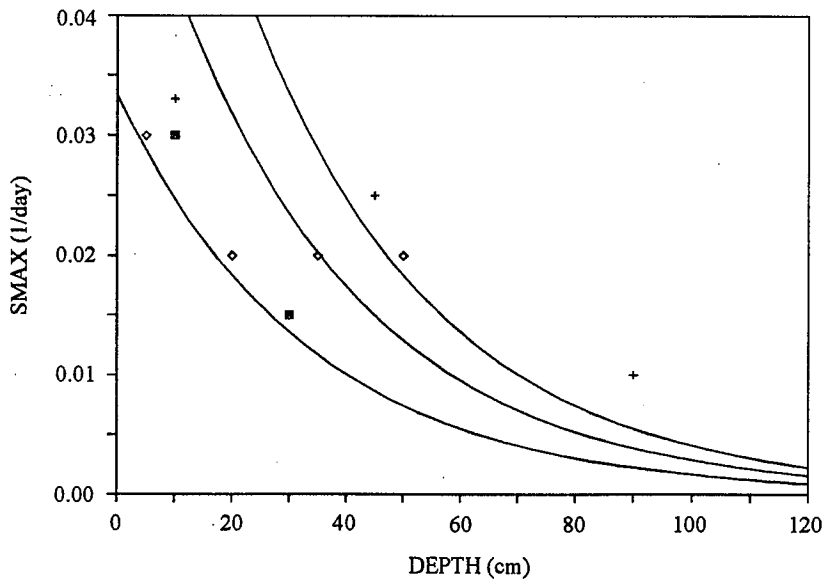


Fig2-8: Maximum root extraction rate for grass as a function of depth. The symbols represent literature data from laboratory experiments (□ from Belmans (1979); ◇ tropical grass data from Badji (1984)) and a field experiment (+ from Flühler et al.(1975)). The solid lines represent extreme curves and a reference curve halfway between both extreme curves



As can be observed from the Figs.2-7 and 2-8, an exponential or linear function could be adopted to describe $S_{\max}(z)$. In the WAVE-model, the linear function is available :

$$S_{\max}(z) = A - Bz \quad (2-63)$$

where A (day^{-1}), and B ($\text{day}^{-1} \text{mm}^{-1}$) are model input parameters. Alternatively one can input S_{\max} -values for each soil compartment separately.

Water uptake is strongly reduced at high pressure head values, near saturation, due to anaerobiosis, and at low pressure heads, due to moisture stress. This phenomenon is described in the WAVE-model by specifying the dimensionless reduction function $\alpha(h)$, which reduces the maximum extraction rate according:

$$S(z, h) = \alpha(h) S_{\max}(z) \quad (2-64)$$

The $\alpha(h)$ in the WAVE-model is characterized by the pressure head values h_0 , h_1 , h_2 , and h_3 (cm) (Fig.2-9). When the pressure head in the soil exceeds h_0 (near saturation), water uptake ceases due to lack of oxygen in the root system. Between, h_1 and h_2 , water uptake is optimal ($\alpha=1$). Below h_3 , water uptake stops due to drought stress. The $\alpha(h)$ -function between h_2 and h_3 can be selected to be linear or hyperbolic. The parameters h_2 and h_3 are less sensitive if drainage calculations are of concern (Diels, 1994). The wilting point value ($h_3 = -16000 \text{ cm}$, $pF = 4.2$) is often taken as a lower limit for the $\alpha(h)$ curve, while h_2 often is set equal to -500 cm . The values of h_0 and h_1 , reflecting anaerobiosis, should be selected with caution. Bakker et al. (1987) presented O_2 -diffusion coefficients of different soils at different air contents. Minimal air contents necessary for a minimal oxygen diffusion ranged between $0.03-0.10 \text{ m}^3 \text{ m}^{-3}$. This corresponds to pressure head values ranging between 20 and 200 cm. The h_0 , and h_1 values should be selected in these ranges.

The $\alpha(h)$ -factor which expresses the effect of pressure head on the root water uptake, is insufficient to describe actual root water uptake. It is still necessary to specify at which depths water will be extracted. Several experiments have shown that water is preferentially extracted near the soil surface. Only when moisture stress occurs is water extracted at larger depths. In the root extraction model of Hoogland et al. (1980) a similar process is mimicked by integrating the root water uptake term from the soil surface to an increasing depth z less or equal to the rooting depth L_r , until the integral becomes equal to the potential transpiration rate. If the integration over the complete rooting depth is insufficient to explain the potential transpiration rate, water stress is considered to occur and the actual transpiration rate is set equal to the integral of $S(h,z)$ over the rooting depth. This concept is written as:

$$T_a = \int_0^{z=L_r} S(h, z) dz \leq T_p \quad (2-65)$$



where T_a is the actual transpiration rate (mm day^{-1}); T_p is the potential transpiration rate (mm day^{-1}); and L_r is the rooting depth (mm). Finally, the root water uptake in each soil compartment is accounted for in the soil water flow equation by adding Eq.(2-64) to the right hand side of the flow equation.

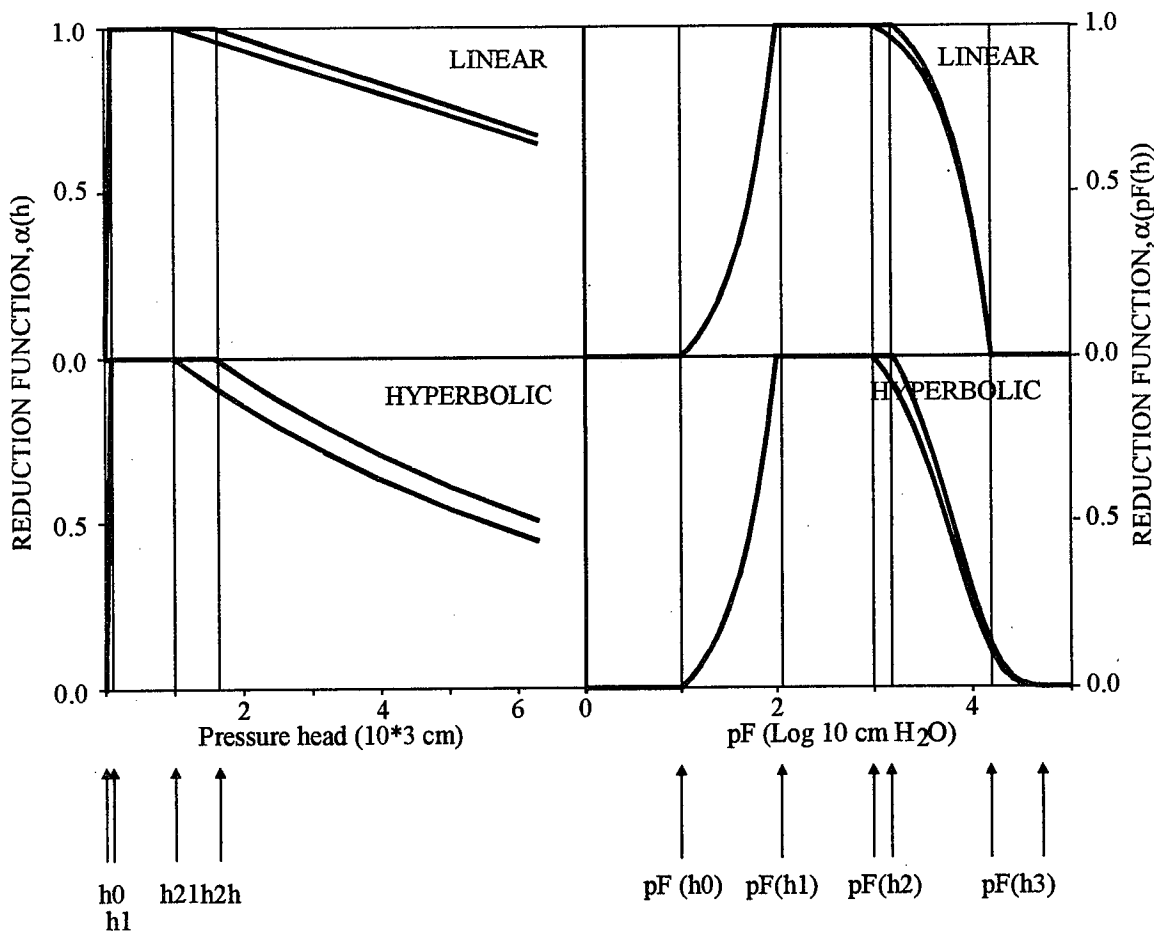


Fig. 2-9: General shape of the dimensionless sink term variable α expressed in terms of pressure head (left) and pF (right). Both a linear (top) and hyperbolic (bottom) decrease of $\alpha(h)$ below the threshold pressure head h_2 are depicted. Curve 1 and 2 are the curves for low and high atmospheric demand, respectively. h_0 : threshold pressure head (cm) above which uptake ceases due to anaerobiosis; h_1 : threshold pressure head below which water uptake is not reduced; h_{2l} : threshold pressure head below which water uptake decreases (linearly or hyperbolically) for low atmospheric demand; h_{2h} : threshold pressure head below which water uptake decrease (linearly or hyperbolically) for high atmospheric demand; h_3 : threshold pressure head below which water uptake ceases due to wilting



Effects of root senescence or severe moisture stress on root water uptake, is simulated in the WAVE-model by specifying an inactivity zone near the surface where the root water uptake is set equal to zero. The date when the roots start to show inactivity and a date when maximum inactivity is reached, is input. In between these dates, the inactivity zone expands linearly with depth, from 0 until a specified depth.

2.5 REFERENCES

- Badji, M., 1984. Utilisation de l'eau du sol par une culture (*Brachiaria Ruziziensis*) en conditions climatiques semi-arides. Analyse expérimentale et simulation numérique. Ph.D. Dissertation, Fac. Agric. Sciences, K.U.Leuven, 157 pp.
- Bakker, J.W., F.R. Boone and P. Boekel, 1987. Diffusie van gassen in de grond en zuurstof diffusiecoëfficiënten in Nederlands akkerbouwgronden. Report 20, ICW, Wageningen, The Netherlands, 44 pp.
- Belmans, C., 1979. Waterstroming in het systeem bodem-plant-atmosfeer: benadering door middel van simulatie. Ph.D. Dissertation, Fac. Agric. Sciences, K.U.Leuven.
- Brooks, R.H. and A.T. Corey, 1964. Hydraulic properties of porous media. Hydrology paper 3, Colorado State University, Fort Collins, Colorado. 27 pp.
- Carnahan, B., H.A. Luther and J.O. Wilkes, 1969. Applied numerical methods. John Wiley and Sons, 604 pp.
- Childs, E.C., 1969. The physical basis of soil water phenomena. Wiley Intersciences, New York.
- Diels, J., 1994. A validation procedure accounting for model input uncertainty: methodology and application to the SWATRER model. Ph.D. Dissertation, Fac. Agric. and Appl. Biol. Sciences, K.U.Leuven, 173 pp.
- Doorenbos, J. and W.O. Pruitt, 1977. Crop water requirements. FAO, Irrigation and drainage paper 24, Rome, Italy.
- Durner, W., 1994. Hydraulic conductivity estimation for soils with heterogeneous pore structure. *Water Res. Res.*, 30(2): 211-223.
- Ehlers, W., 1976. Evapotranspiration and drainage in tilled and untilled loess soil with winter wheat and sugar beet. *Z. Acker- und Pflanzenbau*, 142:285-303.



Ernst, L.F and R.A. Feddes, 1979. Invloed van grondwateronttrekking van beregening en drainwater op de grondwaterstand. Inst. Land and Water Manag. Res. (I.C.W.), Simulation Monographs, PUDOC, Wageningen, The Netherlands, 189 pp.

Feddes, R.A., 1987. Crop factors in relation to Makkink reference crop evapotranspiration. In: J.C. Hooghart (ed.) 'Evaporation and weather'. TNO, Committee on Hydrological Research, nr. 39, The Netherlands.

Feddes, R.A., P.J. Kowalik and H. Zaradny, 1978. Simulation of field water use and crop yield. Simulation Monographs, PUDOC, Wageningen, The Netherlands. 189 pp.

Flühler, H., F. Richard, K. Thalman and F. Borer, 1975. Einfluss der Saugspannung auf den Wasserentzug die Wurzeln einer Grasvegetation. Z. Pflanzenern. Bodenk., 6:583-593.

Gardner, W., 1958. Some steady state solutions of the unsaturated moisture flow equation with application to evaporation from a water table. Soil Sci., 85:228-232.

Gerke, H.H and M.Th. van Genuchten, 1993. A dual-porosity model for simulating the preferential movement of water and solutes in structured porous media. Water Res. Res., 29:305-319.

Gilham, R.W., A. Klute and D.F. Herrmann, 1976. Hydraulic properties of a porous medium. Measurements and empirical representations. Soil Sci. Soc. of Am. J., 40:203-207.

Gregory, P.J., M. McGowan and P.V. Biscoe, 1978. Water relations of winter wheat. 2. Soil water relations. J. Agric. Sci. Camb., 91:103-116.

Haines, W.B., 1930. Studies in the physical properties of soils. The hysteresis effect in capillary properties and the modes of moisture distribution associated therewith. J. Agr. Sci., 20:97-116.

Haverkamp, R., M. Vauclin, J. Touma, P.J. Wierenga and G. Vachaud, 1977. A comparison of numerical simulation models for one-dimensional infiltration. Soil Sci. Soc. of Am. Proc., 41:285-294.

Hoogland, J.C., C. Belmans and R.A. Feddes, 1980. Root water uptake model depending on soil water pressure head and maximum extraction rate. Acta Hortic., 119:123-136.

Huwe, B. and R. Van der Ploeg, 1988. Modelle zur Simulation des Stickstoffhaushaltes von Standorten mit Unterschiedlicher Landwirtschaftlicher Nutzung. Eigenverlag des Instituts für Wasserbau der Universität Stuttgart, Heft 69, 213 pp.



Jones, M.J. and K.K. Watson, 1987. Effect of soil water hysteresis on solute movement during intermittent leaching. *Water Res. Res.*, 23(7):1251-1256.

Jury, W.A., W.R. Gardner and W.H. Gardner, 1991. *Soil Physics*. Fifth Edition, John Wiley and Sons, Inc., 328 pp.

Kool, J.B. and J.C. Parker, 1987. Development and evaluation of closed-form expressions for hysteretic soil hydraulic properties. *Water Res. Res.*, 23(1):105-114.

Makkink, G.F, 1957. Testing the Penman formula by means of lysimeters. *J. Int. of Water Eng.*, 11:277-288.

Maulé, C.P., and D.S. Chanasyk, 1987. A comparison of two methods for determining the evapotranspiration and drainage components of the soil water balance. *Can. J. Soil Sci.*, 67: 43-54.

McGowan, M. and J.B. Williams, 1980. The water balance of an agricultural catchment. 1. Estimation of evaporation from soil water records. *J. of Soil Sci.*, 31:218-230.

Mualem, Y., 1974. A conceptual model of hysteresis. *Water Res. Res.*, 10(3):514-520.

Mualem, Y., 1976. A new model for predicting the hydraulic conductivity of unsaturated porous media. *Water Res. Res.*, 12(3):513-522.

Mualem, Y., 1977. Extension of the similarity hypothesis used for modeling the soil water characteristics. *Water Res. Res.*, 13(4):773-780.

Néel, L., 1942-1943. Théories des lois d'aimantation de Lord Raileigh. *Cah. Phys.*, 12- 13 :19-30.

Philip, J., 1957. The theory of infiltration: The infiltration equation and its solution. *Soil Sci.*, 83:345-357.

Priestly, C.H.B. and R.J.Taylor, 1972. On the assessment of the surfaces of heat flux and evaporation using large scale parameters. *Month. Weth. Rev.*, 100:81-92.

Raes, D., P. van Aelst and G. Wyseure, 1986. Etref, etcrop, etsplit and deficit. Reference manual, Soil and Water Engng. Lab., K.U.Leuven, Belgium. 109 pp.

Remson, I., G.M. Hornberger and F.J. Molz, 1978. *Numerical methods in subsurface hydrology*. Wiley Interscience, New York. 389 pp.

Richards, 1931. Capillary conduction of liquid through porous medium. *Physics*, 1:318-333.



Russo, D., W.A. Jury and G.L. Butters, 1989. Numerical analysis of solute transport during transient irrigation. 1. The effect of hysteresis and profile heterogeneity. *Water Res. Res.*, 25(10):2109-2118.

Scott, P.S., G.J. Farquhar and N. Kouwen, 1983. Hysteretic effects on net infiltration. *Adv. in Infiltration*, 11-883, ASAE St.-Joseph, Michigan, 163-170.

Tietje, O. and M. Tapkenhinrichs, 1993. Evaluation of pedo-transfer functions. *Soil Sci. Soc. of Am. J.*, 57:1088-1095.

van Genuchten, M.Th., 1980. A closed-form equation for predicting the hydraulic conductivity of soil. *Soil Sci. Soc. of Am. J.*, 44:892-898.

van Genuchten, M.Th., 1991. The RETC-code for quantifying the hydraulic functions of unsaturated soils. EPA/600/2-91/065, 83 pp.

van Genuchten, M.Th. and D.R. Nielsen, 1985. On describing and predicting the hydraulic properties of unsaturated soils. *Annales Geophysicae*, 3(5):615-628.

Vauclin, M., R. Haverkamp and G. Vachaud, 1979. Résolution numérique d'une équation de diffusion non-linéaire. Application à l'infiltration de l'eau dans les sols non-saturés. Presses Universitaires de Grenoble, Grenoble, 183 pp.

Vereecken, H., J. Diels, J. van Orshoven, J. Bouma and J. Feyen, 1992. Functional evaluation of pedo-transfer functions for the estimation of soil hydraulic properties. *Soil Sci. Soc. of Am. J.*, 56:1371-1378.

Vereecken, H., J. Maes and J. Feyen, 1990. Estimating unsaturated hydraulic conductivity from easily measured soil properties. *Soil Sci.*, 149(1):1-12.

Vereecken, H., J. Maes, J. Feyen, and P. Darius, 1989. Estimating the soil moisture retention characteristic from texture, bulk density and carbon content. *Soil Sci.*, 148(6):389-403.

Viaene, P., H. Vereecken, J. Diels and J. Feyen, 1994. A statistical analysis of six hysteresis models for moisture retention characteristic. *Soil Sci.* 157(6): 345-353.

Wind, G.P., 1955. Field experiment concerning capillary rise of moisture in heavy clay. *Neth. J. of Agr. Sci.*, 3:60-69.

THE SOLUTE
TRANSPORT MODULE



3 THE SOLUTE TRANSPORT MODULE

3.1 INTRODUCTION

The water transport in soils imposes a convective motion on solutes. Local variations in water flow velocity, induces dispersion of the solute plume during transport. Chemical diffusion, induced by concentration gradients, causes a similar effect. Chemical and physical interactions between solute and soil matrix can retard the overall solute transport. The transfer of solutes is further dispersed by plant uptake and biological transformations. Those processes in turn are strongly controlled by soil temperature and moisture. As a consequence, the transfer of solutes in the soil system is a highly variable and unsteady process.

Before discussing the processes controlling the transfer of solutes in soils, it is relevant to define what is meant by a solute in this context. A solution is a mixture of water and constituents of various chemical composition, which are partially or completely soluble in the soil water phase (De Marsily, 1986). Components in the water phase are normally ionized in proportion to the ionic charge of the element. However, dissolved substances can also be present in an electrically neutral chemical form or aggregated with other molecules and/or ions to form complex substances. Furthermore, it has been observed that salts, considered to be insoluble, can move in a dissolved state as tracers. In the same way, constituents in the form of large molecular aggregates such as colloids, might be present in the soil and move with the liquid phase. All the substances which, in one way or another form part of the soil fluidum, are known as soil solutes as long as they are not part of a mobile phase distinct from the transporting fluid. For many chemical substances on the other hand, a complete mixture with the soil water system does not exist. As such, the transport of many organics is closely related to multiphase flow. In this case processes like volatility, immiscibility and hydrofobicity may complicate the description of the fate of the chemical compound.

The transport of a decaying and sorbing solute in field soils is described numerically with the solute transport module of the WAVE-model. The included solute transport equation is defined in a macroscopic way, indicating that the state variables (e.g. solute concentration) and material characteristics (e.g. soil transport volume) are defined as averages over a Representative Elementary Volume (REV) (Bear, 1972). The developed solute transport model is referred to as the two component or two region convection dispersion model. The model assumes the existence of immobile or stagnant soil water regions, situated at the intra-aggregate or dead end pores and mobile soil water regions. When considering two regions, no complete mixing of the solute in the soil water phase is assumed but rather a solute exchange, which is diffusion limited, controls solute exchange between both soil regions. Transport in the two component medium is described with a couple of equations. For the mobile soil region the convection-dispersion equation holds. In both regions adsorption is assumed to occur reversibly and linearly.



Although the theoretical framework for describing the solute transport phenomena at field scale is still in development, a deterministic point model like the two component model which is developed at the laboratory scale, can be used with variable success to describe solute transport under field conditions.

3.2 THE SOIL SOLUTE TRANSPORT EQUATION

Figure 3-1 illustrates the conceptualisation of the soil system when developing the solute transport equation. Distinction is made between the soil volume occupied by air, the mobile soil water region, the immobile soil water region, the static soil complex defined as the soil complex with adsorption sites in contact with the immobile soil region and the dynamic soil complex with sorption sites in contact with the mobile soil region.

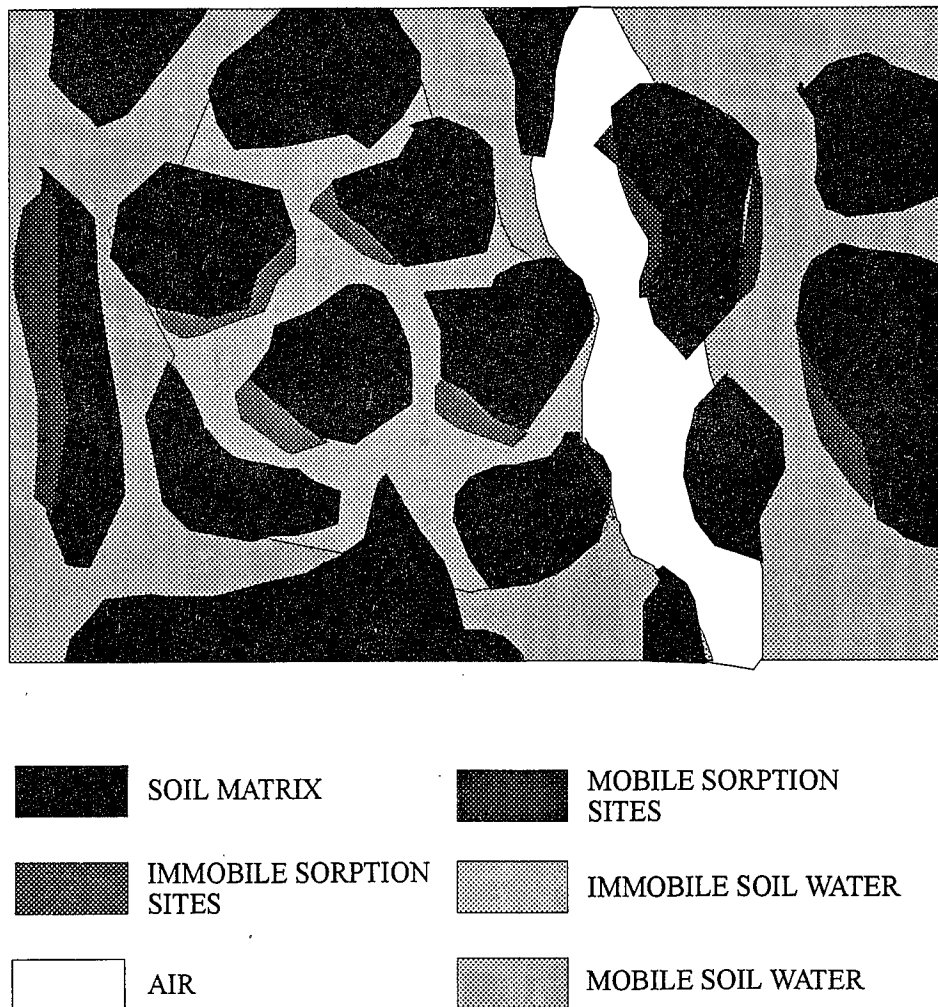


Fig. 3-1: Conceptualisation of the soil system (source: van Genuchten and Wierenga, 1976)



First the solute transport in the mobile soil region is discussed. Transport of solute in the mobile soil region is determined by chemical diffusion, convection and hydrodynamic dispersion. The term diffusion refers to the movement of solute as a result of Brownian motion. The thermal energy causes the particles to move randomly in the phase that contains them. Given a mass of solute in a stagnant water reservoir, then the diffusion flux in water q_{dl} ($\text{kg m}^{-2} \text{ day}^{-1}$) can be defined as the (macroscopic) solute mass going through a unit area across the water reservoir per unit of time. Fick's first law can be used to relate solute flux and concentration gradient:

$$q_{dl} = -Dif \frac{\partial C_m}{\partial x} \quad (3-1)$$

where C is the soil solute concentration (kg m^{-3}); x is the space co-ordinate (m); and Dif is the chemical diffusion coefficient of the considered solute in pure water ($\text{m}^2 \text{ day}^{-1}$). When solute moves by diffusion in the water phase of the soil, the cross sectional area available for diffusion is only a fraction of the total cross sectional area. Due to the tortuous nature of the pores, the diffusion process results in a slower macroscopic vertical spreading than in a pure water system. For this reason an effective diffusion coefficient, $[De (< Dif)] (\text{m}^2 \text{ day}^{-1})$, which depends on the mobile soil water content, θ_m ($\text{m}^3 \text{ m}^{-3}$), is used to describe diffusive solute transport in the mobile soil region:

$$q_{ds} = -De \cdot \theta_m \cdot \frac{\partial C_m}{\partial x} \quad (3-2)$$

where q_{ds} is the diffusional solute flux in the soil mobile region ($\text{kg m}^{-2} \text{ day}^{-1}$).

The value of De can be estimated by the equation of Kemper and Van Schaik (1966):

$$De = \frac{Dif \cdot a \cdot e^{b \cdot \theta_m}}{\theta_m} \quad (3-3)$$

where a and b are empirical constants reported to be approximately $b = 10$ and $0.005 < a < 0.01$ (Olsen and Kemper, 1968). The chemical diffusion coefficient in pure water, Dif , and the parameters a and b are model input.

The term convection refers to the phenomenon where dissolved substances are carried along by the movement of water. Solutes that are carried by the moving water are said to undergo convective, viscous, or mass flow. As such, mass flow is perfectly related to the law determining the transport of water and which was described in a previous chapter of this reference manual. Hence, the convective solute flux going through a unit area equals:



$$q_{cw} = C_m \cdot \theta_m \cdot V_m = C_m \cdot q_w \quad (3-4)$$

where q_{cw} is the convective solute flux density ($\text{kg m}^{-2} \text{ day}^{-1}$) imposed by the convective water flow; q_w is the Darcian water flux ($\text{m}^3 \text{ m}^{-2} \text{ day}^{-1}$); V_m is the average macroscopic pore water velocity (m day^{-1}); and C_m is the solute concentration in the mobile soil region (kg m^{-3}). Owing to the porous nature of the soil, the microscopic pore velocity in the mobile soil region is not equal to macroscopic pore water velocity. The microscopic pore velocity is distributed around the average macroscopic value, in a manner that depends on the pore size and shape. Flow in larger pores is faster than in the small ones and is much faster at the center of a pore than near the periphery. In this way the complexity of the pore system causes mixing of the soil solution along the flow direction, and hence dispersion of the solute. This phenomenon, often referred to as mechanical dispersion is induced by randomly distributed pore velocities and results in a net flow of solute proportional to the velocity. On the basis of the assumption of randomness, one can describe mechanical dispersion in a similar way as chemical diffusion using Fick's law with the diffusion coefficient D_e or D_f replaced by a mechanical dispersion coefficient, denoted D_m ($\text{m}^2 \text{ day}^{-1}$). The latter is assumed to be proportional to the effective average macroscopic pore water velocity:

$$D_m = \lambda \cdot V_m \quad (3-5)$$

where λ (m) is the soil solute dispersivity.

The total macroscopic convective transport of a solute in the mobile soil region is described commonly with an equation that takes into account two modes or components of transport: (i) the average flow velocity component (given by Eq. (3-4)) and (ii) the mechanical dispersion component (Fick's law with D_m). Adding the two components together yields the total convective flux equation, q_{ct} ($\text{kg m}^{-2} \text{ day}^{-1}$):

$$q_{ct} = \theta_m \cdot C_m \cdot V_m + \theta_m \cdot \lambda \cdot V_m \cdot \frac{\partial C_m}{\partial x} \quad (3-6)$$

By adding the diffusive flux (Eq.(3-2)) to the convective flux (Eq.(3-6)), a relation is obtained for the total solute flux travelling along the mobile soil region, q_{tm} ($\text{kg m}^{-2} \text{ day}^{-1}$):

$$q_{tm} = q_{ds} + q_{ct} = -\theta_m \cdot (D_e + D_m) \frac{\partial C_m}{\partial x} + V_m \cdot \theta_m \cdot C_m \quad (3-7)$$

At high flow velocities, or when considerable heterogeneity occurs, the dispersion term is much larger than the diffusion term and Eq.(3-7) simplifies to:

$$q_{tm} = -\theta_m \cdot D_m \cdot \frac{\partial C_m}{\partial x} + V_m \cdot \theta_m \cdot C_m \quad (3-8)$$



where D_m^* is the apparent diffusion coefficient in the mobile soil region ($m^2 \text{ day}^{-1}$). Table 3-1 reports on literature values for pore water velocities, apparent dispersion coefficients, dispersivities, and mobile water contents for undisturbed partially saturated soil.

When a solute is adsorbed, then the total solute mass in a unit soil volume equals the sum of the mass dissolved in the soil solution phase and the mass adsorbed on the soil complex. Both are related according to the equation:

$$C_{tm} = f \cdot \rho \cdot C_{sm} + \theta_m \cdot C_m \quad (3-9)$$

where C_{tm} is the total solute mass in the mobile region (kg solute m^{-3} dry soil); C_{sm} is the adsorbed solute mass on the soil complex (kg kg^{-1} dry soil); ρ is the soil bulk density (kg m^{-3}); and f is the fraction of the adsorption sites situated in contact with the mobile soil region (-). For linear and reversible adsorbing species, the distribution constant is used to relate solute in the soil solution and on the sorption sites or:

$$C_{sm} = k_d \cdot C_m \quad (3-10)$$

where k_d is the solute distribution constant ($\text{m}^3 \text{ kg}^{-1}$). Hence Eq. (3-9) simplifies to:

$$C_{tm} = C_m \cdot (\theta_m + f \cdot \rho \cdot k_d) \quad (3-11)$$

The parameters f , k_d and ρ are model input. Reasonable simulations can be obtained if all sorption sites are assumed to be situated in the mobile soil region ($f = 1$). The distribution constants k_d can be derived from batch sorption experiments or the analysis of breakthrough curve data. The latter method should be preferred, since it enables to identify retardation parameters on undisturbed, scale independent, soil samples. For pesticides, the k_{oc} approach is often used. If this is the case, the k_d value is obtained by multiplying k_{oc} with the fraction of organic carbon.

So far, no interaction between the mobile and the immobile soil region was considered. If however diffusion between both soil regions occur, then this diffusion solute flux, q_{fl} ($\text{kg m}^{-3} \text{ day}^{-1}$) is proportional to the solute concentration difference:

$$q_{fl} = \alpha^* \cdot (C_m - C_{im}) \quad (3-12)$$

where α^* is an empirical transfer coefficient (day^{-1}); and C_{im} is the solute concentration in the immobile soil region (kg m^{-3} solution).

Table 3-1: Literature review of solute transport parameters. Values between brackets represent possible ranges (source: Beven et al., 1993)

Soil type	Vm (cm h ⁻¹)	D _m * (cm ² h ⁻¹)	λ (m)	$\theta m/\theta (-)$	Experimental details
Silt loam	1.52	1.404			Core, 4 replicates
Silt loam, medium sand, sub-angular blocky	0.0417	4.17			Core, 10 replicates
Clay loam/Prismatic	0.0417	0.417			Core, 10 replicates
Loam to silty loam	2.3 (0.6-5.8)	24.0 (1.2-102.8)	0.077 (0.01-0.218)		Core, 4 replicates
Clay loam	2.709 (1.7-4.1)- 0.225 0.171	4.04 (1.65-6.44) 5.642 3.367	150.6 0.251 0.197		Core, 5 replicates
Clay loam	2.941 (0.74-6.34)	23.0 (2.55-75.5)	0.06 (0.03-0.14)	0.41	Core, 18 replicates
Silty clay loam to sandy loam	1.409 (0.77-1.76)	0.230 (0.06-0.57)			Core, 6 replicates, grass soil
Silty clay loam to sandy loam	52.4 (46.7-57.6)	5.55 (2.72-7.58)		0.38 (0.32-0.58)	Core, 6 replicates, forest soil
Silty clay loam	3.04	160.4	0.526	0.68	Core, 1 replicate, (0.073 m ² diameter, 30 m length)
Silty clay loam	1.52	54.2	0.357	0.95	Core, 1 replicate (0.073 m ² , 30 m length)
Silty clay loam	0.76	18.6	0.243	1.0	Core, 1 replicate (0.073 m ² , 30 m length)
Silty clay loam	3.04	370	1.217	0.61	Core, 1 replicate (0.073 m ² , 55 m length, upward flux)
Silty clay loam	1.53	31.5	0.206	0.44	Core, 1 replicate (0.073 m ² , 55 m length, upward flux)
Silty clay loam	0.76	15.5	0.203	0.33	Core, 1 replicate (0.073 m ² , 55 m length, upward flux)
Silty clay loam	0.76	13.5	0.177	0.42	Core, 1 replicate (0.073 m ² , 55 m length, downward flux)
Silty clay loam	0.38	8.4	0.220	0.47	Core, 1 replicate (0.073 m ² , 55 m length, downward flux)
Loamy fine sand	1.01 (0.18-2.22)	20.9 (3.9-46.2)	0.0087(0.0077-0.0094)		Core, several replicates (0.002 diameter, 0.3 m length)
Loamy fine sand	0.08	2.71	34.		Core, 1 replicate (0.70 m diameter, 6 m length)
	1.826 (0.008-15.28)	8.776 (0.35-66.5)	0.055 (0.02-0.26)		Field, 42.3 m ² , up to 1.824 m depth
Clay, silty clay	0.1625 (0.130-0.218)	1.531 (0.93-3.54)	0.094 (0.04-2.72)		Field, 64 m ² , 0.75 m depth
Silty clay loam, silt	0.290 (0.197-0.367)	16.14 (6.5-47.9)	0.524 (0.21-1.41)		Field, 37.2 m ² , 3.0 m depth, water applied semi-weekly
Silty clay loam, silt	0.293 (0.162-0.533)	21.76 (1.56-108.)	0.445 (0.09-0.95)		Field, 37.2 m ² , 3.0 m depth, water applied bi-weekly
Sandy loam, regosol	0.0163	0.060	0.039		Field, 94 m ² , 3.0 m depth, Bromide as tracer
Sandy loam, regosol	0.022	0.047	0.021		Field, 94 m ² , 3.0 m depth, Chloride as tracer
Sandy loam	0.146 (0.071-0.46)	2.229 (1.13-6.67)	0.165 (0.14-0.21)		Field, 446.5 m ² , 2.7 m depth
Silty clay loam, silt	5.00 (4.38-5.75)	88.90 (79.2-99.9)	0.178 (0.14-0.23)		Field, 3.35 m ² , 3.0 m depth
Silty clay loam, silt	4.75 (0.42-29.92)	149.6 (1.9-920.)	0.288 (0.05-0.66)		Field, 3.35 m ² , 3.0 m depth
Loamy sand	0.146 (0.117-0.179)	2.488 (1.31-3.00)	0.197 (0.17-0.26)		Field, 0.64 ha, 1.2-1.8 m depth
Loam, loamy sand			0.102		Field scale



The continuity equation for the solute in the soil mobile region, for an infinitesimal small volume of soil is written as:

$$\frac{\partial C_{tm}}{\partial t} = \frac{\partial q_{tm}}{\partial x} + q_f \quad (3-13)$$

In combination with Eqs. (3-8, 3-11, 3-12), Eq. (3-13) reduces to the solute transport equation for the mobile soil region:

$$\frac{\partial(\theta_m C_m)}{\partial t} + \frac{\partial(f \cdot \rho \cdot k_d \cdot C_m)}{\partial x} = \frac{\partial}{\partial x} \left(\theta_m \cdot D_m^* \frac{\partial C_m}{\partial x} \right) - \frac{\partial(q_w \cdot C_m)}{\partial x} + \alpha^* \cdot (C_m - C_{im}) \quad (3-14)$$

Similarly, mass conservation in the immobile soil region yields:

$$\frac{\partial(\theta_{im} \cdot C_{im})}{\partial t} + (1-f) \cdot \rho \cdot k_d \frac{\partial C_{im}}{\partial t} = -\alpha^* \cdot (C_m - C_{im}) \quad (3-15)$$

When no immobile water is present, then Eq.(3-14) simplifies to the classical convection dispersion equation (Warrick et al., 1971; Bresler, 1972).

3.3 NUMERICAL SOLUTION OF THE SOLUTE TRANSPORT EQUATION

3.3.1 THE SOLUTION PROCEDURE

In order to solve Eqs. (3-14) and (3-15) by finite difference technique, the same time and space discretisation as for the water flow equation is adopted. The following parameters and state variables are initialised for each soil compartment: the soil moisture content (θ); the soil pore water velocity (V_m); the soil bulk density (ρ); the chemical diffusion parameters (Dif, a, b); the hydrodynamic dispersivity (λ); the ratio mobile versus total moisture content (θ_m/θ); the transfer coefficient between the mobile and the immobile soil region (α^*); the mass distribution coefficient (k_d) and the fraction of the sorption sites in the mobile or immobile soil region (f).

The solute transport equations (Eqs.(3-14) and (3-15)) are expanded in finite difference formulations. To ensure convergence and to minimise numerical dispersion, a Crank Nicolson numerical scheme is used to solve the transport equation in the mobile soil region. Second order terms are included in the discretisation scheme. Full details of the discretization scheme are given in [Tillotson et al. (1980)]. Expanding the first term of Eq. (3-14) yields:



$$\left(\frac{\theta_{m_i}^{j+1} C_{m_i}^{j+1} - \theta_{m_i}^j C_{m_i}^j}{\Delta t} \right) - \left(\frac{\Delta t V_{m_i}^{j+1/2} (\theta_{m_i}^{j+1} - \theta_{m_i}^j)}{16 \Delta x^2} \right) * \\ \begin{cases} V_{m_{i-1/2}}^{j+1/2} (C_{m_{i-1}}^{j+1} + C_{m_{i-1}}^j - C_{m_i}^{j+1} - C_{m_i}^j) \\ -V_{m_{i+1/2}}^{j+1/2} (C_{m_i}^{j+1} + C_{m_i}^j - C_{m_{i+1}}^{j+1} - C_{m_{i+1}}^j) \end{cases} \quad (3-16)$$

where i denotes the space index from the i -th compartment; and j the time index. The second term of Eq.(3-14), the adsorption term, is discretised as follows:

$$f_i \cdot \rho_i \cdot k d_i \left(\frac{(C_{m_i}^{j+1}) - C_{m_i}^j}{\Delta t} \right) \quad (3-17)$$

The term containing the apparent diffusion coefficient is developed according to:

$$\frac{D_{m_{i-1/2}}^{j+1/2} \cdot \theta_{m_{i-1/2}}^{j+1/2}}{2 \cdot \Delta z^2} (C_{m_{i-1}}^{j+1} + C_{m_{i-1}}^j - C_{m_i}^{j+1} - C_{m_i}^j) - \frac{D_{m_{i+1/2}}^{j+1/2} \cdot \theta_{m_{i+1/2}}^{j+1/2}}{2 \cdot \Delta z^2} (C_{m_i}^{j+1} + C_{m_i}^j - C_{m_{i+1}}^{j+1} - C_{m_{i+1}}^j) \quad (3-18)$$

while expansion of the convection term results in:

$$-\beta_1 \frac{q_{w_{i-1/2}}^{j+1/2}}{2 \Delta x} (C_{m_{i+1}}^j + C_{m_{i-1}}^{j+1}) + \beta_2 \frac{q_{w_{i+1/2}}^{j+1/2}}{2 \Delta x} (C_{m_i}^j + C_{m_i}^{j+1}) \\ -\beta_3 \frac{q_{w_{i+1/2}}^{j+1/2}}{2 \Delta x} (C_{m_{i+1}}^j + C_{m_{i-1}}^{j+1}) + \beta_4 \frac{q_{w_{i-1/2}}^{j+1/2}}{2 \Delta x} (C_{m_i}^j + C_{m_i}^{j+1}) \quad (3-19)$$

If the flux in the i -th compartment is negative, then $\beta_1=1$ and $\beta_4=0$. If, however, this flux is positive, then $\beta_1=0$ and $\beta_4=1$. A positive flux in the $i+1$ -th compartment results in $\beta_3=1$ and $\beta_2=0$; while the opposite results in $\beta_3=0$ and $\beta_2=1$. Defining the following variables:

$$AB_i = \frac{D_{m_{i-1/2}}^{j+1/2} \cdot \theta_{m_{i-1/2}}^{j+1/2}}{2 \Delta x^2} + \frac{\Delta t \cdot V_{m_i}^{j+1/2} \cdot V_{m_{i-1/2}}^{j+1/2} (\theta_{m_i}^{j+1} - \theta_{m_i}^j)}{16 \cdot \Delta x^2} \\ BB_i = \frac{D_{m_{i+1/2}}^{j+1/2} \cdot \theta_{m_{i+1/2}}^{j+1/2}}{2 \Delta x^2} + \frac{\Delta t \cdot V_{m_i}^{j+1/2} \cdot V_{m_{i+1/2}}^{j+1/2} (\theta_{m_i}^{j+1} - \theta_{m_i}^j)}{16 \cdot \Delta x^2} \\ CB_i = \frac{q_{w_{i-1/2}}^{j+1/2}}{2 \cdot \Delta x} \\ DB_i = \frac{q_{w_{i+1/2}}^{j+1/2}}{2 \cdot \Delta x} \quad (3-20)$$

and substituting, yields the finite difference analogue of Eq.(3-14):



$$\begin{aligned}
 & \frac{\theta_{m_i}^{j+1} C_{m_i}^{j+1} - \theta_{m_i}^j C_{m_i}^j}{\Delta t} - AB_i(C_{m_{i-1}}^{j+1} + C_{m_{i-1}}^j - C_{m_i}^{j+1} - C_{m_i}^j) \\
 & + BB_i(C_{m_i}^{j+1} + C_{m_i}^j - C_{m_{i+1}}^{j+1} - C_{m_{i+1}}^j) + f_i \cdot \rho_i \cdot k d_i \left(\frac{C_{m_i}^{j+1} - C_{m_i}^j}{\Delta t} \right) \\
 & = -\beta_1 \cdot CB_i(C_{m_{i-1}}^j + C_{m_{i-1}}^{j+1}) + \beta_2 \cdot DB_i(C_{m_i}^j - C_{m_i}^{j+1}) \\
 & + \beta_3 \cdot DB_i(C_{m_{i+1}}^j + C_{m_{i+1}}^{j+1}) - \beta_4 \cdot CB_i(C_{m_i}^j - C_{m_i}^{j+1}) - \alpha^*(C_{m_i}^j - C_{im_i}^j)
 \end{aligned} \tag{3-21}$$

Rearranging the terms in Eq.(3-21) yields the following equation:

$$AL_i(C_{m_{i-1}}^{j+1} + BL_i(C_{m_i}^{j+1} + CL_i(C_{m_{i+1}}^{j+1})) = DL_i \tag{3-22}$$

where:

$$\begin{aligned}
 AL_i &= -AB_i + \beta_1 \cdot CB_i \\
 BL_i &= \frac{\theta_{m_i}^{j+1}}{\Delta t} + AB_i + BB_i + \frac{f_i \cdot \rho_i (k d_i)}{\Delta t} - \beta_2 \cdot DB_i + \beta_4 \cdot CB_i \\
 CL_i &= -BB_i - \beta_3 \cdot DB_i \\
 DL_i &= C_{m_{i-1}}^j (AB_i - \beta_1 \cdot CB_i) \\
 & + C_{m_i}^j \left(\frac{\theta_{m_i}^{j+1}}{\Delta t} - AB_i - BB_i + \frac{f_i \cdot \rho_i (k d_i)}{\Delta t} + \beta_1 \cdot DB_i - \beta_4 \cdot CB_i \right) \\
 & + C_{m_{i+1}}^j (BB_i + \beta_3 \cdot DB_i) - \alpha^*(C_{m_i}^j - C_{im_i}^j)
 \end{aligned} \tag{3-23}$$

Equation (3-22) is easily derived for each node except for the top and bottom node. Two similar equations are derived when expanding the top and bottom boundary transport equation. For the top node, the following expression holds:

$$BL_1 \cdot C_{m_1}^{j+1} + CL_1 \cdot C_{m_2}^{j+1} = DL_1 \tag{3-24}$$

while for the bottom node the equation yields:

$$AL_n \cdot C_{m_{n-1}}^{j+1} + BL_n \cdot C_{m_n}^{j+1} = DL_n \tag{3-25}$$

So, for n equations with n unknowns, it is possible to obtain the concentration for each node on the j+1-th time step. The unknown vector is found by solving Eqs. (3-22, 3-24, 3-25) simultaneously using the Thomas algorithm (Remson et al., 1978). Writing Eqs. (3-22, 3-24, 3-25) in matrix format yields:



$$\begin{pmatrix} BL_1 & CL_1 \\ AL_2 & BL_2 & CL_2 \\ & AL_3 & BL_3 & CL_3 \\ & & & \end{pmatrix} \begin{pmatrix} C_{m1}^{j+1} \\ C_{m2}^{j+1} \\ C_{m3}^{j+1} \\ \vdots \\ C_{mn-1}^{j+1} \\ C_{mn}^{j+1} \end{pmatrix} = \begin{pmatrix} DL_1 \\ DL_2 \\ DL_3 \\ \vdots \\ DL_{n-1} \\ DL_n \end{pmatrix} \quad (3-26)$$

The coefficient matrix is tri-diagonal. Hence, the unknown vector (C_{m1}^{j+1} , C_{m2}^{j+1} , ..., C_{mn}^{j+1}) can be obtained, using the Thomas algorithm.

In addition to the solution of the transport equation in the mobile soil region, the mass balance equation in the immobile soil region Eq.(3-15) is solved explicitly. Defining g as:

$$g = \theta_{im} + (1-f) \cdot \rho \cdot k_d \quad (3-27)$$

and substituting, reduces Eq.(3-15) to:

$$\frac{\partial(g \cdot C_{im})}{\partial t} = -\alpha^*(C_m - C_{im}) \quad (3-28)$$

Expanding the left-hand side of Eq.(3-28) in a Taylor series and ignoring the higher order terms yields:

$$\frac{\partial(g \cdot C_{im})}{\partial t} = \frac{g \cdot C_{imi}^{j+1} - g \cdot C_{imi}^j}{\Delta t} - \frac{\Delta t \cdot \partial^2(g \cdot C_{im})}{2 \cdot \partial t^2} \quad (3-29)$$

The expansion of the second order term in Eq.(3-29) yields:

$$\frac{\partial^2(g \cdot C_{im})}{\partial t} = \frac{\partial}{\partial t}(-\alpha^*(C_m - C_{im})) = \frac{-\alpha^* \cdot C_{mi}^{j+1} + \alpha^* \cdot C_{mi}^j}{\Delta t} + \frac{\alpha^* \cdot C_{imi}^{j+1} - \alpha^* \cdot C_{imi}^j}{\Delta t} \quad (3-30)$$

Substituting Eq. (3-30) into (3-29) and (3-28) and rearranging, the mass balance equation for the immobile soil region becomes:

$$AG_i \cdot C_{imi}^{j+1} = BG_i \cdot C_{imi}^j + \frac{\alpha^* \cdot C_{mi}^{j+1}}{2} + \frac{\alpha^* \cdot C_{mi}^j}{2} \quad (3-31)$$

where:



$$\begin{aligned} AG_i &= \frac{\theta_{im_i}^{j+1}}{\Delta t} + \frac{(1-f_i) \cdot \rho_i \cdot k_{d_i}}{\Delta t} + \frac{\alpha_i^*}{2} \\ BG_i &= \frac{\theta_{im_i}^j}{\Delta t} + \frac{(1-f_i) \cdot \rho_i \cdot k_{d_i}}{\Delta t} - \frac{\alpha_i^*}{2} \end{aligned} \quad (3-32)$$

Notwithstanding the use of an implicit numerical scheme and keeping second order terms in the finite difference analogue, numerical dispersion influences model calculations. Numerical dispersion increases when the compartment size increases. To quantify the impact of numerical dispersion, the development of a solute plume was calculated with the numerical model, given a pulse type top boundary condition and a steady-state water flow condition. Solute resident concentrations predicted by the model were used to fit an analytical solution of the transport equations through it. The solution proposed by van Genuchten and Alves (1982) was used. The optimised apparent diffusion coefficient was compared with the model input dispersivity times the simulated pore water velocity. This comparison yielded a linear relationship, with a slope close to one and intercept equal to 0.13 times the compartment size. This intercept is a measure of the induced numerical dispersion. A standard correction on the apparent dispersion constant in the WAVE-model has been made according to these results.

3.3.2 DEFINITION OF THE UPPER BOUNDARY CONDITION

To solve the solute transport equation, an additional numerical equation, similar to Eq.(3-21), needs to be defined for the top node. A flux type boundary condition is used to define the top boundary in the WAVE-model.

$$\begin{aligned} J_s &= C_f \cdot q_w \quad \text{for } q_w < 0.0 \quad (\text{infiltration}) \\ J_s &= 0. \quad \text{for } q_w > 0.0 \quad (\text{evaporation}) \end{aligned} \quad (3-33)$$

where C_f equals the solute flux concentration (kg m^{-3}) and J_s the solute mass flux ($\text{kg m}^{-2} \text{s}^{-1}$). To define C_f , an artificial solute mass reservoir is assumed to exist outside the soil profile. When solute is applied (with a fertilisation or irrigation event), it dissolves in the mass of water entering the profile during the day of solute application (or the first day when infiltration occurs). Hence, the solute mass flux J_s is determined by the water flow across the soil surface, filling or depleting the hypothetical reservoir. During infiltration, solute mass enters only the mobile soil region. Assuming zero dispersion in the hypothetical reservoir, the solute concentration at the soil surface is set equal to $C_f = J_s/q_w = C_s$. In case of evaporation, the solute concentration at the soil surface equals zero ($C_f = C_s = 0$). Taking into account above considerations, the finite difference equation for the soil mobile region at the top becomes:



$$\begin{aligned}
 & C_{m_1}^{j+1} \left(\frac{\theta_{m_1}^{j+1}}{\Delta t} + AB_1 + BB_1 + \frac{f_1 \cdot \rho_1 \cdot kd_1}{\Delta t} - \beta_2 \cdot DB_1 + \beta_4 \cdot CB_1 \right) \\
 & + C_{m_2}^{j+1} (-BB_1 - \beta_3 \cdot DB_1) = \\
 & C_s^j (AB_1 - \beta_1 \cdot CB_1) - C_s^{j+1} (AB_1 + \beta_1 \cdot CB_1) \\
 & + C_{m_1}^j \left(\frac{\theta_{m_1}^{j+1}}{\Delta t} - AB_1 - BB_1 + \frac{\rho_1 \cdot kd_1 \cdot f_1}{\Delta t} + \beta_2 \cdot DB_1 - \beta_4 \cdot CB_1 \right) \\
 & + C_{m_2}^j (BB_1 + \beta_3 \cdot DB_1)
 \end{aligned} \tag{3-34}$$

with

$$\begin{aligned}
 AB_1 &= \frac{\Delta t \cdot V_{m_1 i}^{j+1/2} \cdot q_{w_{l-1/2}}^{j+1/2} (\theta_{m_1}^{j+1} - \theta_{m_1}^j)}{16 \cdot \Delta x^2} \\
 BB_1 &= \frac{\Delta t \cdot V_{m_1}^j \cdot V_{m_1+1/2}^{j+1/2} (\theta_{m_1}^{j+1} - \theta_{m_1}^j)}{16 \cdot \Delta x^2} \\
 CB_1 &= \frac{q_{w_{l-1/2}}^{j+1/2}}{2 \cdot \Delta x} \\
 DB_1 &= \frac{q_{w_{l+1/2}}^{j+1/2}}{2 \cdot \Delta x}
 \end{aligned} \tag{3-35}$$

and which can be rearranged to:

$$BL_1 \cdot C_{m_1}^{j+1} + CL_1 \cdot C_{m_2}^{j+1} = DL_1 \tag{3-36}$$

3.3.3 DEFINITION OF THE LOWER BOUNDARY CONDITION

In the WAVE-model, a zero concentration gradient at the bottom of the flow domain is considered:

$$\left. \frac{\partial C_m}{\partial x} \right|_{x=L} = 0 \tag{3-37}$$

In discretised form, the bottom boundary condition definition is defined as:

$$C_{m_{n+1}}^{j+1} = C_{m_n}^{j+1} \tag{3-38}$$

Using Eq.(3-38) the finite difference scheme for the lower boundary node becomes:



$$\begin{aligned}
 & C_{m_n}^{j+1} \left(\frac{\theta_{m_n}^{j+1}}{\Delta t} + AB_n + BB_n + \frac{f_n \cdot \rho_n \cdot kd_n}{\Delta t} - \beta_2 \cdot DB_n - \beta_3 \cdot DB_n + \beta_4 \cdot CB_n \right) \\
 & + C_{m_{n-1}}^{j+1} (-AB_n - \beta_1 \cdot CB_n) = \\
 & + C_{m_n}^j \left(\frac{\theta_{m_n}^{j+1}}{\Delta t} - AB_n - BB_n + \frac{\rho_n \cdot kd_n \cdot f_n}{\Delta t} + (\beta_2 + \beta_3) \cdot DB_n - \beta_4 \cdot CB_n \right) \\
 & + C_{m_{n-1}}^j (AB_n - \beta_1 \cdot CB_n)
 \end{aligned} \tag{3-39}$$

with

$$\begin{aligned}
 AB_n &= \frac{D_{m_{n-1/2}}^{j+1/2} \cdot \theta_{m_{n-1/2}}^{j+1/2}}{2 \Delta x^2} + \frac{\Delta t \cdot V_{m_n}^{j+1/2} \cdot V_{m_{n-1/2}}^{j+1/2} (\theta_{m_n}^{j+1} - \theta_{m_n}^j)}{16 \cdot \Delta x^2} \\
 BB_n &= \frac{\Delta t \cdot V_{m_n}^{j+1/2} \cdot V_{m_{n+1/2}}^{j+1/2} (\theta_{m_n}^{j+1} - \theta_{m_n}^j)}{16 \cdot \Delta x^2} \\
 CB_n &= \frac{q_{w_{n-1/2}}^{j+1/2}}{2 \cdot \Delta x} \\
 DB_n &= \frac{q_{w_{n+1/2}}^{j+1/2}}{2 \cdot \Delta x}
 \end{aligned} \tag{3-40}$$

3.4 REFERENCES

- Bear, J. 1972. Dynamics of fluids in porous media. Elsevier, New York, London, Amsterdam, 764 pp.
- Beven, K.J., D.Ed. Henderson and Alison D. Reeves, 1993. Dispersion parameters for undisturbed partially saturated soil. J. of Hydrol., 143:19-43.
- Bresler, E., 1973. Simultaneous transport of solute and water under transient flow conditions. Water Res. Res., 9(4): 975-986.
- De Marsily, G., 1986. Quantitative hydrogeology. Groundwater hydrology for engineers. Academic Press Inc., 440 pp.
- Kemper, W.D. and J.C. Van Schaik, 1966. Diffusion of salts in clay water systems. Soil Sci. Soc. of Am. Proc., 30:534-540.
- Olsen, S.R. and W.D. Kemper, 1968. Movement of nutrients to plant roots. Advances in Agronomy, 20:91-151.
- Remson, I., G.M. Hornberger and F.J. Molz, 1978. Numerical methods in subsurface hydrology. Wiley Interscience, New York, 389 pp.



van Genuchten, M.Th. and W.J. Alves, 1982. Analytical solutions of the convection dispersion solute transport equation. U.S.Dept. of Agronomy, Tech. Bull. 1661, 151 pp.

Warrick, A.W., J.W. Biggar and D.R. Nielsen, 1971. Simultaneous solute and water transport for an unsaturated soil. Water Res. Res., 7:1216-1225.

THE HEAT TRANSPORT

MODULE



4 THE HEAT TRANSPORT MODULE

4.1 INTRODUCTION

Most soil biological and bio-chemical processes are influenced by soil temperature. Processes like nitrogen mineralisation e.g., occur at an optimal rate in optimal temperature conditions. The correct assessment of these processes therefore involves a correct description of the soil temperature. Heat flow in the WAVE-model is simulated one-dimensionally. The heat flow module is similar to the model of Tillotson et al. (1980) and Wagenet and Hutson (1989). The calculation of the soil thermal properties is based on work of de Vries (1952), as adopted by Wierenga et al. (1969) and Wagenet and Hutson (1990).

4.2 THE SOIL HEAT FLOW EQUATION

To model the transport of heat in porous media, the one-dimensional heat flow equation is used:

$$\frac{\partial T}{\partial t} = \frac{\partial}{\partial x} \left(\frac{\lambda(\theta)}{\rho \cdot C_p} \frac{\partial T}{\partial x} \right) \quad (4-1)$$

where T is the soil temperature ($^{\circ}\text{C}$); $\lambda(\theta)$ is the thermal conductivity ($\text{J m}^{-1} \text{s}^{-1} ^{\circ}\text{C}^{-1}$); ρ is the wet bulk density (kg m^{-3}); and C_p is the specific heat capacity of the soil ($\text{J kg}^{-1} ^{\circ}\text{C}^{-1}$). Neglecting the heat capacity of the soil gaseous phase, the volumetric heat capacity of the soil is governed by the heat capacity of the soil solid and water phase or:

$$\rho \cdot C_p = \rho_s \cdot C_s + \theta \cdot \rho_w \cdot C_w \quad (4-2)$$

where ρ_s is the bulk density of the soil solid phase; ρ_w the density of water; C_s is the specific gravimetric heat capacity of the soil solids ($840 \text{ J kg}^{-1} ^{\circ}\text{C}^{-1}$); C_w is the specific gravimetric heat capacity of water ($4.2 \text{ kJ kg}^{-1} ^{\circ}\text{C}^{-1}$). The thermal conductivity is calculated in the WAVE-model as reported by Wierenga et al. (1969). Considering soil as a continuous medium of either water or air and solids dispersed in it, then the thermal conductivity can be approximated as:

$$\lambda = c \cdot \frac{\sum_{i=0}^n k_i \cdot X_i \cdot \lambda_i}{\sum_{i=0}^n k_i \cdot X_i} \quad (4-3)$$

where n is the number of different components, X_i is the volume fraction of the i -th component (-), λ_i is the thermal conductivity of the i -th component ($\text{J m}^{-1} \text{s}^{-1} ^{\circ}\text{C}^{-1}$),



and c is an empirical correction factor (-). The volume fraction of quartz, organic matter and other solids is default set equal to 0.54, 0.045 and 0.015 respectively, while the value of c equals 1.65, for $\theta < 0.22$, and 0.0 for $\theta > 0.22$ (Skaggs and Smith, 1967). The subscript zero refers to the continuum medium, e.g. air for dry soil or water for moist soil, with $k_0=1$. Other values of k_i may be calculated from:

$$k_i = \frac{1}{3} \sum_{j=1}^3 \left(1 + \left(\frac{\lambda_i}{\lambda_0} - 1 \right) g_j \right)^{-1} \quad (4-4)$$

where g_j is a dimensionless factor depending on the particle shape of the i -th component, with $g_1+g_2+g_3=1$. The values of λ_i for quartz, organic matter, other solids and air at 20 °C are default equal to 20.4, 0.6, 0.7 and 0.0615 mCal cm⁻¹ sec⁻¹ °C⁻¹. The apparent thermal conductivity of the air filled pores is taken to be $\lambda_a + \lambda_v$, where λ_a is the thermal conductivity of the air and λ_v accounts for the heat movement by vapour across the gas-filled pore. For water contents above 0.20, the air in the soil water pores is considered to be saturated and a value of 0.176 mCal cm⁻¹ sec⁻¹ °C⁻¹ is used for λ_v . It is assumed that the value of λ_v decreases linearly from 0.176 mCal cm⁻¹ sec⁻¹ °C⁻¹ at a moisture content of 0.2 to 0. at oven-dryness. For quartz and solid particles, g_j is set equal to 0.125, 0.125, 0.750 respectively. For organic matter $g_1=g_2=0.5$, while $g_3=0.0$. Values of g_1 and g_2 for the air particles are assumed to decrease linearly from 0.333 in water saturated soil to 0.105 at a soil water content of 0.2. Below this water content, g_1 and g_2 are assumed to decrease linearly to a value of 0.015 at oven dryness.

4.3 NUMERICAL SOLUTION OF THE HEAT FLOW EQUATION

4.3.1 THE SOLUTION PROCEDURE

The right hand term of Eq.(4-1) is expanded as a Taylor series and rearranged in an implicit central difference scheme:

$$\frac{\partial}{\partial x} \left(\frac{\lambda(\theta)}{\rho \cdot C_p} \frac{\partial T}{\partial x} \right) = \frac{1}{x_{i+1} - x_{i-1}} \left(\frac{\lambda_{i-1/2}^{j-1/2} (T_{i-1}^{j-1} + T_{i-1}^j + T_i^{j-1} + T_i^j)}{2 \cdot \rho_{i-1/2} \cdot C_{p,i-1/2}^{j-1/2} \cdot (x_i - x_{i-1})} \right) - \left(\frac{\lambda_{i+1/2}^{j-1/2} (T_i^{j-1} + T_i^j + T_{i+1}^{j-1} + T_{i+1}^j)}{2 \cdot \rho_{i+1/2} \cdot C_{p,i+1/2}^{j-1/2} \cdot (x_{i+1} - x_i)} \right) \quad (4-5)$$

Equation (4-5) is formulated for each node. The rearranged system of linear equations has a tri-diagonal form and can be solved using the Thomas algorithm (Remson et al., 1978).

4.3.2 DEFINITION OF THE UPPER BOUNDARY CONDITION

The upper boundary condition for the soil temperature is defined using the method of Kirkham and Powers (1972). The method considers the daily variation of soil



temperature at the surface as a result of the fluctuation of the daily solar radiation. The foregoing is described using a sine function:

$$T = T_a + \gamma \sin\left(\frac{2\pi t}{p}\right) \quad (4-6)$$

where T is the actual soil surface temperature ($^{\circ}$ C), T_a is the daily average soil surface temperature ($^{\circ}$ C), γ is the amplitude of the soil surface temperature ($^{\circ}$ C) (usually taken equal to the difference between maximum and minimum temperature), p is the period for completing one cycle (usually one day) and t the time (day).

4.3.3 DEFINITION OF THE LOWER BOUNDARY CONDITION

For the lower boundary condition, a constant soil temperature (default fixed at 7° C) is assumed.

4.4 REFERENCES

- de Vries, D.A., 1952. The thermal conductivity of soil. Meded. Landbouwhogeschool, Wageningen, 52, 72 pp.
- Kirkham, D., and W.L. Powers, 1972. Advanced soil physics. John Wiley and Sons, N.Y.
- Remson, I., G.M. Hornberger and F.J. Molz, 1978. Numerical methods in subsurface hydrology. Wiley Interscience, N.Y., 389 pp.
- Skaggs, R.W. and E.M. Smith, 1967. Apparent thermal conductivity of soil as related to soil porosity. Paper 67-114 presented at the Annual meeting of the ASAE at Saskatoon, Skatchewan, 27-30 June.
- Tillotson, W.R., C.W. Robbins, R.J. Wagenet and R.J. Hanks, 1980. Soil, water, solute and plant growth simulation. Bulletin 502, Utah State Agr. Exp. Stn. Logan, Utah, 53 pp.
- Wagenet, R.J. and J.L. Hutson, 1989. LEACHM, a process based model of water and solute movement, transformations, plant uptake and chemical reactions in the unsaturated zone. Centre for Env. Res., Cornell University, Ithaca, N.Y., 147 pp.
- Wierenga, P.J., D.R. Nielsen, and R.M. Hagan, 1969. Thermal properties of a soil based upon field and laboratory measurements. Soil Sci. Soc. Am. Proc., 33:354-360.

THE CROP GROWTH MODULE



5 THE CROP GROWTH MODULE

5.1 INTRODUCTION

The crop leaf area, root length and root density are needed to calculate the soil water and nitrogen balance in a cropped soil. If these time variant functions are not specified as model input, then they can be calculated using a crop growth model. A crop growth model enables the calculation of energy fluxes in the crop in terms of carbon assimilation, based on the photosynthetic process. A fraction of the assimilated energy is used to maintain the crop. The remaining part can be applied to build structural bio-mass. The growth rates for the structural bio-mass, are next divided in growth rates of the different plant components. The crop specific distribution keys vary as a function of the plant development stage. The growth rate of the crop components is finally translated into leaf area, root length and root density extension rates.

The crop growth model, included in WAVE, is a simple universal and comprehensive crop growth model. The model, with the acronym SUCROS, was developed at the Center for Agro-biological Research (CABO), Wageningen, The Netherlands (van Keulen, 1982; Spitters et al., 1988). It calculates the crop development rate, dry matter accumulation rate of the different plant organs and LAI development rate, as functions of a set of climatic (radiation and temperature) and plant phenologic parameters. The model is extended to calculate daily root length and root density profiles. The potential crop growth is limited when water stress in the root zone of the plant occurs. Crop parameters for winter wheat (barley), spring wheat (barley), maize, potato and sugar beets, estimated from a set of field trials mainly under Dutch conditions, are available in the WAVE-version. So far, the model can only be used for these five crops, which represent a large part of the field cropping area in Western Europe. This chapter gives a brief outline of the universal crop growth model SUCROS. More detailed information can be found in the publications of Penning de Vries and Van Laar (1982); Spitters et al. (1986); Spitters (1986) and Spitters et al. (1988).

5.2 CALCULATION OF THE PLANT DEVELOPMENT RATE

In order to account for the climatic conditions during the growing season, a time scale, called the development stage, which is proportional to the accumulated effective temperature sum, is used. The effective temperature (T_e) is defined as the difference between the average daily temperature (T) and the base temperature (T_b) below which crop growth ceases. The effective temperature sum (S_t) is defined as:

$$S_t = \sum_{t_0}^t T_e \cdot \Delta t \quad (5-1)$$



where t is the actual time (day); t_0 is the initial time corresponding to crop emergence (day); Δt the time step (= 1 day); and $T_e = \max(0, T - T_b)$, is the effective temperature ($^{\circ}\text{C}$).

Table 5-1 lists a review of base temperatures and the critical effective temperature sum required ($S_{t,\text{crit},1}$ and $S_{t,\text{crit},2}$) to fulfil the vegetative and reproductive phase for winter wheat, spring barley, spring wheat and grain maize.

For crops showing crop florescence and maturity in the same year, a normalised time scale can be defined. By definition, plant florescence occurs when the plant development stage in the normalised time scale equals one ($DVS' = 1$), while crop maturity is reached at time scale two ($DVS' = 2$). Using this definition, the actual crop development stage can be calculated as:

$$\begin{aligned} DVS' &= \frac{S_t}{S_{t,\text{crit},1}} \quad \text{during the vegetative ; and} \\ DVS' &= 1 + \frac{S_t}{S_{t,\text{crit},2}} \quad \text{during the reproductive phase.} \end{aligned} \quad (5-2)$$

The development rate (DVR) is defined as:

$$DVR = \frac{\partial DVS}{\partial t} \approx \frac{\Delta DVS}{\Delta t} = \frac{\Delta S_t}{\Delta t \cdot S_{t,\text{crit}}} = \frac{\sum_{t_0}^{t_i} T_e \cdot \Delta t - \sum_{t_0}^{t_{i-1}} T_e \cdot \Delta t}{\Delta t \cdot S_{t,\text{crit}}} = \frac{(T_e^{t=i}) \Delta t}{\Delta t \cdot S_{t,\text{crit}}} = \frac{T - T_b}{S_{t,\text{crit}}} \quad (5-3)$$

or

$$\begin{aligned} DVR &= \left(1 / S_{t,\text{crit}}\right) \cdot T - \left(T_b / S_{t,\text{crit}}\right) && \text{for } T > T_b \\ DVR &= 0 && \text{for } T < T_b \end{aligned} \quad (5-4)$$

In this approach, the development rate is a linear function of the actual temperature. The slope and intercept of this linear function can be derived from the Table 5-1. For winter wheat, spring wheat and corn, at least two points of the linear $DVR(T)$ function are needed as model input.

For perennial crops, which show no clear florescence during the growing season, the development stage is not normalised. In this case, the plant development stage is equal to the calculated temperature sum. For sugar beets and potatoes, the base temperature equals 2°C . Development ceases when a threshold maximum temperature is exceeded (for sugar beets, if $T_e > 19^{\circ}\text{C}$; for potatoes, if $T_e > 29^{\circ}\text{C}$).



Table 5-1: Critical temperature sum, base temperature and initiation time required to fulfil the crop vegetative and reproductive phases for maize, winter wheat and spring wheat

Crop	Vegetative phase t0	Tb	St,crit1	Reproductive phase t0	Tb	St,crit2	Remark	Ref.
Winter wheat	1 January	0	1255	Anthesis	0	909		(1)
		0	1000	Anthesis	0	950	U.K, Denmark	(2)
		0	1050	Anthesis	0	1000	U.K Ireland Netherlands Germany	(2)
		0	1125	Anthesis	0	1000	Germany Netherlands Belgium	(2)
		0	1200	Anthesis	0	1000	Luxembourg	
		0	1250	Anthesis	0	1000	Germany	(2)
		0	1300	Anthesis	0	1000	France	
		0	1350	Anthesis	0	1000	France	(2)
		0	795	Flowering	0	909	Italy	
		0	800	Heading	0	750	Spain	
Spring wheat	emergence	10	425	Silking	10	425	Portugal	(2)
		6	730	Silking	6	730	Italy	
		6	695	Silking	6	800	Spain	
		6	695	Silking	6	860	Portugal	(2)
		6	775	Silking	6	880	Greece	
		6	855	Silking	6	900	Spain	
		6	935	Silking	6	920	South Spain	
							Greece	
							Southern Italy	
							Southern Spain	(2)
Spring barley								
Corn								

Legend: (1): Spitters et al., 1988; (2): Boons-Prins et al., 1993



5.3 CALCULATION OF THE DAILY CROP ASSIMILATION RATE

5.3.1 PHOTOSYNTHETIC RESPONSE OF INDIVIDUAL LEAVES

The calculation of the carbon assimilation rate is based on the leaf response curve to photosynthetic active radiation (PAR). Because the rate of photosynthesis decreases with decreasing light intensity, the following light response curve is used to relate the rate of gross photosynthesis of leaf to the intensity of adsorbed radiation:

$$A_L = A_m \left(1 - e^{-\frac{\epsilon I_L}{A_m}} \right) \quad (5-5)$$

where A_L is the gross CO_2 -assimilation rate of a unit leaf area within the canopy ($\text{kg CO}_2 \text{ m}^{-2} \text{ leaf s}^{-1}$); A_m is the potential CO_2 -assimilation rate of a unit leaf area for light saturation ($\text{kg CO}_2 \text{ m}^{-2} \text{ leaf s}^{-1}$); ϵ is the initial light use efficiency ($\text{kg CO}_2 \text{ J}^{-1}$); and I_L is the PAR absorbed by the leaf ($\text{W m}^{-2} \text{ leaf}$). When light saturation is reached, the CO_2 -assimilation rate reaches its maximum level A_m . The leaf response curve is characterised by two parameters: ϵ and A_m . In Tables 5-2 and 5-3 literature values for the A_m and ϵ are given for five crops.

The potential assimilation rates are reduced in case of leaf senescence or unfavourable temperature conditions. This effect is achieved by multiplying the A_m value with a temperature (REDUCT_TEMP_AMAX) or senescence (REDUCT_DVS_AMAX) reduction function. Values of the reduction functions as reported in literature are listed in the Tables 5-4 and 5-5.

Table 5-2: A_m values for the five specified crops

Crop	A_m (kg/ha/h)	Remarks	Ref.
Winter Wheat	40	T=10-25	(1)
	35-45		(2)
Spring Wheat	40		(3)
	35		(1)
Spring Barley	40	T=25	(2)
	35		(1)
Corn	60	T= 25	(1)
	70		(2,3)
Potato	30	T=20	(1,2,3)
Sugar Beet	38	T=20	(1)
	45		(2,3)

Legend: (1) Penning de Vries et al., 1988; (2) Boons-Prins et al., 1993; (3) Spitters et al. (1988).

Table 5-3: ϵ values for five crops

Crop	ϵ (kg/ha/h)/(J/m ² /s)	Remarks	Ref.
Winter Wheat	0.50	T=10-25	(1)
	0.45		(2)
Spring Wheat	0.45	T=25	(3)
	0.40		(1)
Spring Barley	0.45	T=25	(2)
	0.40		(1)
Corn	0.40	T=25	(1)
	0.45		(2,3)
Potato	0.50	T=20	(1)
	0.45		(2,3)
Sugar Beet	0.56	T=20	(1)
	0.45		(2,3)

Legend: (1) Penning de Vries et al., 1988; (2) Boons-Prins et al., 1993; (3) Spitters et al. (1988).

Table 5-4: Reduction of the maximum gross assimilation rate of a leaf (RED_TEMP_AMAX) as a function of ambient temperature

Crop	Temperature (°C)	RED_TEMP AMAX	Ref.
Winter Wheat	0.	0.01	(3)
	8.	0.01	
	10.	0.40	
	15.	0.90	
	25.	1.00	
	35.	0.00	
	0.	0.0001	(1)
	10.	1.00	
	25.	1.00	
Spring Wheat	35.	0.01	
	50.	0.01	
	0.	0.01	(2)
	10.	0.60	
	15.	1.00	
Barley	25.	1.00	
	35.	0.00	
	50.	0.01	
	-20.	0.001	(1)
	0.	0.01	
Spring Barley	5.	0.40	
	10.	0.70	
	15.	0.9	
	20.	1.0	



	25.	1.0	
	30.	0.9	
	35.	0.8	
	40.	0.5	
Spring Barley	0.	0.01	(2)
	10.	0.6	
	15.	1.0	
	25.	1.0	
	35.	0.0	
Corn	-10.	0.01	(3)
	9.	0.05	
	16.	0.80	
	18.	0.94	
	20.	1.00	
	30.	1.00	
	40.	0.75	
	0.	0.01	(1)
	5.	0.01	
	10.	0.10	
	15.	0.50	
	20.	0.80	
	25.	1.00	
	35.	1.00	
	40.	0.90	
	45.	0.75	
	50.	0.07	
	0.	0.01	(2)
	9.	0.05	
	16.	0.80	
	18.	0.94	
	20.	1.00	
	30.	1.00	
	36.	0.95	
	42.	0.56	
Potato	-10.	0.01	(3)
	3.	0.01	
	10.	0.75	
	15.	1.00	
	20.	1.00	
	26.	0.75	
	33.	0.01	
	45.	0.01	
	-20.	0.00	(1)
	-5.	0.01	
	5.	0.02	
	15.	0.80	
	20.	1.00	
	25.	1.00	
	30.	0.80	
	37.	0.00	
	0.	0.01	(2)
	3.	0.01	
	10.	0.75	
	15.	1.00	



	20.	1.00	
	26.	0.75	
	33.	0.01	
Sugar Beet	-10	0.01	(3)
	3.	0.01	
	10.	0.75	
	15.	1.00	
	20.	1.00	
	26.	0.75	
	33.	0.01	
	45.	0.01	
	0.	0.01	(1)
	5.	0.01	
	10.	0.75	
	20.	1.0	
	35.	1.0	
	40.	0.9	
	45.	0.01	
	0.	0.01	(2)
	3.	0.60	
	10.	0.80	
	15.	1.00	
	20.	1.00	
	30.	0.95	
	35.	0.83	
	40.	0.60	

Legend: (1) Penning de Vries et al., 1988; (2) Boons-Prins et al., 1993; (3) Spitters et al. (1988).



Table 5-5: Reduction of the maximum gross assimilation rate of a leaf (RED_DVS_AMAX) as a function of the development stage

Crop	DVS	RED_DVS_AMAX	Ref.
Winter Wheat	0.0	1.0	(2)
	1.0	1.0	
	2.0	0.5	
Spring Wheat	0.0	1.0	(3)
	1.0	1.0	
	2.0	0.5	
	2.5	0.0	
Spring Barley	0.00	1.0	(2)
	1.00	1.0	
	2.00	0.5	
Corn	0.00	1.0	(2)
	1.25	1.0	
	1.50	0.9	
	1.75	0.7	
	2.00	0.3	
	0.0	1.00	(3)
	1.3	1.00	
	1.6	0.50	
	2.0	0.25	
	2.5	0.25	
Potato	0.00	1.0	(2)
	1.57	1.0	
	2.00	0.0	
Sugar Beet	0.00	0.5	(2)
	1.00	1.0	
	1.13	1.0	
	1.80	0.8	
	2.00	0.8	
	0.00	0.50	(3)
	500.00	1.0	
	700.00	1.0	
	1700.00	0.8	
	3000.00	0.6	

Legend: (1) Penning de Vries et al., 1988; (2) Boons-Prins et al., 1993; (3) Spitters et al. (1988).



5.3.2 GLOBAL, DIRECT AND DIFFUSE IRRADIANCE AT THE TOP OF THE CROP CANOPY

In this paragraph, the calculation of the absorbed radiation in the crop canopy, I_L , as a function of the incident radiation (irradiation) and time, is explained. The daily total global radiation ($\text{J cm}^{-2} \text{ day}^{-1}$), measured with a pyranometer or Gunn Bellani Integrator, is input in the model. Total refers to the sum of visible and near infrared light (330-3000 nm), while global refers to the radiation coming from all directions (diffuse and direct). The irradiation is partitioned in two ways: according to the wavelength in photosynthetically active radiation (PAR, 400-700 nm) and according to the direction in direct (from a point source) and diffuse radiation. The PAR is assumed to be 50 % of the total radiation. The diffuse flux is the result of scattering of sun rays by clouds, gases and dust in the atmosphere. The proportion of the diffuse flux in the total radiation is thus proportional to the degree of scattering. The atmospheric transmission, T_d , is defined as:

$$T_d = \frac{\text{DTR}}{\text{DTRM}} \quad (5-6)$$

where DTR is the measured global radiation ($\text{J cm}^{-2} \text{ day}^{-1}$), and DTRM ($\text{J cm}^{-2} \text{ day}^{-1}$) the quantity of radiation energy which should have reached the earth in the absence of the atmosphere. The value of DTRM can, for a given day and latitude, be calculated from theoretical considerations (van Keulen and Wolf, 1986). The latitude is input in the model. The relation between T_d and the direct/global ratio (or diffuse/global ratio) appears to be constant. This empirical relation, which is depicted in Fig. 5-1, is used to calculate the direct (P_d) and diffuse ($1-P_d$) fraction of the global radiation. The difference between direct and diffuse radiation is important for the canopy photosynthesis. Using this figure, and assuming a constant transmission during the day, the instantaneous direct and diffuse photosynthetic active radiation flux, at the top of the canopy ($E_{0,dr}$ and $E_{0,df}$), as well as the daily totals, are calculated using the following expressions:

$$\begin{aligned} E_0 &= \text{DPAR} * \frac{\sin B * (1 + 0.4 * \sin B)}{\sin BE} \\ E_{0,df} &= (1 - P_d) * \text{DPAR} * \frac{\sin B}{\sin BE} \\ E_{0,dr} &= E - E_{0,df} \end{aligned} \quad (5-7)$$

where E_0 , $E_{0,dr}$, $E_{0,df}$ are the instantaneous photosynthetic active, direct and diffuse radiation flux at the top of the crop canopy ($\text{J cm}^{-2} \text{ s}^{-1}$); $\sin B$, the sinus of the solar elevation (-); $\sin BE$, the daily integral of $\sin B$ with a correction of lower atmospheric transmittance at lower solar elevation (-); P_d the direct/diffuse irradiance ratio (-); and DPAR the daily total photosynthetic radiation ($\text{J cm}^{-2} \text{ day}^{-1}$). The value of the solar elevation is, for a given Julian day and latitude, calculated from theoretical calculations. The P_d value is derived from the Fig. 5-1. The DPAR value is set equal to 50 % of the measured daily global radiation (DTR).

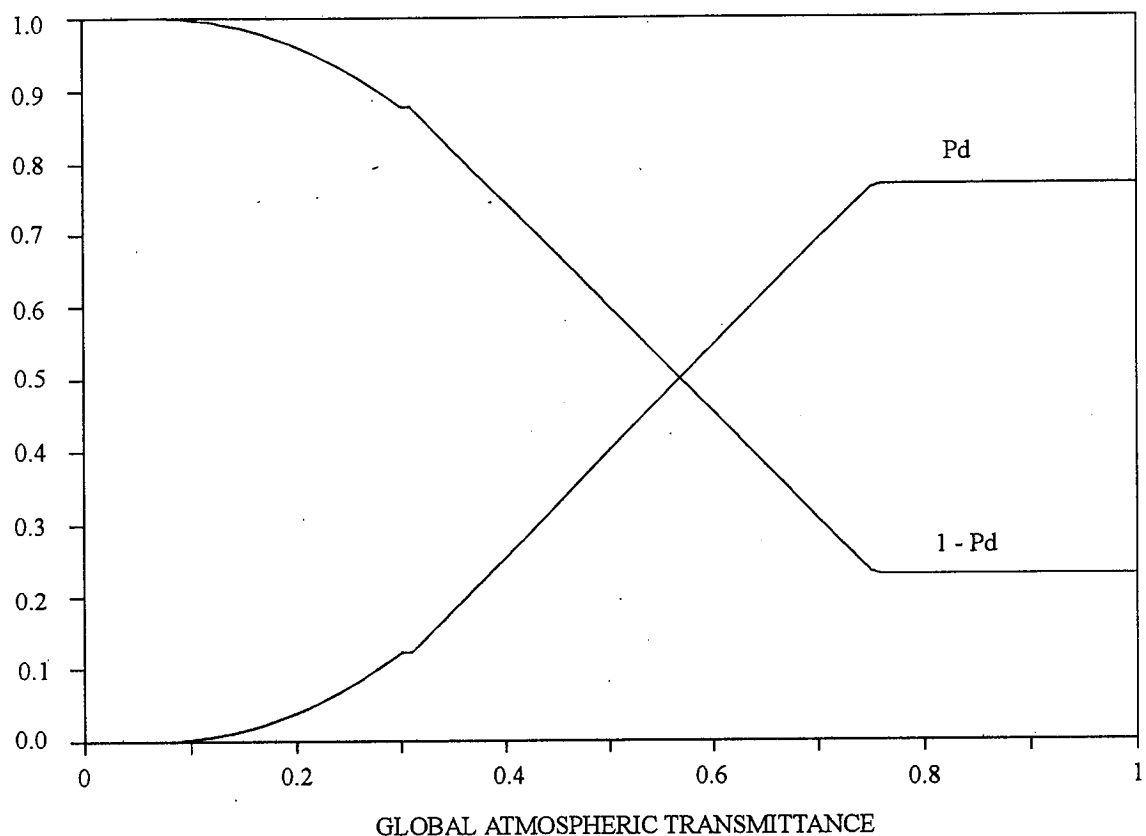


Fig.5-1: Relation between the daily average values of the direct/global ratio (P_d) and the global atmospheric transmittance (T_d)

5.3.3 CROP CANOPY REFLECTION

A fraction of the radiation energy piercing through the crop canopy, is reflected directly, and is not considered for the calculation of the absorbed energy. If a crop canopy consists of horizontally positioned leaves with a hemispherical reflectance and if the leaf transmittance coefficient and reflection coefficient are each equal to half the scattering coefficient σ , and if soil reflection is ignored, then for large LAI-values a simple model for crop reflectance can be written as:

$$f = \frac{1 - \sqrt{1 - \sigma}}{1 + \sqrt{1 - \sigma}} \quad (5-8)$$

where σ is the scattering coefficient of the leaves (dimensionless fraction). The scattering coefficient is input in the model. Usually, the value of σ is set equal to 0.20.



5.3.4 PENETRATION OF THE DOWNWARD RADIATION FLUX IN THE CROP CANOPY

After correcting for crop reflectance, the downward moving radiation flux attenuates in the canopy due to light absorption. The following attenuation function is considered in the crop model.

$$E_L = (1-f) \cdot E_0 \cdot e^{-kL} \quad (5-9)$$

where L (m) is the transformed canopy depth equal to the depth integral of the leaf area index integrated from the top of the canopy downwards; E_L is the radiation flux at depth where the depth integral of the LAI equals L ($J m^{-2} s^{-1}$); E_0 is the radiation at the top of the canopy ($J m^{-2} s^{-1}$); and k is the crop canopy extinction coefficient (m^{-1}). For the direct and diffuse component of the radiation flux, Eq.(5-9) can be written as:

$$\begin{aligned} E_{L,df} &= (1-f) \cdot E_0 \cdot e^{-kdfL} \\ E_{L,dr} &= (1-f) \cdot E_0 \cdot e^{-kdrL} \end{aligned} \quad (5-10)$$

where kdf and kdr (m^{-1}) are the extinction coefficients for direct and diffuse radiation. When penetrating through the canopy, the direct radiation flux ($E_{L,dr}$) divides in a direct component ($E_{L,dr,dr}$), which does not encounter any obstacle along its travel path, and a diffuse component ($E_{L,dr,df}$) which meets foliage along its travel path. The latter is not absorbed and scattered back in the canopy. For any depth in the canopy the following relation holds:

$$E_{L,dr} = E_{L,dr,dr} + E_{L,dr,df} \quad (5-11)$$

The direct component of the radiation flux equals:

$$E_{L,dr,dr} = E_{0,dr} \cdot e^{-kblL} \quad (5-12)$$

where kbl (m^{-1}) is the extinction coefficient for a hypothetical crop, with black leaves.

In a first approach the extinction coefficient kdf is modelled using the scattering coefficient ($\sigma=0.20$):

$$kdf' = 0.8 \cdot \sqrt{1-\sigma} \quad (5-13)$$

This approximated extinction coefficient assumes a spherical leaf angle distribution within the canopy. In reality, however, leaves are grouped together in clusters. A cluster factor is defined as the ratio of the actual extinction coefficient for diffuse radiation to the extinction coefficient for a canopy with spherical angle distribution, which is defined as:



$$\text{CLUSTF} = \frac{\text{kdf}}{\text{kdf}'} \quad (5-14)$$

The actual extinction coefficient of the crop canopy for diffuse light (kdf), is input. Literature values are given in Table 5-6. The defined cluster factor is used to calculate kbl and kdr according:

$$\begin{aligned} \text{kdr} &= 0.5 \cdot \text{CLUSTF} \cdot \frac{\sqrt{1-\sigma}}{\sin B} \\ \text{kbl} &= \frac{0.5 \cdot \text{CLUSTF}}{\sin B} \end{aligned} \quad (5-15)$$

where σ is the scattering coefficient and $\sin B$ is the sinus of the solar elevation.

Table 5-6: Extinction coefficients for diffuse light within the canopy of different crops (source: Boon-Prins et al., 1993; Spitters et al., 1988)

Crop	kdf (m^{-1})
Winter Wheat	0.60
Spring Wheat	0.60
Corn	0.65
Potato	1.00
Sugar Beet	0.69

5.3.5 CALCULATION OF THE DAILY RATES OF THE LIGHT ABSORPTION AND CO₂ ASSIMILATION

The attenuation of any radiation component within the crop canopy by a leaf layer at a depth between L and L+dL can be approximated as:

$$I_L = \frac{dE_L}{dL} = (1-f) \cdot E_0 \cdot k \cdot e^{-kL} \quad (5-16)$$

where I_L is the light absorption rate per unit area ($\text{J m}^{-2} \text{ leaf s}^{-1}$). According to the structure of Eq.(5-16) the calculations are no longer performed on the basis of a hypothetical horizontal layer, but on the basis of the area of the leaves. The absorption rates for the different radiation terms yield:

$$\begin{aligned} I_{L,df} &= (1-f) \cdot E_{0,df} \cdot kdf \cdot e^{-kdf \cdot L} \\ I_{L,dr} &= (1-f) \cdot E_{0,dr} \cdot kdr \cdot e^{-kdr \cdot L} \\ I_{L,dr,dr} &= (1-\sigma) \cdot E_{0,df} \cdot kbl \cdot e^{-kbl \cdot L} \\ I_{L,dr,df} &= I_{L,dr} - I_{L,dr,dr} \end{aligned} \quad (5-17)$$



A fraction of the leaf layer dL , is directly exposed to the sun. This sunlit leaf area fraction ($f_{L,sl}$) decreases with depth, proportional to the attenuation of the direct component of the direct radiation flux or:

$$f_{L,sl} = e^{-kbl \cdot L} \cdot CLUSTF \approx \frac{E_{L,dr,dr}}{E_{0,dr}} \quad (5-18)$$

The absorption rate of the shaded leaf area ($f_{L,sh}$) is equal to the sum of the absorption rate of the diffuse flux and the diffuse component of the direct flux:

$$I_{L,sh} = I_{L,df} + I_{L,dr,df} \quad (5-19)$$

The sunlit leaf area absorbs the same quantity of radiation increased with the direct component of the direct flux. For this latter fraction no attenuation as a function of depth is assumed or:

$$I_{L,sl} = I_{L,sh} + (1 - \sigma) \cdot kbl \cdot E_{0,df} \quad (5-20)$$

Combination of the Eqs. (5-19) and (5-20) with the mathematical expression for the total instantaneous assimilation rate of a layer in the canopy (Eq. 5-5) yields:

$$A_{L,T} = A_{L,sh} \cdot f_{L,sh} + A_{L,sl} \cdot f_{L,sl} \quad (5-21)$$

where $A_{L,T}$ is the total instantaneous assimilation rate ($\text{kg CO}_2 \text{ m}^{-2} \text{ leaf s}^{-1}$); $A_{L,sl}$ is the instantaneous assimilation rate of the sunlit leaves ($\text{kg CO}_2 \text{ m}^{-2} \text{ leaf s}^{-1}$); and $A_{L,sh}$ is the instantaneous assimilation rate of the shaded leaves ($\text{kg CO}_2 \text{ m}^{-2} \text{ leaf s}^{-1}$). The daily total carbon assimilation of a crop, A ($\text{kg CO}_2 \text{ m}^{-2} \text{ day}^{-1}$), is obtained by integrating the instantaneous assimilation rates per unit leaf layer over the total leaf area (LAI) and over the daylight period or:

$$A = \int_{-\tau^*}^{+\tau^*} \int_{0}^{LAI} A_{L,T} \cdot dL \cdot d\tau \quad (5-22)$$

where $-\tau^*$ and $+\tau^*$ represent sunrise and sunset time respectively. In order to solve previous equation numerically the three point Gauss integration method is used. With this integration method, a good approximation of the defined integral in the interval $[0, 1]$ can be obtained by using:

$$\int_0^1 y \cdot dx = \frac{w_1 \cdot y(x_1) + w_2 \cdot y(x_2) + w_3 \cdot y(x_3)}{w_1 + w_2 + w_3} \quad (5-23)$$

where $x_1 = 0.5 - \sqrt{0.15}$; $x_2 = 0.5$; $x_3 = 0.5 + \sqrt{0.15}$; and where $w_1 = 1$; $w_2 = 1.6$; and $w_3 = 1$.



Using this integration method, three depths are selected in the normalised interval L/LAI for which $A_{L,T}$ is calculated using Eq.(5-21). The procedure is then repeated for three different time periods during the day. The results are weighed and summed to obtain the total daily carbon assimilation of the crop.

5.4 CALCULATION OF THE DRY MATTER GROWTH RATE OF THE DIFFERENT PLANT COMPONENTS

The assimilated carbon in the crop canopy is converted into structural bio-mass. Using the global photosynthetic reaction, 44 moles of glucose are created for each 30 moles of carbon used. Hence, the glucose assimilation rate, A_g ($\text{kg CH}_2\text{O m}^{-2} \text{ day}^{-1}$) can be calculated as:

$$A_g = A \frac{30}{44} \quad (5-24)$$

where A is the daily total carbon assimilation rate ($\text{mol CO}_2 \text{ m}^{-2} \text{ day}^{-1}$). Part of the assimilated energy, converted in the glucose form, is used to maintain the existing crop. The maintenance energy differs between the different plant components. For example, 30 g of glucose is daily needed to maintain 1 kg of leaves under optimal conditions. The roots and stems of crops in general, the cobs of maize, the crown of sugar beet and the metabolic active parts of the storage organs need, on average, 15 g of glucose per kg of dry matter per day. These values are default in the model. The respiration rate of the inactive part of the storage organs, however, differs between crop species. Values for the maintenance energy of the inactive part of the storage organs are input and listed in Table 5-7. Ambient temperature and plant senescence control the maintenance demand. This is considered in the model by multiplying the calculated potential respiration with a temperature (a Q_{10} -relation) and senescence (the proportion green versus total leaf weight) reduction factor, as shown in Eq. (5-25):

$$R_m = \left(\sum M_i \cdot W_i \right) \left(Q_{10}^{\frac{T-25}{10}} \right) \left(\frac{WLVG}{WLVT} \right) \quad (5-25)$$

where R_m is the total maintenance demand rate ($\text{kg CH}_2\text{O m}^{-2} \text{ day}^{-1}$); M_i is the maintenance demand rate for the crop component i per unit dry matter ($\text{kg CH}_2\text{O kg}^{-1} \text{ DM day}^{-1}$); W_i is the weight of the crop component i per unit area (kg DM m^{-2}); $WLVG$ is the weight of green leaves per unit area (kg DM m^{-2}); $WLVT$ is the weight of leaves per unit area (kg DM m^{-2}); Q_{10} is the base coefficient ($Q_{10}=2$); and T is the daily mean temperature ($^{\circ}\text{C}$).



Table 5-7: Maintenance energy of the storage organs of different crops (Boons-Prins et al., 1993; Spitters et al., 1988)

Crop	M_STORAGE_ORGAN (kg CH ₂ O kg ⁻¹ DM day ⁻¹)
Winter wheat	0.0100
Spring wheat	0.0100
Corn	0.0100
Potato	0.0045
Sugar beet	0.0030

The remaining part of the assimilated energy can be used to build up structural biomass. Hence, the net growth rate of dry matter is calculated as:

$$GWT = \frac{A_g - R_m}{ASRQ} \quad (5-26)$$

where GWT is the net dry matter growth rate per unit area (kg DM m⁻² day⁻¹); A_g is the daily glucose assimilation rate (kg CH₂O m⁻² day⁻¹); R_m is the maintenance demand rate (kg CH₂O m⁻² day⁻¹); and ASRQ the conversion efficiency coefficient (kg DM kg⁻¹ CH₂O). The energy needed to constitute structural material depends on the chemical composition and the energy needed to form the different chemical elements in the different plant components. In Table 5-8 values for the chemical composition of the different plant organs together with the energy costs to form these components are given. These values are used to calculate the conversion efficiency coefficient for a particular plant organ. For green leaves, the leave conversion efficiency coefficient is calculated as:

$$\begin{aligned} ASRLVG &= \\ &0.52 * 1257 + 0.25 * 1887 + 0.05 * 3.189 + 0.05 * 2.2231 + 0.05 * 0.954 + 0.08 * 0.12 \\ &= 146 \text{ kg CH}_2\text{O kg}^{-1} \text{ DM} \end{aligned} \quad (5-27)$$

The respiration coefficients for the leaves (1.46), stems (1.51), and roots (1.44) are assumed to be the same for the different crops in the model. The respiration coefficient for the storage organs is taken from Table 5-9.



Table 5-8: Mean chemical composition of the different plant organs (CH = Carbon hydrates (%), PROT = protéines(%), LIP = lipides (%), LIG = lignines (%), ORG = organic acids (%), MIN = minerals (%)); mean glucose demand for creating the element (kg CH₂O kg⁻¹ DM) and average global glucose requirement (ASR_i (kg CH₂O kg⁻¹ DM)) to form the different plant organs

Glucose requirement	CH 1.275	PROT 1.887	LIP 3.189	LIG 2.231	ORG 0.954	MIN 0.120	ASR _i
Leaves	52	25	5	5	5	8	1.46 ←
Stems	62	10	2	20	2	4	1.51 ←
Roots	56	10	2	20	2	10	1.44 ←
Storage Organs	76	12	2	6	2	2	1.41

Table 5-9: Conversion efficiency for the storage organs of different crops (kg CH₂O kg⁻¹ DM)

Crop	ASR _{storage organs}	Ref.
Winter Wheat	1.41	(1,3)
	1.415	
Spring Wheat	1.41	(3)
Spring Barley	1.41	(2)
Corn	1.49	(1,3)
	1.491	
Potato	1.28	(3,1,2)
	1.285	
	1.17	
Sugar Beet	1.29	(3,1,2)
	1.294	
	1.21	

Legend: (1) Penning de Vries et al., 1988; (2) Boons-Prins et al., 1993; (3): Spitters et al., 1988.

The crop conversion efficiency coefficient ASRQ, is obtained by weighing the different component efficiency coefficients according to their dry matter fraction in the plant or:

$$\text{ASRQ} = \sum F_i \cdot \text{ASR}_i \quad (5-28)$$

where F_i is the dry matter fraction of component i (-); and ASR_i is the component conversion efficiency coefficient (kg CH₂O kg⁻¹ DM).

Subsequently, the net dry matter growth rate of the crop is partitioned among the different crop components. The partitioning key F_i (-), which distributes the assimilated dry matter to the different plant components, is a function of the plant



phenological stage expressed in terms of plant development stage (DVS). The distribution keys are crop specific and need to be specified as model input (Table 5-10). Given F_i , the net growth rate of a particular plant component, GW_i ($\text{kg DM m}^{-2} \text{ day}^{-1}$), yields:

$$GW_i = F_i \cdot GWT \quad (5-29)$$

For winter and spring wheat, the fraction of the total dry matter allocated to the shoot (F_{sh}) is input together with the shoot fraction allocated to the leaves (F_{lv}) and stems (F_{st}). The fraction of shoot dry matter allocated to the storage organs is calculated as:

$$F_{so} = 1 - F_{lv} - F_{st} \quad (5-30)$$

The fraction of the total dry matter allocated to the roots equals:

$$F_{rt} = 1 - F_{sh} \quad (5-31)$$

For corn, a similar procedure is followed. However, for the calculation of the shoot dry matter allocated to the storage organs, the fraction allocated to the maize cobs (exclusive grains) is explicitly accounted for. Hence Eq.(5-30) reduces to:

$$F_{so} = 1 - F_{lv} - F_{st} - F_{cob} \quad (5-32)$$

The fraction of the shoot dry matter going to the maize cob (exclusive grains) is model input (see Table 5-11). The leave sheets are considered to be a part of F_{st} , while F_{lv} is constituted of the leave blades.

For sugar beets, the shoot fraction (F_{sh}) includes the leave laminae fraction (F_{lv}), the petioles and midribs (F_{st}) and crown fraction of the shoot dry matter ($F_{crown}=1-F_{sh}-F_{st}$). The below ground dry matter ($1-F_{sh}$) consists of fibrous roots ($F_{rt}=Frac_fibrous_root*(1-F_{sh})$), and storage material in the beet (F_{so}). The fraction fibrous roots of the below ground dry matter is input in the model (see Table 5-12).

For potato, the distribution keys are calculated using default empirical equations, which are a function of the potato maturity class. The maturity class is input. Values for the maturity class range between 2.5 (late cultivars) and 9.5 (early cultivars).

potato maturity class



Table 5-10: Fraction of the total dry matter partitioned to the shoots (Fsh) and fraction of the shoot dry matter allocated to the leaves (Flv) and stems (Fst), for different crops as a function of the crop development stage

Crop	Dvs	Fsh	Dvs	Flv	DVS	Fst	Ref.
Spring Wheat	0.00	0.50	0.00	0.65	0.00	0.35	1,2
Spring Barley	0.10	0.50	0.10	0.65	0.10	0.35	
	0.20	0.60	0.25	0.70	0.25	0.30	
	0.35	0.78	0.50	0.50	0.50	0.50	
	0.40	0.83	0.70	0.15	0.70	0.85	
	0.50	0.87	0.95	0.00	0.95	1.00	
	0.60	0.90	2.50	0.00	1.05	0.00	
	0.70	0.93			2.50	0.00	
	0.80	0.95					
	0.90	0.97					
	1.00	0.98					
	1.10	0.99					
	1.20	1.00					
	2.50	1.00					
Barley	0.00	0.35	0.00	0.82	0.00	0.18	3
	0.51	0.45	0.25	0.75	0.25	0.30	
	0.72	0.85	0.51	0.55	0.51	0.45	
	0.95	1.00	0.60	0.50	0.60	0.50	
	2.10	1.00	0.72	0.23	0.72	0.77	
			0.83	0.01	0.83	0.99	
			0.95	0.00	0.95	1.00	
			2.10	0.00	1.21	0.00	
					2.10	0.00	
Spring Wheat	0.00	0.50	0.00	0.90	0.00	0.10	3
	0.33	0.50	0.19	0.83	0.19	0.17	
	0.53	0.75	0.26	0.85	0.26	0.15	
	1.00	1.00	0.45	0.82	0.45	0.18	
	2.10	1.00	0.60	0.32	0.60	0.68	
			0.86	0.15	0.86	0.85	
			1.00	0.26	1.00	0.34	
			1.26	0.00	1.26	0.27	
			2.10	0.00	1.50	0.00	
					2.10	0.00	
Winter Wheat	0.0	0.50	0.00	0.65	0.00	0.35	2
	0.1	0.50	0.10	0.65	0.10	0.35	
	0.2	0.60	0.25	0.70	0.25	0.30	
	0.3	0.78	0.50	0.50	0.50	0.50	
	0.4	0.83	0.70	0.15	0.70	0.85	
	0.5	0.87	0.95	0.00	0.95	1.00	
	0.7	0.93	2.00	0.00	1.05	0.00	



	0.9	0.97			2.00	0.0	
	1.2	1.00					
	2.0	1.00					
	0.00	0.40	0.00	0.90	0.00	0.10	3
	0.32	0.50	0.33	0.85	0.33	0.15	
	0.60	0.75	0.43	0.83	0.43	0.17	
	1.00	1.00	0.53	0.75	0.53	0.25	
	2.10	1.00	0.62	0.56	0.62	0.44	
			0.77	0.20	0.77	0.80	
			0.95	0.09	0.95	0.64	
			1.14	0.05	1.14	0.62	
			1.38	0.00	1.38	0.00	
			2.00	0.00	2.1	0.00	
Corn	0.0	0.60	0.00	0.70	0.00	0.30	1,2
	0.1	0.63	0.33	0.70	0.33	0.30	
	0.2	0.66	0.88	0.15	0.88	0.85	
	0.3	0.69	0.95	0.00	0.95	1.00	
	0.4	0.73	2.00	0.00	1.05	0.00	
	0.5	0.77			2.00	0.00	
	0.6	0.81					
	0.7	0.85					
	0.8	0.90					
	0.9	0.94					
	1.0	1.00					
	2.5	1.00					
	0.00	0.50	0.00	0.49	0.00	0.51	3
	0.67	0.75	0.35	0.59	0.35	0.41	
	1.37	1.00	0.67	0.20	0.67	0.66	
	2.10	1.00	1.0	0.12	1.00	0.64	
			1.18	0.09	1.18	0.31	
			1.37	0.00	1.37	0.00	
			2.10	0.00	2.10	0.00	
Sugar Beets	0.	0.00	0.	0.85	0.	0.10	1
	400.	0.70	370.	0.85	370.	0.10	
	900.	0.52	665.	0.48	665.	0.43	
	901.	0.22	820.	0.23	820.	0.67	
	3000.	0.22	3000.	0.23	3000.	0.67	

Legend: (1) Penning de Vries et al., 1988; (2) Boons-Prins et al., 1993; (3) Spitters et al., 1988



Table 5-11: Fraction of the shoot dry matter allocated to the maize cob, the maize grains not included (source: Spitters et al., 1988)

DVS	Fcob
0.	0.00
0.8	0.00
0.95	0.55
1.1	1.00
1.2	0.00
2.5	0.00

Table 5-12: Fraction of the below ground dry matter allocated to the fibrous roots of sugar beet (source: Spitters et al., 1988)

DVS	Frac fibrous root
0.	1.00
400.	1.00
500.	0.50
1000.	0.10
2000.	0.03
3000.	0.03

5.5 LEAF AREA DEVELOPMENT

Distinction is made between the area of the green leaves, dead leaves and ears for wheat species. In the model, two stages are distinguished for the computation of the green leaf area index (LAI_G). During the crop juvenile stage, leaf area development is mainly driven by temperature. An exponential equation is used to describe the leaf area development:

$$LAI_G^t = LAI_G^0 \cdot e^{k_{LAI} \cdot t} \quad (5-33)$$

where LAI_G^0 is the green leaf area index at emergence (m^2 leaf m^{-2} soil); LAI_G^t is the green leaf area index at time t (m^2 leaf m^{-2} soil); t is the time (day) and k_{LAI} is the actual LAI development rate coefficient (day^{-1}). The k_{LAI} is calculated as:

$$k_{LAI} = k_L \cdot T_e \quad (5-34)$$

where T_e is the effective temperature for this day ($^\circ C$); and k_L is the crop specific LAI development coefficient (m^2 leaf m^{-2} soil $^\circ C^{-1}$ day^{-1}), which is model input (see Table 5-13). Expanding Eq.(5-33) yields an expression of the leaf area development rate during the crop juvenile phase ($GLAI_G^t$ (m^2 leaf m^{-2} soil day^{-1})) calculated as an average over a time step Δt :



$$\begin{aligned}
 \frac{\text{LAI}_G^{t+\Delta t} - \text{LAI}_G^t}{\Delta t} &= \frac{\text{LAI}_G^0 \cdot e^{k_{\text{LAI}} \cdot (t+\Delta t)} - \text{LAI}_G^0 \cdot e^{k_{\text{LAI}} \cdot (t)}}{\Delta t} = \frac{\text{LAI}_G^0 \cdot e^{k_{\text{LAI}} \cdot (t)} \cdot e^{k_{\text{LAI}} \cdot (\Delta t)} - \text{LAI}_G^0 \cdot e^{k_{\text{LAI}} \cdot (t)}}{\Delta t} \\
 &= \frac{\text{LAI}_G^t \cdot (e^{k_{\text{LAI}} \cdot (\Delta t)} - 1)}{\Delta t} = \text{GLAI}_G^t
 \end{aligned} \tag{5-35}$$

The juvenile growth stage terminates when the green leaf area exceeds $0.75 \text{ m}^2 \text{ leaf m}^{-2} \text{ soil}$ or when a critical development stage is attained ($\text{DVS} > 0.3$ for wheat; $\text{DVS} > 450 \text{ }^\circ\text{C day}$ for potatoes and sugar beets). In the later crop stages, crop growth is increasingly restricted by the supply of assimilate. Hence, the growth rate of green LAI is obtained by multiplying the dry matter growth rate of green leaves with the specific leaf area i.e.:

$$\text{GLAI}_G^t = \text{GWLV}_G^t * \text{SLA} \tag{5-36}$$

where GWLV_G^t is the dry matter growth rate of green leaves ($\text{kg DM m}^{-2} \text{ soil day}^{-1}$) and SLA is the specific leaf area ($\text{m}^2 \text{ leaf kg}^{-1} \text{ DM}$). Except for corn, for which SLA varies as a function of DVS, the SLA is considered to be constant during the growing season (see Table 5-13).

Table 5-13: Green leaf area growth rate parameters for different crops (source: Spitters et al., 1988; Boon-Prins et al., 1993)

Crop	k_L ($\text{m}^2 \text{ m}^{-2} \text{ }^\circ\text{C}^{-1} \text{ day}^{-1}$)	SLA ($\text{ha leaf kg}^{-1} \text{ DM}$)
Winter Wheat	0.007	0.002
	0.007	0.002
Spring Wheat	0.014	0.0022
Spring Barley	0.007	0.002
Corn	0.0294	(DVS= 0.0) 0.0040 (DVS=0.7) 0.001 (DVS=2.5) 0.001 0.0294 (DVS=0.0) 0.0035 (DVS=0.78) 0.0016 (DVS=2.00) 0.0016
Potato	0.012	0.003
	0.012	(DVS=0.0) 0.003 (DVS=1.1) 0.003 (DVS=2.0) 0.0015
Sugar Beet	0.0156	0.002
	0.0160	0.002



The leaf area growth rate decreases during the late season mainly due to senescence, but also due to self shading or chilling temperatures. This process is described in the model by considering a dead leaf area growth rate which is subtracted from the green leaf area growth rate. The growth rate of the dead leaf area is calculated as:

$$\text{GLAI}_D^t = \frac{\text{LAI}_G^t \cdot (e^{k_{D_LAI} \cdot (\Delta t)} - 1)}{\Delta t} \quad (5-37)$$

where GLAI_D^t equals the dead leaf area growth rate ($\text{m}^2 \text{ death leaf m}^{-2} \text{ soil day}^{-1}$) and k_{D_LAI} , the dead leaf area growth rate constant ($\text{m}^2 \text{ death leaves m}^{-2} \text{ soil day}^{-1}$). The following procedures are used to asses k_{D_LAI} for different crops.

For winter and spring wheat, k_{D_LAI} is composed of a component to account for senescence ($k_{D_LAI_SENES}$) and self shading ($k_{D_LAI_SHADE}$). If DVS<1, then $k_{D_LAI_SENES} = 0$. If, however, DVS>1, this parameter is taken from an input table, which specifies $k_{D_LAI_SENES}$ as a function of DVS (Table 5-14). The potential $k_{D_LAI_SENES}$ increases with increasing DVS. This is mimicked by multiplying the potential $k_{D_LAI_SENES}$ with a DVS dependent weighing function, which is input in a separate table (Table 5-15). The component of the k_{D_LAI} , due to self shading is calculated with the empirical equation:

$$0.0 < k_{D_LAI_SHADE} = 0.03 \left(\frac{\text{LAI}_G^t - \text{LAI}_{cr}}{\text{LAI}_{cr}} \right) < 0.03 \quad (5-38)$$

The critical leaf area, LAI_{cr} , for which this process starts, is input and usually set equal to 4.0. The actual k_{D_LAI} is taken as the maximum of $k_{D_LAI_SENES}$ and $k_{D_LAI_SHADE}$ rate coefficient.

A similar procedure is used for spring wheat or spring barley, but the $k_{D_LAI_SENES}$ is not weighed in function of the development stage. Hence only LAI_{cr} and $k_{D_LAI_SENES}(Te)$ are input.

For corn, the k_{D_LAI} consists of three components, the $k_{D_LAI_SENES}$, the $k_{D_LAI_SHADE}$ and $k_{D_LAI_CHILL}$. All components are calculated using default empirical equations. Only the critical leaf area, LAI_{cr} is input.

For potato, the $k_{D_LAI_SENES}$ and $k_{D_LAI_SHADE}$ are calculated using default empirical equations. Only the LAI_{cr} is input.

For sugar beets, a slightly modified senescence rate constant is used. The $k_{D_LAI_SENES_MOD}$ ($\text{m}^2 \text{ m}^{-2} \text{ }^\circ\text{C day}^{-1}$) is input in the model as a function of DVS (Table 5-16).

The calculated dead leaf area growth rate is used to estimate the contribution of dead leaves in the total dry matter weight:



$$GWLVD = GLAID * \frac{WLVG}{LAIG} \quad (5-39)$$

where GWLVD is the dry matter growth rate of the dead leaves ($\text{kg DM m}^{-2} \text{ soil day}^{-1}$); GLAID is the leaf area growth rate of the dead leaves ($\text{m}^2 \text{ leaf m}^{-2} \text{ soil day}^{-1}$); WLVG is the dry matter of green leaves ($\text{kg DM m}^{-2} \text{ soil}$); and LAIG is the green leaf area ($\text{m}^2 \text{ leaf m}^{-2} \text{ soil}$).

Table 5-14: Senescence component of the growth rate coefficient of the death leaf area ($\text{m}^2 \text{ leaf m}^{-2} \text{ soil day}^{-1}$) as a function of effective temperature for winter wheat and spring wheat (source: Spitters et al., 1988)

Crop	Te (°C)	k _{D_LAI_SENES} ($\text{m}^2 \text{ m}^{-2} \text{ day}^{-1}$)
Winter Wheat	0.	0.03
	10.	0.03
	15.	0.04
	30.	0.09
Spring Wheat	0.	0.03
	10.	0.03
	15.	0.04
	30.	0.09

Table 5-15: Weighing function for the senescence component of the death leaf area growth rate as a function of development stage (source: Spitters et al., 1988)

Crop	DVS (-)	WEIGHT_KD_ LAI SENES
Winter Wheat	0.00	0.00
Winter Barley	0.59	0.00
	0.60	0.085
	0.89	0.085
	0.90	0.500
	1.09	0.500
	1.10	1.000
	2.50	1.000



Table 5-16: Modified senescence component of the growth rate coefficient of the death leaf area (m^2 leaf m^{-2} soil $^{\circ}C$ day $^{-1}$) as a function of development stage for sugar beet (source: Spitters et al., 1988)

Crop	DVS ($^{\circ}C$)	$k_{D_LAI_SENES_MOD}$ ($m^2 m^{-2} ^{\circ}C day^{-1}$)
Sugar beet	0.	0.0000
	600.	0.0000
	1000.	0.00022
	1500.	0.00050
	2500.	0.00075

When the DVS exceeds 0.8 wheat ears also play an important role in the photosynthetic process. For the calculation of the carbon assimilation rate, the one sided ear area ratio is added to the LAI of the green leaves. The growth rate of the ear area is expressed according to:

$$GEAI = EAR * (WLV + WST + WSO) \quad (5-40)$$

where GEAI is the total ear area growth rate (m^2 ear m^{-2} soil day $^{-1}$) and EAR is the ear area ratio growth rate (m^2 ear kg^{-1} DM day $^{-1}$). In the model, the initial ear area index (EAI) and EAR ($0.000063 m^2$ ear kg^{-1} DM day $^{-1}$) are input.

5.6 ROOTING DEPTH AND ROOT DENSITY DEVELOPMENT

At emergence an initial rooting depth of 3.5 cm is assumed. The increase in root depth is driven by temperature and is expressed with the following empirical expression:

$$DAINCR = 0.22 * TEMPFACT \quad (5-41)$$

where DAINCR is the rooting depth growth rate (cm day $^{-1}$). The temperature factor (TEMPFACT) is set equal to an effective temperature and 0.22 ($cm ^{\circ}C^{-1}$ day $^{-1}$) is an empirical constant. When air temperature drops below zero during the growing season, a correction mechanism is included to account for the heat capacity of the soil on soil temperature. The rooting depth increases until a maximal value, specified by the user, is reached. Compiled literature values for maximal rooting depth are given in Table 5-17.

The root density is calculated independently from the rooting depth, using the simulated dry matter in the root system and a mean value for the specific root length (cm root g^{-1} soil). To calculate the root density development, the accumulated root weight is translated into enlarged root length using a mean specific root length factor



(cm root g⁻¹ soil). The accumulated root length is then divided into the different soil compartments using a weighing factor. The equation yields:

$$RDENS_i = \frac{SPECWEIG * WRT * WEIGHT_i}{10^8 * \Delta x_i} \quad (5-42)$$

where RDENS_i is the root length density of the compartment i (cm root cm⁻³ soil), WRT the total root dry matter weight (kg root DM ha⁻¹ soil), SPECWEIG the specific root weight (cm root g⁻¹ root DM) and Δx_i the thickness of compartment i (cm). The weighing function WEIGHT_i and the specific root weight SPECWEIG are input in the model and can be selected from Table 5-17.

Table 5-17: Crop specific root data taken from literature reviews: (1) Van Noordwijk and Brouwer, 1991; (2) Winlo B.P., 1974. Values between brackets are estimated ranges

Crop	Maximum rooting depth (cm)	SPEC-WEIG (m g ⁻¹)	WEIGHT (00-30 cm)	WEIGHT (30-60 cm)	WEIGHT (60-90 cm)	Ref.
Winter wheat	90.3 (34-160) (75-105)	174 (70-268)	0.65 (0.57-0.78)	0.25 (0.19-0.30)	0.09 (0.02-0.13)	1
						2
Barley	57.5 (20-140) (90-105)	160 (112-202)	0.64 (0.55-0.76)	0.29 (0.15-0.43)	0.05 (0.009-0.07)	1
						2
Oats	67 (40-100) (60-75)	59 (21-97)	0.65 (0.55-0.76)	0.29 (0.25-0.43)	0.04 (0.01-0.08)	1
						2
Corn	105 (40-183) (60-90)	101 (8.2-280)	0.65 (0.5-0.87)	0.25 (0.06-0.44)	0.08 (0.-0.22)	1
						2
Sugar beet	66 (40-90) (130-200)	34.6 (122-741)	0.81 (0.58-0.84)	0.19 (0.15-0.26)	0.03 (0.-0.15)	1
						2
Potato	64 (20-100) (100-130)	234	0.65 (0.62-0.69)	0.29 (0.29-0.30)	0.04 (0.-0.08)	1
						2



5.7 REFERENCES

- Boons-Prins, E.R., G.H.J. de Koning, C.A. van Diepen and F.W.T. Penning de Vries, 1993. Crop specific parameters for yield forecasting across the European Community. Simulation Report CABO-TT (32), Wageningen, The Netherlands, 43 pp.
- Penning de Vries, F.W.T., D.M. Jansen, H.F.M. Ten berge and A.H. Bakema, 1988. Simulation of eco-physiological processes of growth of several annual crops. Simulation Monographs, PUDOC-IRRI, Wageningen, The Netherlands.
- Penning de Vries, F.W.T. and H. van Laar, 1982. Simulation of plant growth and crop production. Simulation Monographs, PUDOC, Wageningen, The Netherlands.
- Spitters, C.J.T., H. van Keulen and D.W.G. Van Kraailingen, 1988. A simple but universal crop growth simulation model, SUCROS87. In: R. Rabbinge, H. Van Laar and S. Ward (eds.). Simulation and systems management in crop protection. Simulation Monographs, PUDOC, Wageningen, The Netherlands.
- Spitters, C.J.T., H.A.J. Toussaint and J. Goudriaan, 1986. Separating the diffuse and direct component of global radiation and its implications for modelling canopy photosynthesis. Part I. Components of incoming solar radiation. Agricultural and Forest Meteorology, 38:217-229.
- Spitters, C.J.T., 1986. Separating the diffuse and direct components of global radiation and its implications for modelling canopy photosynthesis. Part II. Calculation of canopy photosynthesis. Agricultural and Forest Meteorology, 38:231-242.
- van Keulen, H. and J. Wolf, 1986. Modelling of agricultural production : weather, soils and crops. Simulation Monographs, PUDOC, Wageningen, The Netherlands, 464 pp.
- van Keulen, H., F.W.T. Penning de Vries and E.M. Drees, 1982. A summary model for crop growth. In: Penning de Vries F.W.T. and H. van Laar (eds.). Simulation of plant growth and crop production. Simulation Monographs, PUDOC, Wageningen, The Netherlands, 87-97.
- Van Noordwijk, M and G. Brouwer, 1991. Review of quantitative root length data in agriculture. In: B.L. McMichael and H. Persson (eds.) Plant roots and their environment. Elsevier, 515-525.
- Winlo, B.P., 1974. A practical guide to irrigation. NCAE, Silsoe, England, 60

THE NITROGEN FATE

MODULE



6 THE NITROGEN FATE MODULE

6.1 INTRODUCTION

The fate of nitrogen in the soil is determined by different processes (Fig.6-1). Nitrogen can enter the soil environment through atmospheric deposition (rainfall and dry deposition), fertilizer application, organic matter addition or through nitrogen fixation by rhizobia. Nitrogen can leave the soil environment through nitrogen denitrification, volatilization, plant uptake or leaching. Mineralization from organic into mineral nitrogen, immobilization from mineral nitrogen in organic matter, nitrification from ammonia to nitrate and denitrification change the form, and so, the properties of nitrogen in the soil. Each of these processes has been the subject of intensive studies. Simulation models have been used for the description of the different subprocesses (Van Veen, 1977; Rachhpal-Singh and Nye, 1988; Verbruggen, 1985; De Willigen and Noordwijk, 1987, amongst others). However, to be of use for policy makers and to be able to solve a number of problems, an integrated model of the nitrogen cycle is required.

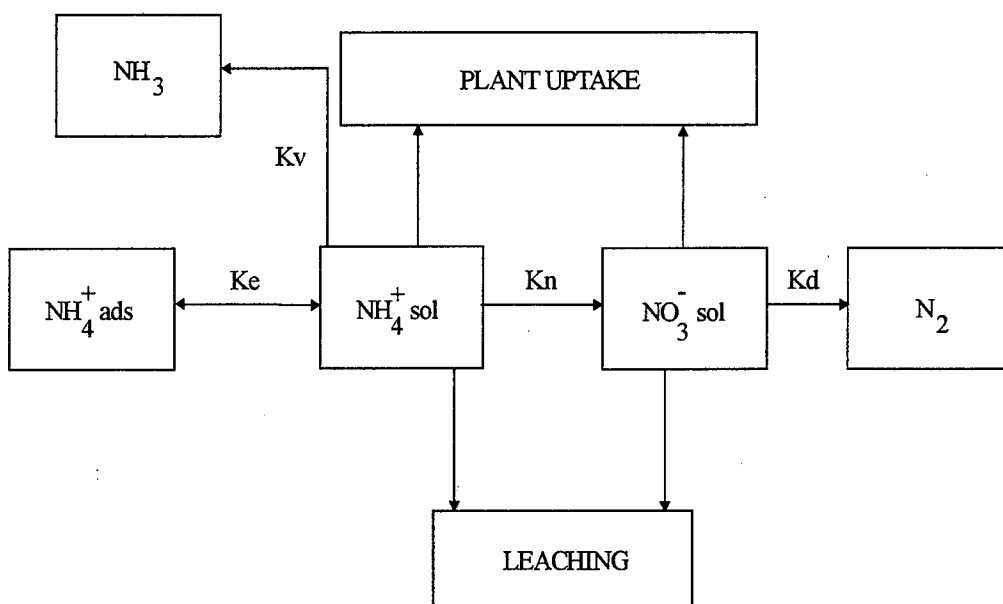


Fig.6-1 : Schematic flow chart of the nitrogen cycle.

Different levels of complexity exist for describing the nitrogen transfer and transformation processes. The complexity level of a selected model will strongly depend on the desired level of explanation. A simple, first order decay model for the mineralization of the organic nitrogen might give a good description of the mineralization processes shortly after an organic matter addition. However such a model might fail to describe the long term mineralization process involving the



decomposition of the organic matter fractions. A detailed model description, on the other hand reduces the model applicability for extrapolative purposes. Parameters describing the transformation processes of nitrogen for a wide set of soil and management scenarios are still lacking at this moment.

The nitrogen module used in the WAVE-model, was originally developed by Vereecken et al. (1990, 1991) and named SWATNIT (Simulating WATer and NITrogen). The nitrogen module describes the transformation processes for the organic and inorganic nitrogen in the soil. Also, the uptake of nitrogen by the plants is described by means of a sink term added to the transport equation. The potential transformation rates, which are model input, are reduced for temperature and moisture content in the soil profile. The model compromises research findings with field results. For the processes which are believed to be better understood and for which relevant data are available a more complex approach is used. Other processes, such as soil denitrification or volatilization, are described using simple kinetics.

6.2 MODELLING OF NITROGEN TRANSFORMATIONS IN SOILS

6.2.1 MINERALIZATION OF THE SOIL ORGANIC NITROGEN

Organic nitrogen transformations and resulting mineralization of organic carbon and nitrogen are described using a three pool concept as reported by Johnsson et al. (1987) and shown in Fig.6-2. These authors distinguish a fast cycling pool of organic matter/microbial bio-mass complex (soil litter pool), receiving fresh organic matter and a slow cycling pool of stabilized decomposed products (soil humus pool). Because of the different properties of the applied slurry or manure, a third pool (soil manure pool) is distinguished. The soil bio-mass, which constitutes 1 to 5 % of the soil organic matter, though being the eye of the needle where all the organic material at least once passes through (Jenkinson and Ladd, 1981; Dendooven, 1990), is not modelled explicitly. However, it is assumed that the nitrogen demand for the internal cycling of carbon and nitrogen in the three pools, which is modelled explicitly, is regulated by a constant C/N ratio of the soil bio-mass, which is model input. In addition, it is assumed that the C/N ratio of the turn-over metabolites equals the C/N ratio of the soil bio-mass. Consequently, this C/N ratio controls the soil mineral nitrogen release from the three organic matter pools.

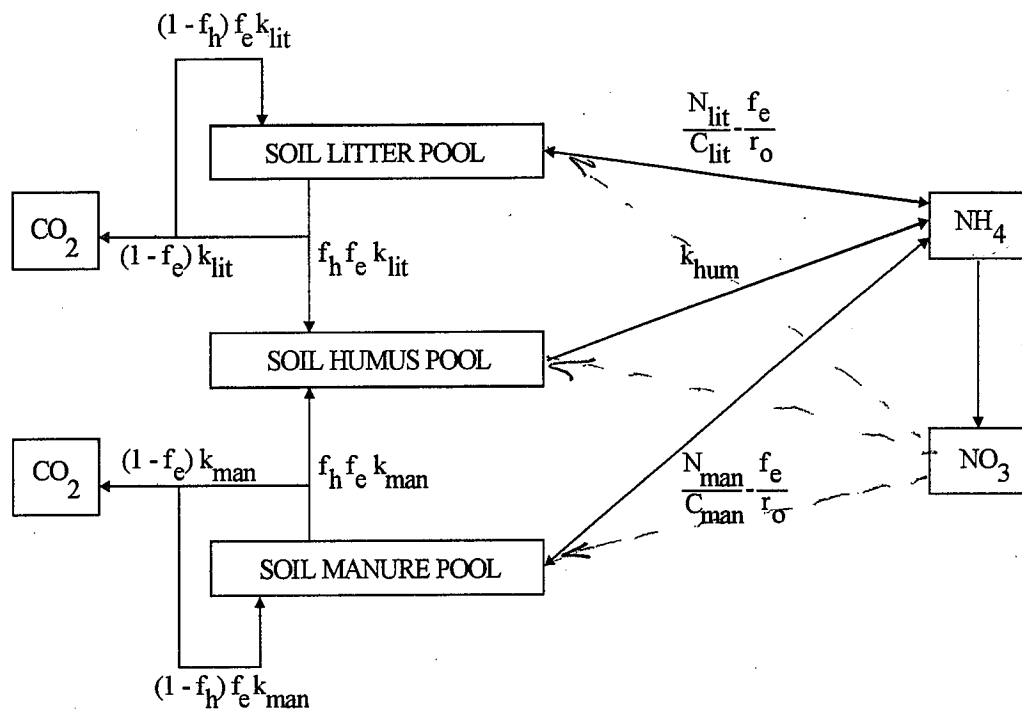


Fig. 6-2: Organic matter turnover concept as applied in the nitrogen fate module (Johnsson et al., 1987)

The turnover of the carbon in the litter pool is represented by the upper loop in Fig. 6-2. The fraction of C in te litter pool which is turned over per unit time equals $k_{lit} \cdot C_{lit}$. The turn-over efficiency f_e (-) determines which fraction is effectively transformed into new organic matter through the bio-mass and which fraction is decomposed. The humification constant f_h determines next which fraction of the effectively turned-over C goes to the humus pool. Hence, the net increase of C in the litter pool is written as:

$$\frac{\partial C_{lit}}{\partial t} = IN - OUT = [(1 - f_h)f_e - 1]k_{lit}C_{lit} \quad (6-1)$$

where C_{lit} is the carbon content of the litter pool (kg C m^{-3} soil); f_h is the dimensionless humification constant (-); f_e is the dimensionless turn-over efficiency (-); k_{lit} is the decomposition rate of the litter (day^{-1}).

During the turn-over of the litter-C, N-immobilization or N-mineralization can occur, depending on the C/N ratio's of the litter (C_{lit}/N_{lit}) and the bio-mass (r_o). From Eq. (6-1) it follows that the net increase of the N-content in the litter pool is written as:

$$\frac{\partial N_{lit}}{\partial t} = \left[(1 - f_h)f_e \frac{1}{r_o} - \frac{N_{lit}}{C_{lit}} \right] k_{lit}C_{lit} \quad (6-2)$$



where N_{lit} is the N-content of the litter pool (kg N m^{-3} soil) and r_o is the bio-mass C/N ratio. In Eq. (6-2) it is assumed that the turn-over metabolites have the same C/N ratio as the bio-mass (r_o).

For the manure pool, a similar turn-over loop is represented in the Fig. 6-2. Equation similar to Eqs. (6-1) and (6-2) can be written as follows:

$$\frac{\partial C_{man}}{\partial t} = [(1 - f_h)f_e - 1]k_{man}C_{man} \quad (6-3)$$

$$\frac{\partial N_{man}}{\partial t} = \left[(1 - f_h)f_e \frac{1}{r_o} - \frac{N_{man}}{C_{man}} \right] k_{man}C_{man} \quad (6-4)$$

where C_{man} and N_{man} are respectively the C content (kg C m^{-3} soil) and N-content (kg N m^{-3} soil) in the manure pool; and k_{man} is the decomposition rate of the manure pool (day^{-1}). It is assumed that the same f_e and f_h constants apply for the litter and manure pools. From Fig. 6-2 it can be seen that the net increase rate of C and N in the humus pool is written as:

$$\begin{aligned} \frac{\partial C_{hum}}{\partial t} &= f_e f_h (k_{lit}C_{lit} + k_{man}C_{man}) - k_{hum}C_{hum} \\ \frac{\partial N_{hum}}{\partial t} &= \frac{f_e f_h}{r_o} (k_{lit}C_{lit} + k_{man}C_{man}) - k_{hum}N_{hum} \end{aligned} \quad (6-5)$$

where C_{hum} and N_{hum} are respectively the C content (kg C m^{-3} soil) and N content (kg N m^{-3} soil) in the humus pool; and k_{hum} is the decomposition rate of the humus pool (day^{-1}). All C/N turn-over reactions represented in Fig. 6-2 can result in a net production or consumption of ammonium, depending on the C/N ratio's of the bio-mass and the three pools. As the increase of $\text{NH}_4^+ \text{-N}$, due to mineralization is equal to the decrease of organic N in the three organic matter pools, we obtain from the Eqs. (6-2), (6-4) and (6-5):

$$\frac{\partial N_{\text{NH}_4^+}}{\partial t} = \left[\frac{N_{lit}}{C_{lit}} - \frac{f_e}{r_o} \right] k_{lit}C_{lit} + \left[\frac{N_{man}}{C_{man}} - \frac{f_e}{r_o} \right] k_{man}C_{man} + k_{hum}N_{hum} \quad (6-6)$$

Eq.(6-6) determines whether mineralization (right hand side of the equation is positive) or immobilization (right hand side is negative) is occurring. In case no ammonium is available for immobilization, nitrate is used as given by the following equation:

$$\frac{\partial N_{\text{NO}_3^-}}{\partial t} = -\frac{f_e}{r_o} (k_{lit}C_{lit} - k_{man}C_{man}) \quad (6-7)$$



Equations (6-1) to (6-7) are integrated numerically using the Euler integration method. The resulting mineralization/immobilization rates enter the sink term of the solute transport equation.

In order to account for soil water and temperature effects on the organic matter turn-over, the potential rate constants, k_{lit} , k_{man} and k_{hum} are reduced. It is assumed that between a low ($pF=3$) and high ($pF=2$) critical moisture content no reduction occurs. In non-optimal conditions a reduction factor is derived by linear interpolation between 1 and 0 in the moisture content interval ($\theta(pF=3)-\theta(\text{oven dryness})$), and between 0 and 1 in the moisture content interval ($\theta(\text{saturation})-\theta(pF=2)$). The effect of soil temperature is considered through a default Q_{10} ($Q_{10}=3$) reduction function.

$$\text{REDTEMP} = 3^{\left(\frac{T-16}{10}\right)} \quad (6-8)$$

where T is the soil temperature ($^{\circ}\text{C}$).

A compilation of literature data on the bio-mass C/N ratio r_0 , is listed in Table 6-1.

For solving the mineralization equations the organic matter pools need to be initialized. The distribution of the organic matter in both the nitrogen and carbon fraction of the three pools is model input. Paul and Juma (1981) stated that 92 % of the organic matter in the soil can be situated in the stable humic pool. This figure can be used to initialize the humus pool. The remaining soil organic matter can then be distributed equally over the litter and manure pool. In practice, a warm-up period of several years to equilibrate the nitrogen and carbon content in the different pools is recommended.

The turn-over of the organic matter is further controlled by the carbon turn-over efficiency. The carbon turn-over efficiency equals the fraction of the mineralized carbon which turns over in the organic matter immediately and hence is not lost as carbon dioxide. This fraction governs the amount of immobilized or mineralized nitrogen through the given constant C/N ratio of bio-mass and metabolization products. Carbon turn-over efficiency values range between 10 and 60 % depending on the kind of substrate or decomposing micro-organisms. Compiled literature data (Dendooven, 1990) for this parameter are given in Table 6-2. A part of the soil organic carbon which turns over is incorporated in the humus pool of the soil. This fraction is controlled by the humification coefficient which can be set equal to e.g. 0.2 (Johnson et al., 1987). The carbon turn-over efficiency constant and humification coefficient are model input.



Table 6-1: C/N ratio's of soil bio-mass as reported in literature (source: Dendooven, 1990)

C/N ratio ro	Bio-mass type
6	C/N Bio-mass
8	C/N Bio-mass
6	C/N Bio-mass
8	C/N Bio-mass
8	C/N Bio-mass
30	C/N Bio-mass structural
3	C/N Bio-mass metabolic
6	C/N Bio-mass
6	C/N Bio-mass
8	C/N Bio-mass
8	C/N Bio-mass
10	C/N Bio-mass
6	C/N Bio-mass
10	Bio-mass
3	Protein
1.31	RNA
17	Bacterial polysacchariden
5	Bacterial cells
10	Fungi
5	Actinomycetes
3-7	Bacteria
5	Bacillus Cereus
8-18	Bacillus Cereus + extra cellular products
2-4	Enterobacter Aerogenes
4-5	Klebsiella Aerogenes
4-9	Candida Utilis
5.2	Yeast
11-22	Fungi
5-43	Fungi
6-21	Fungi
4-21	Fungi
5-27	Fungi
5	Bacteria
15	Fungi
5	Yeast (grown on carbohydrate)
4	Bacterium (methanol)



*Table 6-2: Efficiency constants of the carbon assimilation as reported in literature
(source: Dendooven, 1990)*

f_e	Description
0.5	Carbonaceous compounds in soil
0.4	Efficiency of carbon assimilation
0.6	Efficiency of carbon assimilation for metabolite C, metabolite C+N, decomposable C, slowly decomposable C
0.4	Active fraction, stabilized C+N, old C+N
0.6	Efficiency of carbon assimilation
0.4-0.6	Efficiency of carbon assimilation assuming only aerobic growth
0.6	Glucose utilization efficiency
0.4	Well decomposable pool
0.2	Active, but protected, and old pool
0.25	Recalcitrant pool utilization efficiency
0.35-0.37	Bacteria
0.18	Bacteria poor aeretion
0.38	Bacteria high aeretion
0.40	Bacteria
0.61	Aerobacter, glycerol limited
0.55	Candida utilis
0.60	Bacteria in situ
0.60	Fungi in situ
0.40	Soil organisms in situ
0.05-0.10	Bacteria
0.3-0.4	Fungi
0.15-0.30	Actinomycetes
0.40-0.80	Bacillus Cereus
0.23-0.37	Bacillus Cereus
0.60	Heterotrophs, average over many papers
0.40-0.65	Klebsiella, glycerol limited
0.53-0.59	Candida Utilis, glycerol limited
0.58-0.68	Candida Utilis, methanol limited
0.58	Yeast (carbohydrate)
0.58	Bacteria (methanol)
0.50	Yeast (n-paraffin)
0.48-0.55	Pennicillium Chrysogenum

The mineralization or immobilization of soil organic matter from the different pools is governed by the potential decomposition rates. Literature values of possible decomposition rates, for the different organic matter fractions, are given in the Tables 6-3, 6-4 and 6-5.



Table 6-3: Decomposition rate of soil litter as reported in literature (source: Dendooven, 1990)

k_{lit} (day⁻¹)	Type
0.04	Rye straw in Nigeria
0.01	Rye straw in England
0.008	Wheat straw (summer)
0.003	Wheat straw (year)
0.08	Wheat straw (laboratory)
0.0822	Litter in virgin grass land
0.00986	Litter in cultivated land
0.02	Roots, well decomposable
0.002	Roots, recalcitrant
0.2	Soluble compounds as in straw
0.08	(Hemi-)cellulose as in straw
0.2	Proteins as in straw
0.02	Lignin as in straw
0.0155	Decomposable plant material
0.0008	Resistant plant material

Table 6-4: Decomposition rate of soil manure as reported in literature

k_{man} (day⁻¹)	Reference
0.035	Johnson et al., 1987
0.0014	Wadman and Ehlert, 1989
0.0020	Wadman and Ehlert, 1989
0.001	Gilmour and Gilmour, 1980

Table 6-5: Decomposition rate of soil humus as reported in literature

k_{hum} (day⁻¹)	Reference
0.00007	Vereecken et al., 1990
0.0070	Nuske and Richter, 1981
0.0015	Nuske and Richter, 1981
0.0005	Richter and Nordmeyer, 1982
0.00052	Richter et al., 1982
0.00022	Richter et al., 1982
0.0011	Nordmeyer and Richter, 1985
0.0059	Nordmeyer and Richter, 1985



6.2.2 DENITRIFICATION

Due to the anaerobic respiration of soil bacteria, soil nitrate-nitrogen is reduced to gaseous nitrogen forms such as N_2O and N_2 . The soil pH, the texture, the organic carbon supply, the amount of crop residues, the soil temperature, the soil mineral nitrate availability, the soil aeration and moisture status, among others, are factors controlling the denitrification in field conditions. In the nitrogen module of WAVE, a first order kinetic approach is used to assess the soil denitrification. The anaerobic respiration is not linked to turn-over model for the organic matter. The following equations are used:

$$\frac{\partial [\text{NO}_3^-]}{\partial t} = k_{\text{denit}} \cdot [\text{NO}_3^-] \quad (6-9)$$

where NO_3^- is the nitrate concentration in the soil water and k_{denit} is a first order denitrification constant (day^{-1}).

Few studies are available yielding potential denitrification rates for a range of soil types. Breeuwsma et al. (1991) report on potential soil denitrification rates, based on the soil texture, carbon content and mean groundwater level. The following relations are suggested for sandy and clay soils under Dutch conditions:

$$\begin{aligned} k_{\text{denit}} &= 0.41 * \text{Carbon}(\%) - 0.35 * \text{mean groundwater level (m)} \text{ for sandy soils} \\ k_{\text{denit}} &= 0.51 - 0.049 * \text{Clay}(\%) + 0.20 * \text{Carbon}(\%) \text{ for clay soils} \end{aligned} \quad (6-10)$$

The potential denitrification rate is reduced using the Q_{10} temperature reduction function (Eq.(6-8)). The effect of the soil moisture status on denitrification is assessed through the use of the soil water reduction factor for denitrification, R_w (Johnsson et al. 1987; Aulakh et al., 1992):

$$\begin{aligned} R_w &= \left(\frac{\theta - \theta_d}{\theta_s - \theta_d} \right)^d && \text{if } Se > 0.8 \\ R_w &= 0. && \text{if } Se < 0.8 \end{aligned} \quad (6-11)$$

where θ_d is a critical threshold value, corresponding to a saturation degree of 0.80, and d an empirical constant, set equal to 2.

6.2.3 VOLATILIZATION

In the soil environment ammonia might be present in gaseous form. If conditions are favourable ($\text{pH} > 7.5$) and the partial pressure head gradient between NH_3 in the soil and the atmosphere is sufficiently large, ammonia gas can volatilize. Ammonia volatilization in WAVE is simulated using a first order kinetic approach.



6.2.4 NITRIFICATION

Nitrification, which transforms ammonia-N to nitrate-N and which is ruled by heterotrophic soil organisms, is modelled using a first order kinetic equation. Since soil nitrification is controlled by the soil bio-mass, the former defined temperature and water reduction (see section 6.2.1) mechanisms are applied.

6.2.5 HYDROLYSIS OF UREA

The hydrolysis of urea, which is a basic constituent of many inorganic and organic fertilizers, is modelled using a first order kinetic approach. Again, temperature and water stress reduction mechanisms are considered (see section 6.2.1).

6.2.6 UPTAKE OF AMMONIA AND NITRATE

The nitrogen uptake by plants is described using a macroscopic uptake model as proposed by Mc Isaac et al. (1985) and adapted by Huwe and van der Ploeg (1988). The macroscopic uptake component restricts the nitrogen uptake rate to a potential level.

If crop growth is not modelled, the potential uptake rate ($\partial N / \partial t_p$) is calculated as:

$$\begin{aligned} \left. \frac{\partial N}{\partial t} \right|_p &= A * t * (G - t) && \text{for } t < G \\ \left. \frac{\partial N}{\partial t} \right|_p &= 0 && \text{for } t \geq G \end{aligned} \quad (6-12)$$

where G the time when the plant N uptake stops (day), A a parameter to assure that in non-stressed conditions the maximum N uptake is reached ($\text{mg m}^{-2} \text{ day}^{-3}$). Integrating Eq. 6-12 yields $N = AGt^2/2 - At^3/3$ which in optimal conditions ($t=0, N=0; t=G, N=N_{\max}$) enables to calculate A as $A = N_{\max}/(G^2/2 - G^3/3)$. The user has to specify a value for G and for the maximum N uptake (mg m^{-2}). To simplify the input, G is input as a fraction of the total growing season. Hence, its value must range between 0 and 1.

If crop growth is modelled the potential uptake rate is simulated as:

$$\left. \frac{\partial N}{\partial t} \right|_p = \left. \frac{\partial N}{\partial t} \right|_{leaves} + \left. \frac{\partial N}{\partial t} \right|_{stems} + \left. \frac{\partial N}{\partial t} \right|_{roots} \quad (6-13)$$

where the right hand term of Eq.(6-13) refer to the nitrogen demand of the leaves, stems and roots, respectively. The potential uptake rates for leaves, stems and roots is modelled with:



$$\begin{aligned}
 \left. \frac{\partial N}{\partial t} \right|_{p, \text{leaves}} &= WLV * XNCLE - N_{\text{leaves}} \\
 \left. \frac{\partial N}{\partial t} \right|_{p, \text{stems}} &= WST * XNCST - N_{\text{stems}} \\
 \left. \frac{\partial N}{\partial t} \right|_{p, \text{roots}} &= WRT * XNCRT - N_{\text{roots}}
 \end{aligned} \tag{6-14}$$

where WLV, WST, WRT is the accumulated dry matter (kg ha^{-1}); XNCLE, XNCST, XNCRT the potential fraction of nitrogen N in the crop dry matter ($\text{kg N kg}^{-1} \text{ DM}$); and N_{stems} , N_{leaves} and N_{roots} is the nitrogen N accumulated in the leaves, the stems and the storage organs. The fraction of the nitrogen N in the leaves, XNCLE, is input as a function of crop development stage. The fraction of nitrogen N in the stems and roots is assumed to be 50 % of the fraction in the leaves.

The potential nitrogen uptake rate is further divided in a convective and diffusive fraction. The potential convective nitrogen uptake rate ($\text{mg m}^{-2} \text{ day}^{-1}$) is defined as:

$$\left. \frac{\partial N}{\partial t} \right|_{\text{conv}} = \int_0^{z_{\max}} S_w \cdot C_m \cdot dx \tag{6-15}$$

where z_{\max} is the rooting depth at time t (mm), C_m is the concentration of either nitrate or ammonia in the soil water (mg l^{-1}), and S_w is the convective root water uptake rate (day^{-1}). The convective root water uptake is calculated in the water flow module of WAVE. The convective uptake rate is limited to the potential uptake rate. If the convective uptake rate is smaller than the potential, a potential diffusive nitrogen uptake rate is calculated:

$$\left. \frac{\partial N}{\partial t} \right|_{\text{difp}} = \left. \frac{\partial N}{\partial t} \right|_p - \left. \frac{\partial N}{\partial t} \right|_{\text{conv}} \tag{6-16}$$

The maximum diffusive nitrogen uptake rate, for both nitrate and ammonia, is calculated as:

$$\left. \frac{\partial N}{\partial t} \right|_{\text{dif max}} = \int_0^{z_{\max}} \frac{2 \cdot \pi \cdot RDENSi \cdot RORAD \cdot Dif(\theta) \cdot Cmi \cdot \theta}{10^5 \cdot D0} dx \tag{6-17}$$

where RDENSi is the root density (cm l^{-1}); RORAD the mean root radius (mm); Dif(θ) is the chemical diffusion coefficient in a soil ($\text{mm}^2 \text{ day}^{-1}$); $1/D0$ the travel distance resistance between the bulk soil solution and the root (1/mm); Cmi the concentration of either nitrate or ammonia in the soil solution (mg l^{-1}) and dx the depth increment (mm). The maximum diffusive uptake rate is limited to the potential diffusive uptake rate. If the SUCROS-model is used, RDENSi is directly obtained



from the crop growth module ($1000 * \text{RLDFL} (\text{cm cm}^{-3}) = \text{RDENSi} (\text{cm l}^{-1})$). If no crop growth model is used, the root density function is simulated with an exponential decreasing function :

$$\text{RDENS} = \text{RDENS}_0 \cdot e^{-\text{alfa_rdens} \cdot x} \quad (6-18)$$

where $\text{RDENS}_0 (\text{cm l}^{-1})$, the root density at the soil surface and $\text{alfa_rdens} (-)$ are model input.

The total actual uptake rate is calculated as the sum of the actual convective and the diffusive uptake rate or:

$$\frac{\partial N}{\partial t} \Big|_{act} = \frac{\partial N}{\partial t} \Big|_{conv} + \frac{\partial N}{\partial t} \Big|_{dif} \quad (6-19)$$

If crop growth is modelled, the actual uptake rate in the different crop components is modelled according to:

$$\begin{aligned} \frac{\partial N}{\partial t} \Big|_{act, leaves} &= \frac{\partial N}{\partial t} \Big|_{pot} \left(\frac{\partial N}{\partial t} \Big|_{act} - \frac{\partial N}{\partial t} \Big|_{pot} \right) - \frac{\partial N}{\partial t} \Big|_{storage, organs} \left(\frac{WLV}{WLV + WST} \right) \\ \frac{\partial N}{\partial t} \Big|_{act, stems} &= \frac{\partial N}{\partial t} \Big|_{pot} \left(\frac{\partial N}{\partial t} \Big|_{act} - \frac{\partial N}{\partial t} \Big|_{pot} \right) - \frac{\partial N}{\partial t} \Big|_{storage, organs} \left(\frac{WST}{WLV + WST} \right) \\ \frac{\partial N}{\partial t} \Big|_{act, roots} &= \frac{\partial N}{\partial t} \Big|_{pot} \left(\frac{\partial N}{\partial t} \Big|_{act} - \frac{\partial N}{\partial t} \Big|_{pot} \right) \\ \frac{\partial N}{\partial t} \Big|_{act, storageorgans} &= \frac{\partial N}{\partial t} \Big|_{pot} = (WSO * XNCSO - N_{storage, organs}) * REDFACT \end{aligned} \quad (6-20)$$

The reduction factor is calculated using:

$$\begin{aligned} \text{REDFACT} &= 1 - \sqrt{1 - \text{NITRED}} \\ 0 \leq \text{NITRED} &= \left(\frac{\text{ANCL} - \text{RLNCL}}{\text{RMNCL} - \text{RLNCL}} \right) \leq 1 \end{aligned} \quad (6-21)$$

where ANCL is the actual nitrogen fraction in the leaves, RMNCL the leaf nitrogen threshold concentration for unrestricted growth assumed to be $0.5 * \text{XNCLE}$ and RLNCL the leaf nitrogen threshold concentration below which there is no growth anymore, assumed to be equal to $0.005 \text{ kg N kg}^{-1} \text{ DM}$. The potential fraction of nitrogen N of the storage organs, XNCSO ($\text{kg N kg}^{-1} \text{ DM}$), is set default equal to



0.0125 kg N kg⁻¹ DM for winter and spring wheat, 0.025 kg N kg⁻¹ DM for potatoes and maize and 0.075 kg N kg⁻¹ DM for sugar beet. This uptake model of the different crop components is based on the PAPRAN model (Seligman and van Keulen, 1981).

6.3 REFERENCES

Aulakh, M.S., J.W. Doran and A.R. Mosier, 1992. Soil denitrification significance, measurements and effects of management. *Advances in Soil Sci.*, 18:2-42.

Dendooven, L., 1990. Nitrogen mineralization and nitrogen cycling. Ph.D dissertation, Faculty of Agric. Sciences, K.U. Leuven, Belgium, 112 pp.

De Willigen, P. and M. Van Noordwijk, 1987. Roots, plant production and nutrient use-efficiency. Ph.D. dissertation, Agricultural University Wageningen, The Netherlands, 282 pp.

Gilmour, J.T. and G.M. Gilmour, 1980. A simulation model for sludge decomposition in soil. *J. Environ. Quality*, 9(2):194-199.

Huwe, B. and R. Van der Ploeg, 1988. Modelle zur Simulation des Stickstoffhaushaltes von Standorten mit Unterschiedlicher landwirtschaftlicher Nutzung. Eigenverlag des Instituts für Wasserbau der Universität Stuttgart, Heft 69. 213 pp.

Jenkinson, D.S and J.N. Ladd, 1981. Microbial biomass in soil. Measurement and turnover. In : E.A. Paul and J.N. Ladd (eds.). *Soil Biochemistry*. Dekker, N.Y: 415-471.

Johnsson, H., L. Bergstrom, P. Jansson and K. Paustiaen, 1987. Simulating nitrogen dynamics and losses in a layered agricultural soil. *Agric. Ecosystems and the Environ.*, 18:333-356.

Nordmeyer, H. and J. Richter, 1985. Incubation experiments on nitrogen mineralization in loess and sandy soils. *Plant and Soil*, 83:433-445.

Nuske, A. and J. Richter, 1981. N-mineralization in loss parabrown earthes: Incubation experiments. *Plant and Soil*, 59:237-247.

McIsaac, D. Martin and D. Watts, 1985. Users guide to NITWAT-a nitrogen and water management model. Agr. Eng. Dept. University of Nebraska, Lincoln, Nebraska.

Paul, E.A. and N.G. Juma, 1981. Mineralization and immobilization of soil nitrogen by micro-organisms. In: F.E. Clark and T. Rosswall (eds.) *Ecol. Bull.*, 33:179-195.



Rachhpal-Singh and P.H. Nye, 1988. A model of ammonia volatilization from applied urea. IV. Effect of method of urea application. *J. of Soil Sci.*, 39:9-14.

Richter, J. and H. Nordmeyer, 1982. Stickstoffmineralization und Verfugbarkeit in Lossockenboden. 94 VDFLUFA Kongres, Munster, 121-129.

Richter, J., A. Nuske, W. Habenicht and J. Bauer, 1982. Optimized N-mineralization parameters of loess soils from incubation experiments. *Plant and Soil*, 68:379-388.

Seligman, N.G. and H. van Keulen, 1981. PAPRAN: A simulation model of annual pasture production limited by rainfall and nitrogen. In: M.J. Frissel and J.A. van Veen (eds.) *Simulation of nitrogen behaviour of soil-plant systems*. PUDOC, Wageningen, The Netherlands: 192-221.

Van Veen, J. 1977. The behaviour of nitrogen in soil. Ph.D. dissertation, Agric. University Wageningen, The Netherlands, 164 pp.

Verbruggen, J., 1985. Simulatie van het denitrificatie proces. Ph.D. dissertation. Faculty of Agric. Sciences, K.U.Leuven, Belgium, 180 pp.

Vereecken, H., M. Vanclooster and M. Swerts, 1990. A simulation model for the estimation of nitrogen leaching with regional applicability. In: R. Merckx and H. Vereecken (eds.). *Fertilization and the environment*. Leuven Academic Press, Belgium. 250-263.

Vereecken, H., M. Vanclooster, M. Swerts and J. Diels, 1991. Simulating water and nitrogen behavior in soil cropped with winter wheat. *Fert. Res.*, 27: 233-243.

Wadman, W.P. and P.A.I. Ehlert, 1989. Environmental effects of organic manures in sugar beet production. 52th winter congress IIRB, Brussels, 15-16 February 1989: 93-101.

DESCRIPTION OF THE
MODEL INPUT AND
OUTPUT



7 DESCRIPTION OF THE MODEL INPUT AND OUTPUT

7.1 INTRODUCTION

The WAVE-model consists of a series of modules simulating the behaviour of water and solutes in the soil-plant continuum. The current modules available are:

- WAT : a module for calculating the water balance in the soil-plant continuum;
- SOL : a module for calculating the solute balance in the soil-plant continuum;
- TEMP: a module for calculating the heat balance in the soil-plant continuum;
- NIT : a module for simulating the nitrogen balance in the soil-plant continuum;
- CROP: a module for simulating crop growth.

7.2 THE INPUT

Model predictions for a specific scenario require that values are specified for both the input variables and the model parameters. Input variables are those variables by which the environment effects the delineated system, as represented by the model. Model parameters are constants in the mathematical relationships present in the model. They determine the behaviour of the system and are site specific. In the subsequent, no distinction is made between model parameters or model input variables. As both should be specified by the model user, we call them 'input'. Input are those values which the programme needs for correct execution. For a given set of input the programme calculates the transport and transformation of matter and energy in the soil, crop and vadose environment. The programme is general because it can be used to calculate the behaviour of water and agrochemicals in the complex soil-crop environment for a multitude of different sets of input or scenario's.

7.2.1 DEFINITION OF THE INPUT SYNTAX

INPUT FILES:

The programme reads its input from external ASCII-files, so-called input charts, which can be prepared using a conventional text editor. Each input file consists of a number of lines.

LINE:

A line is a sequence of ASCII-characters, ending with a carriage return. A line is either blank or not.

- blank : a blank line contains no characters (except for the carriage return or blanks). Blank lines are ignored by the programme.
- non-blank : a non blank line can contain either input fields, comment fields or both.

***INPUT FIELD:***

Input fields are records within a non-blank line and consists of one or different input values. If the first character of a non-blank line is not 'C' or 'c' (i.e. a comment header), the entire line is considered to be the input field. If the line starts with 'C' or 'c', the input field consists of all, if any, ASCII-characters following a colon ':'.

INPUT VALUE:

An input value is a sequence of ASCII-characters within an input field. An input value is either:

- integer : represented in the normal way with digits;
- real : represented in the normal way with digits, a decimal point is used; or
- boolean : represented by the characters 'Y' or 'y' for true, 'N' or 'n' for false.

The input values in an input field are separated by blanks. The input values are supplied to the programme in a well defined order.

BLANKS:

Some editors use control characters to represent blanks. All characters with an ASCII-code less than 39 are considered as blanks by the programme.

COMMENT FIELDS:

Comment fields are records within a non-blank line, starting with 'C' or 'c' and ending with either a colon ':' or carriage return. The user can add comments to the input file to facilitate the interpretation of the input by (other) user(s). The use of comments enhances input readability, but has no meaning for the programme itself. The user can add as many comments he or she wishes. There are two ways to comment an input file. In a first way a comment header is added to a non-blank line, already containing some input values. In this way, comment fields and input fields are combined on the same non-blank line. To distinguish the comment field from the input field, a colon (':') is put between both fields. A second way to add comments to the input file is the addition of a complete comment line. A comment line starts with the letter 'C' or 'c' in the first column of the input line and ends with a carriage return. The system first tests the input for a colon (comment header). This implies that a line, starting with a letter 'C' or 'c' but with a colon, is considered to contain valid input for the system. Note also that the user can add as many comment lines he or she wishes, but only one comment header (colon) per line. An example is given below.

```
18
Y
17.0
```



```
C This is a comment line added to the input file
C Give the number of calculation steps : 18
  Do you want to use model 1? : Y
C
C Give parameter of model 1 (reals) : 17.0
```

**TABLE:**

A table is a series of non blank lines without comment fields. The last line of a table starts with the letters 'et' or 'ET', an acronym for end of table. A table is typically used to input a time series of values (e.g. climate data) or a profile description for values of state variables that vary with depth (e.g. soil moisture content profile). An example is given below.

```
C Please specify the number of fertilizer additions :2
C Specify for each addition a table with application date and amount
C Month Day Amount (mg / m**2)
C -----
04      31      1400.
05      04      2100.
ET
```

It is important to stress the important consequences of the above defined input syntax:

1. The input is free-format since the line and column numbers do not play any role.
2. The order in which the input values is specified, however, is crucial. The programme only scans the input fields for input values. If an input field is empty, it jumps to the next one, regardless the text within comment lines.
3. Only relevant questions, for the simulation at hand, should be answered. This means that if you add extra input lines this will erroneously be interpreted as valid input for the programme. Eg. all input fields related to the crop should be skipped if you specified that there is no vegetation considered in the GENDATA.IN file.

7.2.2 VERIFICATION OF THE INPUT

The programme checks the input on its consistency. The following tests are performed:

- **File_check.**
Does the input file exist in the current working directory?
- **Value_check.**
Are there enough values in the input? The programme checks for lacking or superfluous lines. Only the strictly necessary input may be supplied. An exception to this rule is that more values may be on one line than strictly necessary. If too many values are on a line only leftmost values are read, the rest is ignored.
- **Type_check.**
Is the value of correct type? The programme checks if the value is numeric (real or integer) or boolean.
- **Table_order_check.**
Is the order of the values in a table correct? Many tables contain dates or compartment numbers. This information is used to check the order of the values in the table.
- **Range_check.**
Is the input value in the correct range? The input value is tested against a maximum and a minimum.
- For some input values additional tests are done.



When errors occur the programme will report these in the file 'ERR_FILE' and abort after trying to read all the input files. To make simulations for abnormal input values possible, range checking can be turned off. When range checking is turned off, the programme writes warnings to the 'ERR_FILE' when range errors occur.

7.2.3 INPUT FILES USED BY THE WAVE PROGRAMME

The input files have the extension '.IN'. The general information (e.g. simulation period) which is common for all possible simulation combinations is put together in one file: 'GENDATA.IN'. There are additional files needed when simulating water, solute and heat ('WATDATA.IN', 'SOLDATA.IN', 'TEMPDATA.IN'). Climate data are specified in the 'CLIMDATA.IN' file. When nitrogen is modeled 'SOLDATA.IN' is augmented with 'NITDATA.IN'. If the crop growth is modelled, the file 'CROPDATA.IN' is necessary and parts of the 'NITDATA.IN' and 'WATDATA.IN' are omitted. An overview of the files necessary for each kind of simulation is given below.

a) <u>Modeling water</u>	
i) no vegetation	: GENDATA.IN, WATDATA.IN and CLIMDATA.IN
ii) vegetation (no crop growth model)	: same as a.i
iii) vegetation (crop growth model)	: same as a.i + CROPDATA.IN
b) <u>Modeling heat (no nitrogen)</u>	
i) no vegetation	: same as a.i + TEMPDATA.IN
ii) vegetation (no crop growth model)	: same as a.ii + TEMPDATA.IN
iii) vegetation (crop growth model)	: same as a.iii + TEMPDATA.IN
c) <u>Modeling solute (no nitrogen)</u>	
i) no vegetation	: same as a.i + SOLDATA.IN
ii) vegetation (no crop growth model)	: same as a.ii + SOLDATA.IN
iii) vegetation (crop growth model)	: same as a.iii + SOLDATA.IN
d) <u>Modeling nitrogen</u>	
i) no vegetation	: same as c.i + NITDATA.IN + TEMPDATA.IN
ii) vegetation (no crop growth model)	: same as c.ii + NITDATA.IN + TEMPDATA.IN
iii) vegetation (crop growth model)	: same as c.iii + NITDATA.IN + TEMPDATA.IN

Each of the input files contains different items. In the sample input files, provided with this document, the different items start with a title (comment). To clearly indicate the titles, these have been underlined with a sequence of T's in the sample boxes below. Each input item coincides with a certain aspect of the model.

In practice the programme could be used to simulate the fate of water and agrochemicals for many years, or for many different scenario's. To facilitate this, the different parts of a WAVE input file can be read from separate external text files. A



batch file can then easily be created combining the different files to constitute multiple runs. The name of these 'secondary' files are fixed by the programme. In the samples below the name of the external files are provided in a comment line.

GENDATA.IN

In the 'GENDATA.IN' file general information about the simulation type, the simulation period, the soil profile development (number of soil layers with different characteristics, the number of soil compartments within each layer, the bulk density of each layer), the parameters controlling the time step mechanism and parameters controlling the output are specified.

The programme needs the 'type of simulation' information to decide which input files are necessary and which calculations should be performed. Simulating nitrogen implies that heat and solute transport is modelled. The use of the crop growth model is optional. Notice that you only answer the question about SUCROS when there are plants. As nitrogen is a solute, only answer the questions on nitrogen if you are modeling solutes.

C SIMULATION TYPE	
C TTTTTTTTTTTTTTT	
- ARE THERE PLANTS? (Y/N)	: Y
- IF THERE ARE PLANTS, WILL SUCROS BE USED? (Y/N)	: Y
- IS TEMPERATURE MODELED? (Y/N)	: Y
- ARE SOLUTES MODELED? (Y/N)	: Y
- IS NITROGEN MODELED? (Y/N)	: Y

In order to solve the different transport equations numerically, the soil profile is divided into different soil compartments of equal size. The different compartments are grouped into soil layers. The compartment size and the number of soil layers are specified first. Next the thickness of the different soil layers is specified by giving the number of compartments contained within each soil layer. Selecting a small compartment size, will increase the calculation accuracy, but also the computation time. If heat and/or solute transport is modelled, the soil bulk density is specified.

The sample profile below has a total depth of 260 cm. It consists of 4 distinct pedogenetic soil layers, ranging from 00-30, 30-60, 60-120, and 120-260 cm. The profile is subdivided in compartments of 100 mm. Soil layer 1 and 2 is subdivided in 3 compartments, soil layer 3 in 6, and soil layer 4 in 14 compartments.



```

C SOIL PROFILE DEVELOPMENT
C TTTTTTTTTTTTTTTTTTTTTTTTTTTT

- COMPARTMENT SIZE (MM) ..... : 100.0
- NUMBER OF SOIL LAYERS ..... : 4

C- NUMBER OF COMPARTMENTS FOR EACH SOIL LAYER
C LR NO_OF_COMPARTMENTS
C --
    1 3
    2 3
    3 6
    4 14
ET

C IF MODELING SOLUTES (NITROGEN) OR HEAT TRANSPORT SPECIFY BULK DENSITY
C LR BULK_DENSITY
C KG L-1
C --
    1 1.52
    2 1.52
    3 1.52
    4 1.52
ET

```

In the next part, the ‘simulation time variables’ are specified. The planting or emergence date and the harvest date are only input if plants are present. The ‘year(s)’ of simulation are only specified for the start and the end of calculations.

C SIMULATION TIME VARIABLES
 C TTTTTTTTTTTTTTTTTTTTTTTTTTT
 - START OF CALCULATIONS (Y M D) : 1988 04 19
 - END OF CALCULATIONS (Y M D) : 1989 02 28
 C NEXT TWO DATES ARE ONLY INPUT IF THERE ARE PLANTS
 C IN CASE THE CROP GROWTH IS MODELED THE FIRST DATE IS THE EMERGENCE DATE
 - PLANTING OR EMERGENCE DATE (M D) : 05 22
 - HARVEST DATE (M D) : 11 04

The model uses a variable time step to solve the numerical transport equations. The time step is calculated as a function of the calculated water flux, the maximum allowed water content change in a compartment during a time step, and the water mass balance error in a compartment. The calculated time step is bounded by a minimum and a maximum value. The stop criterium for the iterative numerical solution of the Richards equation is the maximum allowed balance error for one compartment. In general, the parameters concerning the numerical solution should be chosen to minimize both the water and solute balance errors. However, taking very strict values is not recommended for it will make increase the computation time and may even cause the programme to abort if it is unable to achieve the requested accuracy within a reasonable computation time.

The last item of this input chart contains the output control variables. These are explained in section 3.



```

C PARAMETERS CONCERNING PRINTING
C TTTTTTTTTTTTTTTTTTTTTTTTTTT
C - STOP THE PROGRAM WHEN THERE ARE RANGE ERRORS IN THE INPUT? (Y/N): Y
C - IS THE TIME INCREMENT BETWEEN THE PRINTING OF THE SUMMARY TABLES
C   LISTING THE DIFFERENT STATE VARIABLES CONSTANT? (Y/N) .....: Y
C   IF "YES"
C     GIVE THE TIME INCREMENT (DAY) (INTEGER).....: 30
C   IF "NO"
C     1) GIVE THE NUMBER OF DATES THERE IS A SUMMARY TABLE.....:
C     2) GIVE THE DATES AT WHICH THE SUMMARY TABLE MUST BE PRINTED
C     M D
C   -----
C - SPECIFY ISD, THE BOTTOM COMPARTMENT OF THE UPPER PART FOR WHICH THERE IS
C   OUTPUT IN THE SUMMARY FILES .....: 10
C
C - COMPARTMENT RANGES FOR THE TIME SERIES FILES
C   1) NUMBER OF COMPARTMENT RANGES FOR THE TIME SERIES FILES .....: 6
C   2) GIVE THE UPPER AND LOWER COMPARTMENT FOR EACH RANGE
C     UPPER    LOWER
C   -----
C     1       2
C     3       4
C     5       6
C     7       8
C     9      10
C    11      12
ET

```

CLIMDATA.IN

In the CLIMDATA.IN file the climate data required to solve the field water flow equation are specified.

The following sequence must be followed: year, month, day, potential evapotranspiration of a reference crop (mm day^{-1}), precipitation (mm day^{-1}), irrigation (mm day^{-1}), interception capacity (mm), minimum and maximum temperature ($^{\circ}\text{C}$) and global radiation ($\text{J cm}^{-2} \text{ day}^{-1}$). The minimum and maximum temperature are only necessary when the crop growth is modelled or when the behaviour of nitrogen species or heat is studied. The values for daily global radiation are only required if the crop growth is simulated. Notice that it is not an error to specify more data on a line than are actually read by the programme. This is useful when you are first simulating water and afterwards decide to include solute or heat transport.

```

C SPECIFY THE CLIMATOLOGICAL DATA
C IF NITROGEN IS MODELED THEN SPECIFY MIN AND MAX TEMPERATURES
C IF SUCROS OR HEAT IS USED THEN SPECIFY MIN, MAX TEMPERATURES
C   AND GLOBAL RADIATION
C ELSE SKIP LAST THREE COLUMNS
C
C   YR M DAY    ETO      PREC     IRRIG    INTC    MINTEM  MAXTEMP  GLOBAL RAD
C   (MM)        (MM)      (MM)     (MM)     (C)      (C)      (J/CM2/DAY)
C   -----
C   1988   4   19   0.0     5.0     0.0     0.0     8.3     19.0    2027.0
C   1988   4   20   0.0     0.0     0.0     0.0     9.5     14.5    1006.0
C   1988   4   21   2.5    10.0     0.0     0.0     7.0     14.5    1267.0
...
ET

```



WATDATA.IN

The WATDATA.IN file contains the input required to model soil water flow.

The soil hydraulic parameters (moisture retention characteristic, MRC; hydraulic conductivity curve, HCC) are specified for each soil layer, in the initial section of the WATDATA.IN file. When a one-modal porosity model is adopted, a hysteretic or non-hysteretic MRC model can be chosen. For the non-hysteretic case, the five parameters of the van Genuchten equation can be specified. For the universal hysteresis model, no additional parameters are needed. For the second hysteresis model, however, one has to supply the model with an additional shape parameter for the main wetting curve. When no hysteresis is considered, one can select 5 different parametric HCC curves. In case of hysteresis, Mualem's closed form HCC expression (model 5) should be used. When a multi-modal porosity model is adopted, one should not fill out the first section, but continue with the soil layer dependent specification of the van Genuchten and Mualem parameters for each modality.

DESCRIPTION OF THE MODEL INPUT AND OUTPUT



C HYDRAULIC PROPERTIES
C TTTTTTTTTTTTTTTTT

- INPUT FROM EXTERNAL FILE WATPAR.WP? (Y/N): N
- MULTIPOROSITY (Y/N?): N

C IF YOU ARE USING MULTIPOROSITY MODEL FOR THE HYDRAULIC
C PROPERTIES, SKIP THIS PART AND GOTO TO THE MULTI POROSITY
C SECTION

C SINGLE POROSITY
C -----

- SPECIFY THE MOISTURE RETENTION MODEL (NR) (INTEGER): 1
C MODELS AVAILABLE
C NO HYSTERESIS:
C VAN GENUCHTEN SE = $1/(1+(\text{ALPHA}^*\text{H})^{*\text{N}1})^{*\text{M}}$ 1
C WITH SE = $(\text{WC}-\text{WCR})/(\text{WCS}-\text{WCR})$
C HYSTERESIS:
C MUalem UNIVERSAL MODEL BASED ON MUalem MODEL II 2
C MUalem MODEL II 3

- SPECIFY THE HYDRAULIC CONDUCTIVITY MODEL SNR) (INTEGER) ..: 1
C MODELS AVAILABLE
C HYDRAULIC CONDUCTIVITY MODEL NUMBER
C GARDNER(POWER) K = $\text{KSAT}/(1+(\text{BH})^{*\text{N}2})$ 1
C GARDNER (EXPON) K = $\text{KSAT}^*\text{E}^{**}(\text{ALPHA}2^*\text{H})$ 2
C GILHAM K = $\text{A}^*\text{WC}^{**}\text{N}2$ 3
C BROOKS&CORREY K = $\text{KSAT}^*\text{SE}^{**}((2+3*\text{LAMBDA})/\text{LAMBDA})$ 4
C MUalem K = $\text{KSAT}^*\text{SE}^{**}\text{L}^*((1-\text{SE}^{**}(1/\text{M}))^{*\text{M}})^{**2}$ 5

C MOISTURE RETENTION PARAMETERS FOR EACH SOIL LAYER
C -----
C LR WCR WCS ALPHA N M (MODEL 1)
C LR WCR WCS ALPHAW N M (MODEL 2)
C LR WCR WCS ALPHAD ND MD ALPHAW NW MW (MODEL 3)
1 0.078 0.396 0.00525 0.792 1.00
2 0.065 0.400 0.00200 0.690 1.00
3 0.067 0.400 0.00200 0.800 1.00
4 0.030 0.400 0.01500 2.000 1.00

ET
C IN CASE OF A HYSTERESIS MODEL GIVE THE MAXIMUM RELATIVE CHANGE
C IN PRESSURE HEAD (-) ELSE SKIP

C HYDRAULIC CONDUCTIVITY PARAMETERS FOR EACH SOIL LAYER
C -----
C LR KSAT B N (GARDNER POWER FUNCTION)
C LR KSAT ALPHA (GARDNER EXPONENTIAL FUNCTION)
C LR KSAT N (GILHAM)
C LR KSAT LAMBDA (BROOKS AND CORREY)
C LR KSAT L (MUalem)
(CM/DAY)
1 0.84 0.036 1.72
2 4.37 0.095 1.57
3 30.66 0.300 1.58
4 120.60 0.310 1.86

ET

C MULTI-POROSITY MODELS
C -----
C - IF MULTI POROSITY MODEL IS ASSUMED, MOISTURE RETENTION IS DESCRIBED
C WITH A SUM OF DIFFERENT VAN GENUCHTEN EQUATIONS (DURNER, 1994) AND
C THE HYDRAULIC CONDUCTIVITY WITH MUalem's GENERAL MODEL (MUalem, 1976)
C - SPECIFY FOR EACH LAYER
C NR_POR : NUMBER OF POROSITY CLASSES (-)
C WCR : RESIDUAL MOISTURE CONTENT (M3/M3)
C WCS : SATURATED MOISTURE CONTENT (M3/M3)
C L : TORTUOSITY FACTOR OF THE MUalem MODEL
C KSAT : SATURATED CONDUCTIVITY (CM/DAY)
C SPECIFY FOR EACH POROSITY CLASS
C W(NR_POR) : WEIGHT FACTOR FOR EACH PARTIAL MRC
C ALFA(NR_POR) : INVERSE AIR ENTRY VALUE FOR EACH PARTIAL MRC (1/CM) (-)
C N(NR_POR) : N FOR EACH PARTIAL MRC (-)
C M(NR_POR) : M FOR EACH PARTIAL MRC (-)
C IN THE FOLLOWING ORDER
C NR_POR WCR WCS L KSAT
C W(NR_POR) ALFA(NR_POR) N(NR_POR) M(NR_POR)



An example of the input for a double porosity MRC, with residual moisture content 0.011 and saturated moisture content 0.414, and weight factors 0.6 and 0.4 for each partial MRC is given below:

2	0.011	0.414	0.5	125
0.6	0.001	1.2	0.98	
0.4	0.01	1.4	0.88	

The 'water upper boundary condition' is implicitly specified in the 'CLIMDATA.IN' file. Besides the climate data, the user specifies a threshold pressure head value (cm) below which evaporation is limited and a maximum water depth which can be stored in the soil surface before runoff (mm) takes place.

```
C WATER UPPER BOUNDARY CONDITIONS
CTTTTTTTTTTTTTTTTTTTTTTTTTTTTTTT
- INPUT FROM EXTERNAL FILE WATUBC.WU? (Y/N) .....: N
- GIVE THE MINIMUM ALLOWED PRESSURE HEAD AT THE SURFACE (CM): -1.D+07
- MAXIMUM PONDING DEPTH (MM) .....: 0.00
```

The section entitled 'Plant water uptake aspects' groups the input of the K_c -factors, inactivation of the roots near the surface, the leaf area index (LAI), the effective rooting depth and the sink term variables. Remember to skip the entire section if no vegetation is considered.

The evolution of the K_c -factor with time is defined by specifying some discrete points of the K_c -time function. The model interpolates linearly in between these points to generate the K_c -time function on a daily basis. If crop growth is modelled, one can alternatively give K_c -values for specific development stages (DVS-units). In this way the evolution of the K_c -factor can be coupled to the phenological development and the simulated LAI.

In case root senescence occurs, water uptake ceases near the soil surface. The senescence initiation date, the date of maximum inactivity, and depth of inactivity are model input.

Leaf area index ($m^2 m^{-2}$) and rooting depth (mm) are specified by means of a table of discrete points in between which the programme interpolates linearly. If crop growth is modelled, these two tables should be left blank (LAI and rooting depth are simulated).

Next, the reduction of the maximum root water uptake, induced by soil drought or anaerobiosis, as well as the shape of the reduction function (hyperbolic or linear) are input. Finally, the potential soil water uptake rate - depth function is specified. The latter can be input either as a linear relationship or a table with discrete values. In case discrete values are used, values for selected depths ought to be specified. The

DESCRIPTION OF THE MODEL INPUT AND OUTPUT



model interpolates linearly in between these data to generate the Smax-depth values for each compartment.



```

C WATER SINK TERM VARIABLES
C -----
C - IS THE RELATION BETWEEN THE REDUCTION FACTOR OF THE
C   ROOT WATER UPTAKE (ALPHA) AND THE PRESSURE HEAD LINEAR? (Y/N)..: N
C - SPECIFY THE VALUE OF THE PRESSURE HEAD BELOW WHICH THE ROOTS
C   START TO EXTRACT WATER FROM THE SOIL (CM) .....: -10.
C - SPECIFY THE VALUE OF THE PRESSURE HEAD BELOW WHICH THE ROOTS
C   START TO EXTRACT WATER OPTIMALLY FROM THE SOIL (CM) .....: -100.
C - SPECIFY THE VALUE OF THE PRESSURE HEAD BELOW WHICH THE ROOTS CAN NO
C   LONGER EXTRACT WATER OPTIMALLY
C           AT A HIGH EVAPORATIVE DEMAND (CM)..: -5000.
C           AT A LOW EVAPORATIVE DEMAND (CM)..: -5000.
C - THE VALUE OF THE PRESSURE HEAD AT WHICH THE WATER
C   UPTAKE BY THE ROOTS CEASES (WILTING POINT) (CM) .....: -16000.
C - IS THE FUNCTION BETWEEN THE POTENTIAL ROOT WATER UPTAKE
C   AND DEPTH LINEAR ? (Y/N) .....: N
C - IF "YES" SPECIFY THE PARAMETERS OF THE EQUATION
C     SMAX=ARER+BRER*ABS(DEPTH IN MM)
C       1 ARER (INTERCEPT) (DAY-1) .....:
C       2 BRER (SLOPE) (DAY-1 MM-1) .....:
C - IF "NO" INPUT MAXIMAL ROOT WATER UPTAKE FOR EACH COMPARTMENT
C   COMP   SMAX
C         (DAY-1)
C   -----
C       2 0.023
C       3 0.013
C      11 0.013
C      12 0.005
C      14 0.005
C      15 0.001
ET

```

The fourth section of this file contains the data defining 'the lower boundary condition'. If a groundwater table is present the time course of the groundwater table depth is input on selected dates. In between these dates the model interpolates linearly to generate the groundwater depth - time data on a daily basis.



```

C WATER BOTTOM BOUNDARY CONDITION
C TTTTTTTTTTTTTTTTTTTTTTTTTTTTTTT

C - INPUT FROM EXTERNAL FILE WATBBC.WB? (Y/N) ..... : N
C - IS THE GROUNDWATER LEVEL INPUT (MM)? (Y/N) ..... : Y
C   M D GWL
C     (MM)
C   -----
C     4 19 1240.0
C     5 11 1610.0
C     6 12 1884.0
C     7 14 2029.0
C     9 15 2489.0
C    10 17 2089.0
C    11 18 2116.0
C    12 20 1490.0
C     1 19 1431.0
C     1 23 1477.0
C     2 28 1300.0
C     4 18 1300.0
ET

C - IS THE FLUX FROM THE SATURATED ZONE INPUT? (Y/N) ..... : N
C IF THE FLUX FROM THE SATURATED ZONE IS INPUT THEN SPECIFY
C - THE INITIAL GROUNDWATER LEVEL (MM) (REAL) ..... :
C - THE FLUX
C   M D FLUXSAT
C     (MM DAY-1)

C - IS THE FLUX FROM THE SATURATED ZONE CALCULATED? (Y/N) ..... : N
C IF THE FLUX FROM THE SATURATED ZONE IS CALCULATED AS
C A FUNCTION OF THE GROUNDWATER LEVEL, THEN SPECIFY
C - THE INITIAL GROUNDWATER LEVEL (MM) ..... :
C - THE PARAMETERS OF THE EQUATION
C   FLUX=AREL*EXP(BREL*ABS(GROUNDWATER LEVEL))
C     - AREL (MM DAY-1) ..... :
C     - BREL (MM-1) ..... :
C - IS THE PRESS. HEAD OF THE BOTTOM COMPARTMENT INPUT? (Y/N) ..... : N
C - IS THERE A LYSIMETER BOTTOM BOUNDARY CONDITION? (Y/N) ..... : N
C IF THE PRESS. HEAD IS INPUT SPECIFY
C   M D PH
C     (CM)
C   -----
C - IS THE FLUX AT THE BOTTOM OF UNSATURATED ZONE ZERO? (Y/N) ..... : N
C - IS THE PROFILE DRAINING FREELY? (Y/N) ..... : N
C - IS THERE A LYSIMETER BOTTOM BOUNDARY CONDITION ? ..... : N

```

As a fifth part of the WATDATA.IN file are the initial conditions given. If no equilibrium with the groundwater table is considered, either pressure head or moisture content profiles are specified. Notice that you can only specify equilibrium with the groundwater table if the bottom boundary condition is a groundwater table. State variables are specified for selected depths. In between these depths the model interpolates linearly to generate state variables for each compartment.

```

C WATER INITIAL VALUES
C TTTTTTTTTTTTTTTTTTT

C - INPUT FROM EXTERNAL FILE WATINIT.WI? (Y/N) ..... : N
C - SHOULD THE PRESSURE HEAD (CM) AT EACH NODAL POINT BE CALCULATED
C IN EQUILIBRIUM WITH THE INITIAL GROUNDWATER TABLE ? (Y/N) ..... : Y
C - IF "YES" THEN SKIP THIS SECTION
C   AND GOTO SECTION 'WATER PRINTING CONTROL'
C ELSE
C   CONTINUE
C - IS THE PRESSURE HEAD AT EACH NODAL POINT INPUT? (Y/N) ..... :
C - IF "NO"
C   GIVE THE INITIAL MOISTURE CONTENT (CM3 CM-3) FOR EACH COMPARTMENT
C ELSE
C   GIVE THE INITIAL PRESSURE HEAD (CM) FOR EACH COMPARTMENT
C     COMP PH OR MC
C     (CM OR CM3 CM-3)
C   -----

```

The last part of the input chart, contains the variables controlling the output. The user specifies which output files he (or she) wants the model to create.



```
C WATER PRINTING CONTROL
C TTTTTTTTTTTTTTTTTTTTTTTT

- DETAILED ITERATION HISTORY (WAT_HISTOR.OUT) ? (Y/N) .....: N
- SUMMARY FILE (WAT_SUM.OUT) ? (Y/N) .....: Y
- CUMULATIVE TERMS OF THE WATER BALANCE (WAT_CUM.OUT) ? (Y/N) .....: N
- EVAPOTRANSPIRATION AND GROUND WATER TABLE LEVEL (WAT_ET.OUT) ? (Y/N) .....: N

C TIME SERIES
- PRESSURE HEAD (PH.OUT) ? (Y/N) .....: N
- WATER CONTENT (WC.OUT) ? (Y/N) .....: Y
- FLUXES (FLX.OUT) ? (Y/N) .....: N
- ROOT EXTRACT. (RTEX.OUT) ? (Y/N) .....: N
- CUM. ROOT EXTRACT (CRTEX.OUT) ? (Y/N) .....: N
```

SOLDATA.IN

The 'SOLDATA.IN' file contains the additional input for modeling the behaviour of solutes in the soil-plant continuum. When nitrogen is modeled, it is implicitly assumed that the three first solute species are: 1 = urea, 2 = ammonium, 3 = nitrate. Initially, one specifies how many solutes are considered and specifies if the two region concept is invoked.

```
C GENERAL INFORMATION
C TTTTTTTTTTTTTTTTTTTT

NUMBER OF SOLUTES .....: 3
USE THE MOBILE/IMMOBILE CONCEPT? (Y/N) .....: N
```

Thereafter the solute transport parameters should be given as input. This is done for each solute species and each soil layer. The solute transport parameters are: the distribution coefficient of an adsorbing solute, (k_d , L kg^{-1}); the chemical diffusion coefficient of the solute, (D_{if} , $\text{mm}^2 \text{ day}^{-1}$); the empirical coefficients relating the chemical diffusion in a pure liquid with diffusion in the soil medium (a and b); the soil hydrodynamic dispersivity (λ , mm); the fraction mobile versus total water content (θ_m/θ , -); the mass transfer coefficient between the mobile and the immobile water zone (α^* , day^{-1}) and the fraction of the adsorption sites in the mobile zone (f , -).

```
C SOLUTE TRANSPORT PARAMETERS
C TTTTTTTTTTTTTTTTTTTTTTTTTT

C INPUT FROM EXTERNAL FILE SOLPAR.SP? (Y/N) .....: N

C SPECIFY THE PARAMETERS FOR EACH SOLUTE AND SOIL LAYER
C NUMBER PARAMETER
C 1 DISTRIBUTION COEFFICIENT (L KG-1)
C 2 CHEM DIFFUSION IN PURE WATER (MM2 DAY-1)
C 3 A COEFFICIENT
C 4 B COEFFICIENT
C 5 HYDRODYNAMIC DISPERSIVITY (MM)
C 6 MOBILE/TOTAL MOISTURE CONTENT (-)
C 7 MASS TRANSFER COEFFICIENT (DAY -1)
C 8 ADSORBED FRACTION IN THE MOBILE ZONE (-)

C SOLUTE 1
C LR 1 2 3 4 5 6 7 8
C --- --- --- --- --- --- ---
C 1 0.9 0.01 0.01 10. 17.0 0.2 0.0001 0.5
C 2 0.9 0.01 0.01 10. 17.0 0.2 0.0001 0.01
C 3 0.9 0.01 0.01 10. 17.0 0.2 0.0001 0.1
C 4 0.0 0.01 0.01 10. 17.0 0.2 0.0001 0.1
ET
C SOLUTE 2
C ...
```



The ‘top boundary condition’ is specified in the third section. The daily dry (mg m^{-2}) and wet (mg l^{-1}) atmospheric deposition are input. For each known solute application (e.g. in terms of fertilisation) the total mass of solute applied (mg m^{-2}) is specified. Notice that if one simulates the nitrogen balance and if there is an organic fertiliser event, only the mineral part of the nitrogen fertiliser is entered at this location, while the organic part is inputted in the NITDATA.IN file (see below). If fertigation is applied, the solute load of the irrigation water for each solute species (mg m^{-2}) is specified. Notice that irrigation water depths are specified in the CLIMDATA.IN file, while only the solute mass addition with the irrigation water is considered in the SOLDATA.IN file. The frequency of plowing and plowing depth (mm) is specified in the last section of this input item.

C SOLUTE UPPER BOUNDARY CONDITIONS
C TTTTTTTTTTTTTTTTTTTTTTTTTTTTTTTTT

C INPUT FROM EXTERNAL FILE SOLUBC.SU? (Y/N): N

C - DRY AND WET DEPOSITION
C RAINCOSAL = AVERAGE LOAD OF SPECIES I IN PRECIPITATION (MG L-1)
C DDEPSAL = AVERAGE DAILY LOAD OF SPECIES i (MG M-2)
C SPECIES RAINCOSAL DDEPSAL
C -----
1 0.0 00.0
2 0.0 00.0
3 0.0 00.0

ET

C - INORGANIC FERTILIZATION
C NUMBER OF APPLICATIONS OF INORGANIC FERTILISER.....: 2
C DOSE(I) = APPLIED DOSE OF SPECIES I ON SPECIFIED DAY (MG/M**2)
C NOTICE THAT - THERE ARE THREE SOLUTE SPECIES IF N IS MODELLED
C - THE APPLICATIONS ARE NUMBERED 1, 2, . . . , NUMBER
C OF APPLICATIONS
C APPL M D DOSE(SOL1) DOSE(SOL2)...DOSE(NR OF SPEC)
C -----
1 04 21 0.0 7705. 0.0
2 04 30 0.0 14405. 0.0

ET

C - IRRIGATION
C DOSE(I) = APPLIED DOSE OF SPECIES I ON SPECIFIED DAY (MG/M**2)
C NUMBER OF IRRIGATIONS.....: 0
C APPL M D DOSE(SOL1) DOSE(SOL2)...DOSE(NR OF SPEC)
C -----

C - PLOWING
C SPECIFY NUMBER DATE OF PLOWING AND PLOWING DEPTH (MM)
C NUMBER OF TIMES PLOWED.....: 1
C NR M D DEPTH
C -----
1 11 11 270.

ET

In a next section the first order decay rates of the solutes are input for different compartments. The model interpolates linearly between the specified compartments to generate the transformation rates for each compartment. If one simulates the nitrogen balance the decay rates are NOT the classical mineral nitrogen transformation rates! Each solute species decays independently of the other species, which is not the case when modelling inorganic nitrogen transport. Therefore, the urea hydrolysis rate (day^{-1}), ammonia nitrification rate (day^{-1}) and nitrate denitrification rate (day^{-1}) are input in 'NITDATA.IN' (see below). Hence, when modelling soil nitrogen, the first order decay rates in 'SOLDATA.IN' will be zero.



```
C SOLUTE SINK TERM
C TTTTTTTTTTTTTTTT

C INPUT FROM EXTERNAL FILE SOLSINK.SS? (Y/N) .....: N

C SPECIFY THE POTENTIAL FIRST ORDER DECAY RATE FOR EACH SOLUTE (DAY-1)
C THESE RATES ARE 0 FOR NITROGEN SPECIES
C COMP RATES(1..NR_OF_SOL)
C -----
1 0.0 0.0 0.0
5 0.0 0.0 0.0
23 0.0 0.0 0.0
ET
```

The initial values of the solute mass for selected compartments are input in the fifth section. The model interpolates linearly in between these values to initialise the system for each compartment.

```
C SOLUTE INITIAL VALUES
C TTTTTTTTTTTTTTTTTT

C INPUT FROM EXTERNAL FILE SOLINIT.SI? (Y/N) .....: N

C SPECIFY THE INITIAL VALUES FOR THE SOLUTE MASS IN EACH COMPARTMENT
C FOR THE DIFFERENT SOLUTE SPECIES (MG M-2)
C COMP CONC SOLUTES(1..NR_OF_SOL)
C -----
1 0.0 207.6 1257.8
2 0.0 207.6 1257.8
3 0.0 114.0 1143.8
4 0.0 114.0 1143.8
5 0.0 395.2 1037.4
6 0.0 395.2 1037.4
7 0.0 202.6 976.6
8 0.0 202.6 976.6
9 0.0 676.4 1634.0
10 0.0 676.4 1634.0
11 0.0 60.8 1903.8
12 0.0 60.8 79.8
14 0.0 60.8 79.8
15 0.0 60.8 11.0
18 0.0 60.8 11.0
19 0.0 60.8 9.5
ET
```

The final section of the 'SOLDATA.IN' file specifications are given to control the output. For each solute species, the programme can create a separate output file containing a summary of the main programme variable values, a file with cumulative values and time series for specific variables.

```
C SOLUTE PRINTING CONTROL
C TTTTTTTTTTTTTTTTTT

C OUTPUT FOR WHICH SOLUTES? (1.. NR_OF_SOL)
C
(SOLUTE 1 = UREUM IN CASE OF NITROGEN) : 1 N
(SOLUTE 2 = AMMON. IN CASE OF NITROGEN) : 2 N
(SOLUTE 3 = NITRATE IN CASE OF NITROGEN) : 3 Y
ET

C WHAT KIND OF OUTPUT
C
THE SUMMARY TABLE BE PRINTED(SOL_SUM.OUT)? : Y
THE CUMULATIVE TERMS OF THE SOLUTE BALANCE (SOL_CUM.OUT)? : Y

C TIME SERIES
C
THE SOLUTE CONCENTR (CONC.OUT)? : Y
THE SOLUTE FLUXES (FLXS.OUT)? : Y
THE SINK TERM (SINK.OUT)? : Y
```



NITDATA.IN

This file contains the information required to model the fate of nitrogen species in the plant-soil continuum. Because different nitrogen species are kinds of solute, the 'NITDATA.IN' file is proceeded by the 'SOLDATA.IN' file, for which solute 1 = urea, solute 2 = ammonia, and solute 3 = nitrate. Only information which is typical for modelling nitrogen is included in 'NITDATA.IN'.

Additional information is required to characterize the upper boundary condition for modelling nitrogen flow. When crops are grown, part of the crop can contribute to the organic nitrogen pool at harvest. To calculate this contribution, the programme needs information on the nitrogen distribution within the crop at harvest. If there are no crops, this section is ignored. When organic fertilizer is used the number of applications and the organic carbon and nitrogen content (mg m^{-2}) for each application is specified. The inorganic components of the fertilizers are input in the SOLDATA.IN file.

The next section of this input file contains the input related to the nitrogen transformation processes. First the parameters related to the mineralisation-immobilisation and nitrogen uptake are input. The uptake parameters are the average distance between the roots and the soil solution (mm), the average radius of the roots (mm). If no crop growth is modelled, the maximum uptake rate is modelled by specifying the fraction of the growing season the crop effectively grows (-) and the maximum amount of nitrogen a crop can assimilate (mg m^{-2}). In this case, root density is modelled by specifying the maximum density at harvest at the soil surface ($\text{cm root l}^{-1} \text{ soil}$) and a parameter determining the exponential decrease in root density with depth (mm^{-1}). If crop growth is simulated, the last four parameters are not input. Next the nitrogen potential transformation rate constants are specified for some selected compartments, i.e the urea hydrolysis rate (day^{-1}), the ammonia nitrification rate (day^{-1}), the nitrate denitrification rate (day^{-1}), the decomposition rate of the humic soil fraction (day^{-1}), the decomposition rate of the litter soil fraction



(day⁻¹) and the decomposition rate of the manure soil fraction (day⁻¹). The model interpolates linearly between the specified values to obtain transformation rates for each soil compartment.

C NITROGEN TRANSFORMATION PARAMETERS
C TTTTTTTTTTTTTTTTTTTTTTTTTTTTTTTTT

INPUT FROM EXTERNAL FILE NITSINK.NS? (Y/N) : N

C MINERALIZATION
C RO = C/N RATIO OF THE BIOMASS
C FE = SYNTHESIS EFFICIENCY CONSTANT
C FH = HUMIFICATION COEFFICIENT
RO : 10.0
FE : 0.3
FH : 0.4

C PLANT UPTAKE PARAMETERS
C - IF THERE ARE NO PLANTS SKIP THIS PART
C AND GO TO SECTION 'POTENTIAL UPTAKE RATES'
C - SPECIFY
C RORAD = AVERAGE ROOT RADIUS (MM)
C RDO = AVERAGE DISTANCE BETWEEN SOIL SOLUTION AND ROOT SURFACE (MM)
C RORAD : 0.22
C RDO : 0.1

C - IF CROP GROWTH IS MODELLED SKIP THE NEXT SECTION AND GOTO
C THE SECTION 'POTENTIAL TRANSFORMATION RATE CONSTANTS'
C
C G = FRACTION OF GROWING SEASON THERE IS POTENTIALLY UPTAKE
C RNMAXP = MAXIMUM NITROGEN UPTAKE (MG M-2)
C W0_RDWRENS = ROOT DENSITY AT SOIL SURFACE (CM L-1)
C ALFA_RDWRENS = REDUCTION FACTOR OF ROOT DENSITY VERSUS DEPTH (MM-1)
C G :
C RNMAXP :
C W0_RDWRENS :
C ALFA_RDWRENS :

C POTENTIAL TRANSFORMATION RATE CONSTANTS
C TTTTTTTTTTTTTTTTTTTTTTTTTTTTTTTTTTTTT

INPUT FROM EXTERNAL FILE NITDEC.ND? : N

C RKNITRI = NITRIFICATION CONSTANT (DAY-1)
C RKDENIT = DENITRIFICATION CONSTANT (DAY-1)
C RKHYD = UREUM HYDROLYSE CONSTANT (DAY-1)
C RKVOL = VOLATILIZATION CONSTANT (DAY-1)
C RKLIT = DECAY FROM LITTER POOL (DAY-1)
C RKMAN = DECAY FROM MANURE POOL (DAY-1)
C RKHUM = DECAY FROM HUMUS POOL (DAY-1)
C COMP RKNITRI RKDENIT RKHYD RKVOL RKLIT RKMAM RKHUM
C
C -----
4 5.82 0.01 0. 0.0 0.035 0.035 0.00007
5 0.0 0.01 0. 0.0 0.035 0.035 0.00007
22 0. 0.0 0. 0.0 0.0 0.0 0.0000

ET

Subsequently, the initial distribution of the organic matter and the soil organic fractions in the profile are given. The model interpolates between the specified compartments to initialise the organic matter pools for each compartment.



7.3 THE OUTPUT

The programme writes output into ASCII-files. The WAVE model generates three different type of output files, which are denoted with different extensions.

'ERR_FILE'

The programme produces two files with the errors and warnings encountered during execution ('ERR_FILE'). The 'ERR_FILE' is always generated but should be empty if the programme runs successfully.

**.RES'*

For each input chart used, a '*.RES' file is generated by the programme. These files might help the user to discover errors in the input which are not noticed by the programme and not reported in the 'ERR_FILE'.

**.OUT'*

The '*.OUT' files contain the model output. In the '*.IN', the user is prompted which '*.OUT' files the model must generate. The user should carefully select these files as the maximum amount of output files is fixed within the programme. Each aspect of the model (water, solute, nitrogen specific additions to solute, plants and heat) is written to different *.OUT files. The *.OUT file consists of a comment header, explaining the format and units of model output and the actual output.

The '*SUM.OUT' files contain summaries of the main state variables in the programme. Summaries are produced at time intervals by the user defined in the 'GENDATA.IN' file. This time interval is fixed or variable. In the latter case, the user provides the programme with the output dates in 'GENDATA.IN'. Summaries are produced for the complete soil profile or a volume within the soil profile. This volume is characterised with the ISD-compartment (Integrating Soil Depth). The state variables are integrated at a depth of the ISD-compartment. The ISD-compartment is specified in the 'GENDATA.IN' file. The following summary files can be created:

WAT_SUM.OUT	Summary output of the soil water balance
SOL_SUMi.OUT	Summary output of the solute balance for solute species i. When nitrogen is modelled, the summary state variables for urea, ammonia and nitrate are given in SOL_SUM1.OUT, SOL_SUM2.OUT and SOL_SUM3.OUT, respectively
NIT_SUM.OUT	Summary file of the nitrogen balance

The simulated soil state variables values, integrated or averaged over different soil compartments, are written in a 'time series' file, on a daily basis. The user specifies the compartment ranges, for which an average or total value is output, in the



'GENDATA.IN' file. The specified ranges are default for all modules. So the compartment ranges are the same for all state variables. The values in the time series files are instantaneous values of the state variables during the last time step of a day. This means that the values of e.g. FLXS.OUT are the actual values of the solute fluxes at the end of a day. These values do not equal the daily average solute fluxes.

WC.OUT	Average moisture content	$\text{m}^3 \text{ m}^{-3}$
PH.OUT	Average pressure head	cm
FLX.OUT	Flux at the bottom of the selected compartment ranges	mm day^{-1}
RTEX.OUT	Root water extraction rate averages	day^{-1}
CRTEX.OUT	Integrated root water uptake, integrated over time	mm
*CONC.OUT	Integrated solute mass of species i	mg m^{-2}
FLXS*.OUT	Solute flux of species i at the bottom of the selected soil compartment ranges	$\text{mg m}^{-2} \text{ day}^{-1}$
SINK*.OUT	Integrated solute sink term of species i	mg m^{-2}
TEMP.OUT	Average soil temperature	$^{\circ}\text{C}$
ORGNLIT.OUT	Organic N in the litter pool	mg m^{-2}
ORGNMAN.OUT	Organic N in the manure pool	mg m^{-2}
ORGNHUM.OUT	Organic N in the humus pool	mg m^{-2}
ORGCLIT.OUT	Organic C in the litter pool	mg m^{-2}
ORGCMAN.OUT	Organic C in the manure pool	mg m^{-2}
ORGCHUM.OUT	Organic C in the humus pool	mg m^{-2}
NH4UPT.OUT	Integrated NH4+ uptake, integrated over time	mg m^{-2}
NO3UPT.OUT	Integrated NO3- uptake, integrated over time	mg m^{-2}
DENITRIF.OUT	Integrated NO3- denitrified, integrated over time	mg m^{-2}
NITRIFIC.OUT	Integrated NH4+ nitrified, integrated over time	mg m^{-2}
HYDROLYS.OUT	Integrated urea hydrolysed, integrated over time	mg m^{-2}
VOLATIL.OUT	Integrated ammonia volatilised, integrated over time	mg m^{-2}
NH4MIN.OUT	Integrated ammonia mineralised, integrated over time	mg m^{-2}
NO3MIN.OUT	Integrated nitrate mineralised, integrated over time	mg m^{-2}



Specific integrated soil balance terms are written to the WAT_ET.OUT, WAT_CUM.OUT, SOL_CUMi.OUT and NIT_CUM.OUT file.

WAT_ET.OUT	Terms of the soil water top boundary condition
WAT_CUM.OUT	Main terms of the soil water balance
SOL_CUMi.OUT	Main terms of the balance for solute species i
NIT_CUM.OUT	Main terms of the organic nitrogen balance

The simulated crop state variables are written in two ‘time series files’ on a daily basis.

CROP_GRO.OUT	Dry matter of different crop components, integrated over time
CROP_DEV.OUT	LAI, rooting depth and actual reduction functions affecting crop growth

DESCRIPTION OF THE
COMPUTER
PROGRAMME



8 DESCRIPTION OF THE COMPUTER PROGRAMME

8.1 GENERAL CONSIDERATIONS

8.1.1 LIMITING VARIABLE VISIBILITY

A programme can be completely described by the effect it has on its variables. During execution the programme in each step will use a certain subset of programme variables and change the value of the subset. In view of this, it is interesting to create a partition of the programme variables and group the actions on these disjunct subsets of variables in an equal number of modules. This limits the possible effects the programme has on the programme variables at each point of execution to a subset. This makes the programme easier to understand. However in practice a programme is constructed from modules that communicate with each other. The point is to make the interface between the modules as small and clear as possible.

In the WAVE-programme communication between the different parts of the programme is attained in different ways. The information in the general module is necessary for all other modules and is therefore put in a common block that is included in the variable list for all other modules. A problem with common blocks is that not only information is passed but also the variable. It would be preferable that the general information could only be changed in the module for general information and be passed in a read only fashion to the other modules. Unfortunately this is not possible in FORTRAN in an elegant way: the programmer is responsible for correct use of the variables. Between the other modules information is passed through function and subroutine calls. Here again it is not possible to pass actual arguments to functions in a read only fashion: FORTRAN can only pass arguments by reference.

8.1.2 THE 'USES'-RELATIONSHIP

A pragmatic definition for this relationship is: "if A and B are two modules then A 'uses' B if A can only work correctly if B works correctly". Notice that the 'uses'-relationship is not equivalent to the 'calls'-relationship. If A calls B it is possible that A does not depend on the results of B. In this case there is no 'uses' relationship between A and B. An 'uses' relationship is also not always a 'calls'-relationship. In the WAVE-programme, the main programme consists of a sequence of subroutine calls. The sequence of these calls is not random, so there is a 'uses' relationship between some of the subroutines in the sequence. It is good programming practice to limit the 'uses' relations between the modules as this relationship strongly determines the adaptability of the programme. Chapter 8.2.1 of the text explains the programme structure using this 'uses' relationship.



8.1.3 ABSTRACTIONS

Abstractions allow the user to postpone programming decisions. The main abstraction mechanisms used in the new programmes are:

- Use of constant names instead of constants (PARAMETER statement in FORTRAN). The main dimensions of the model (e.g. maximum number of compartments) are constant names in the programme. The file 'CONSTANT' which is used by all programme modules contains all these constant names. Changes of model dimensions are possible by editing this file and recompiling the programme.
- The modules for input and output are comparable to 'abstract data types' for an input and output system, respectively. Each of these modules offers the user a set of functions and procedures for writing and reading values. Decisions on the way the input or output should look like are therefore mainly confined to these modules. Not all input or output uses the input and output system. FORTRAN does not enforce the use of the new set of input output functions so the original FORTRAN read and write functions are still used in the programme when the functionality of the abstract data type was insufficient.
- The FORTRAN 'include' metacommand is used to incorporate all files with common blocks (*.COM) in the programme as well as the 'CONSTANT' file. This way, changes to the common blocks or constant name list are limited to editing a few files instead of all parts of the programme that depend on these common blocks or constant name list.
- Abstractions often used are subroutines and functions. Parametrisation allows generalisation of the arguments for which the subroutines and functions act.

8.2 THE STRUCTURE OF THE WAVE PROGRAMME

8.2.1 GENERAL STRUCTURE OF THE PROGRAMME

In Fig. 1-1 of chapter 1, the flow of information between the main modules was shown as 'uses'-relationships. The arrow points to the module or component being 'used'. Notice that the I/O-modules are not included in Fig. 1-1. All the modules in Fig. 1-1 use the I/O-module for reading and writing to external files. The 'uses'-relationship will determine an appropriate sequence of calculations. In some cases there is a circularity in the 'uses'-relationship. From the uses graph, it is also easy to predict possible implications of programme modifications. Changing the interface of the 'nitrogen'-module, which is only used by the 'crop'-module, has less implications than changing the interface of the 'general information'-module.

For each of the arrows of Fig. 1-1, the information passed between the modules is listed below. This information can be passed using common block variables or functions. First the mechanism for transferring information is presented, next the actual variables in the common block that are used by the module at the tail of the arrow are listed. In some cases the list of variables belonging to the common block are omitted and a short description is given of the common blocks used. The functions are shown with parentheses to distinguish them from the common blocks.



1. GEN.COM; CLIM.COM: Common blocks with general and climate variables.
2. WAT.COM: The variables 'iter', 'flxa', 'flxs', 'phsa', 'phsurf' and 'rTEX' are used to calculate the timestep, 'dt', in subroutine 'calcdt'. The variable 'nr_no_conv' is changed in subroutine 'halve'.
3. ROOT_SUCROS(); RLAI_SUCROS(): Two functions in the crop growth module which are called in the subroutine 'wat_upt' when the crop growth is modelled.
4. CALC_WATREDUCTGROW(): Function called in subroutine 'sucros' to calculate the water stress on crop development.
5. WAT.COM; WAT_SOL(): The subroutine 'wat_sol' calculates all the variables of the water balance needed to calculate the solute behaviour in the solute module using 'wat.com'. This subroutine limits the visibility of the water-module in the solute-module.
6. WAT.COM; WAT_TEMP(): The subroutine 'wat_temp' calculates all the variables of the water balance needed to calculate the heat behaviour in the temperature-module using the variables in 'wat.com'. This subroutine limits the visibility of the water-module in the temperature-module.
7. SOL.COM: Common blocks with the solute variables.
8. WHAT_IS_SOILTEMP(): Subroutine called in 'nit_sink'. Again the visibility of the temperature-module for the nitrogen-module is limited.
9. CALC_NITREDUCGROW(): Function called in subroutine 'SUCROS' to calculate the nitrogen stress on crop development.
10. RDENS_SUCROS(), CALC_XNCLE(), PLANT_WEIGHTS(), SUCR_ANLV(), SUCR_XNCSO(): Functions in the crop growth-module which are called by the subroutine 'nit_upt' and 'nit_sink'.
11. SOL.COM: The solute module does not use the nitrogen module. The nitrogen module however has a side effect upon the solute module when used: a part of the result of the nitrogen module consists in a change of the variables 'sinki', 'sinkm' and 'sink' which are in 'sol.com'.
12. CALC_RTEX, CALC_WC: Functions which yield root water extraction and specific moisture contents when the nitrogen transformations are modelled.

8.2.2 THE STRUCTURE OF EACH MODULE

The source code for each module consists of a number of FORTRAN text files. The text files contain different items such as subroutines, functions, common blocks and a constant list. For each module, the different items of the principle text files are listed below. Each item is proceeded with a comment heading explaining the item content. In addition, intermediate comment lines increase the readability of the source code substantially. Functions can be subroutines or functions in the FORTRAN sense. A function can be private or public. A public function is used by other modules, files or functions within the same or another file. A private function is only used by functions within the file itself. FORTRAN does not distinguish between these two.



THE INPUT MODULE

The source code for this module is written in `in_sys.com` and `in_sys.for`. As mentioned above the input system (also the output system) is an abstract data type (ADT). A type in general is a collection of values and operations that can be applied to these values. In general, operations can be distinguished to create, modify and destroy objects of the type. As an example, a well known type is the 'integer' type. This type consists of the set of integers. An object of type integer is created with variable declaration (in FORTRAN this can be implicit). The objects are changed by assignment and by the operations addition, multiplication,... An integer object in FORTRAN 'disappears' upon termination of the programme. The ADT 'in_sys' consists of the 'input files' to which the operations listed as public functions below can be applied. To create an object of type `in_sys` the operation `INIT_FILE` is used, to 'destroy' this object `END_FILE` is used. During its life time the object is manipulated with the other functions listed below. The `in_sys.for` text file, encompasses the following items:

```
CONSTANT
IN_SYS.COM
IN_SYS.FOR
END_FILE
CHECK_ET
EXTRACT_ONE
HOLD_LINE
INIT_ERR
INIT_FILE
INPUT_ERROR
NEXT_LINE
RD_DATE
RD_INT
RD_LOGIC
RD_REAL
READ_LINE
REPORT_ERR
RM_COMMENT
SET_RANGE_CHECKING
SPACE
WARN_ERR
```



THE OUTPUT MODULE

The output system is also similar to an ADT. The FORTRAN text file encompasses the following items:

```
CONSTANT
OUT_SYS.COM
OUT_SYS.FOR
APPEND_FILE
AVG
BIG_TITLE
CLOSE_FILE
DATE_TITLE
FREE_UNIT
GET_UNIT
HEADING
HEADING_TABLE
OPEN_FILE
SMALL_TITLE
STOP_SIMULATION
SUM
WR_TABLE
```

THE MODULE WITH GENERAL AND CLIMATE INFORMATION

The climatological information is, like the general information used by all the other modules. The source code for this module is in the files:

```
CONSTANT
CLIM.COM
GEN.COM
CLIMDATA.FOR
CLIMDATA
GENDATA.FOR
GENDATA
TIME.FOR
CALCDT
HALVE
DATE
DAY_NR
JDATE
WR_CLIMD.FOR
WR_CLIMDATA
WR_GENDA.FOR
WR_GENDATA
```



THE MODULE FOR CALCULATING THE WATER BALANCE

The FORTRAN text files for the water transport module are in the following files, encompassing the following items:

CONSTANT
CLIM.COM
GEN.COM
WAT.COM
PFK.FOR
 CALC_CON
 CALC_DMC
 CALC_PH
 CALC_WC
 CHECK_TURN_POINT
 INIT_PFK
PRHEAD.FOR
 BALANCE_ERROR
 DMCCON
 PRHEAD
WAT_BOCO.FOR
 CALC_BBOCO
 CALC_UBOCO
 CALGWL
 CHECK_BBOCO
 CHECK_UBOCO
 FIX_UBOCO
 WAT_BOCO
WAT_INTG.FOR
 WAT_INTGR
WAT_PRIN.FOR
 WAT_CUM
 WAT_ET
 WAT_PRINT
 WAT_SUM
 WAT_TSERIES
WAT_UPT.FOR
 CALC_RTEX
 CALC_WAT_DRZ
 CALC_WATREDUCTGROW
 ETSLIT
 RER
WATDATA.FOR
 WATDATA
WR_WATDA.FOR
 WR_WATDATA



THE MODULE FOR CALCULATING THE SOLUTE BALANCE

The FORTRAN text files for the solute transport module are in the following files, encompassing the following items:

CONSTANT
CLIM.COM
GEN.COM
SOL.COM
WAT.COM
SOL_BOZO.FOR
 SOL_BOZO
SOL_INTG.FOR
 SOL_INTGR
SOL_PRIN.FOR
 SOL_CUM
 SOL_PRINT
 SOL_SUM
 SOL_TSERIES
SOL_SINK.FOR
 SOL_SINK
SOLDATA.FOR
 SOLDATA
SOLN.FOR
 SOLN
WAT_SOL.FOR
 CALC_WAT_SOL
WR_SOLDATA.FOR
 WR_SOLDATA

THE MODULE FOR CALCULATING THE NITROGEN BALANCE

The FORTRAN text files for the nitrogen fate module are in the following files, encompassing the following items:

CONSTANT
CLIM.COM
GEN.COM
NIT.COM
SOL.COM
WAT.COM
NIT_BOZO.FOR
 NIT_BOZO
NIT_INTG.FOR
 NIT_INTGR
NIT_PRIN.FOR



NIT_CUM
NIT_PRINT
NIT_SUM
NIT_TSERIES
NIT_SINK.FOR
MINER_IMMOB
NIT_UPT
SEQTRANS
NIT_CORRECT_SINK
NIT_UPT.FOR
CALC_NITREDUCTGROW
CALC_RDENS
NITDATA.FOR
NITDATA
TEMP_PR_FOR_NIT
WR_NITDA.FOR
WR_NITDATA

THE MODULE FOR CALCULATING THE HEAT BALANCE

The FORTRAN files for the heat transport module are in the folowing files, encompassing the following items:

CONSTANT
CLIM.COM
GEN.COM
TEMP.COM
WAT.COM
SOILTEMP.FOR
SOILTEMP
WHAT_IS_SOILTEMP
TEMP_PRI.FOR
TEMP_PRINT
TEMP_TSERIES
TEMPDATA.FOR
TEMPDATA
WAT_TEMP.FOR
CALC_WAT_TEMP
WR_TEMP.FOR
WR_TEMPDATA



THE MODULE FOR CALCULATING CROP GROWTH

The FORTRAN text files for the crop growth module are in the following files, encompassing the following items:

```

CONSTANT
CLIM.COM
CROP.COM
GEN.COM
CROP_PRI.FOR
    CROP_OUT
    CROP_PRINT
CROPDATA.FOR
    CROPDATA
SUCROS.FOR f
    AFGEN
    CALC_XNCLE
    DVS_SUCROS
    PLANT_WEIGHTS
    RDENS_SUCROS
    RLAI_SUCROS
    ROOT_SUCROS
    SUCROS
WR_CROPD.FOR f
    WR_CROPDATA

```

8.3 VARIABLES OF THE PROGRAMME

In the next paragraphs a list of variables in each of the files containing common blocks are presented. For each variable a short description of its meaning and its dimensions are given. In case the variable is composite, its components can have different dimensions. In that case the dimensions are denoted by (*).

8.3.1 GEN.COM: GENERAL INFORMATION

DEVSTOP	maximum allowed balance error	(day ⁻¹)
DSP	depth of the soil profile	(mm)
DT	time step	(day)
DTHM	maximum change in volumetric moisture content	(cm ³ cm ⁻³)
DTMAX	maximum allowed time step	(day)
DTMIN	minimum allowed time step	(day)
DX	thickness of the compartments	(mm)
DXINTER	distance between the nodes of the compartments	(mm)
FROM	upper compartment number for the compartment ranges used for creating time series output	(-)



HARVEST_DATE	the crop is harvested at the beginning of this date (day)	
IPRCT	switch for constant time interval between the output for summary files (-)	
ISD	number of the compartment for which additional information is output in the summary file (-)	
ISUCR	switch for using the crop growth model	
NCS	number of compartments. (-)	
NCSL	number of compartments in each layer (-)	
NDAY	cardinal number of the actual simulation day (first day = 1) (-)	
NDSIM	number of simulation days (-)	
NDTS	number of time steps since the start of the day (-)	
NLA	array with the layer number for each compartment (-)	
NPL	number of soil layers (-)	
NPR	number of days summary file output should be produced (-)	
NR_OF_POINTS	number of compartment ranges for which time series output is created (-)	
NTS	number of the actual time step (-)	
PLANT_DATE	crop is planted at the beginning of the day (day)	
PRINTING_TIME	array with the dates at the end of which the summary file is created (-)	
RANGE_ERR	switch for checking the input files for range errors (-)	
SIMNIT	switch for modeling nitrogen species (-)	
SIMPLANT	switch for modeling crop development (-)	
SIMSOL	switch for modeling solutes (-)	
SIMTEMP	switch for modeling the behaviour of heat (-)	
T	actual simulation time calculated as the sum of the julian date of the first day (tinit) and the elapsed time since the beginning of the simulation (day)	
TEND	julian day number of the last simulation day (day)	
TINIT	julian day number of the first simulation day (day)	
TMD	time at the end of the actual day of simulation (day)	
TO	lower compartment number for the compartment ranges used for creating time series output (-)	
TPRINT	if the interval between the summaries is constant, this variable contains the constant printing interval (day)	
X	vertical distance from the soil surface, positive upward (mm)	
YEARIN	year in which the simulation starts (-)	

8.3.2 CLIM.COM: CLIMATE INFORMATION

ET0	daily evapotranspiration of a reference crop	(mm day ⁻¹)
FIN	interception capacity of the vegetation	(mm)
HSH	daily global radiation	(J day ⁻¹ cm ⁻²)



PREC	daily precipitation	(mm day ⁻¹)
RIRR	daily irrigation	(mm day ⁻¹)
TMAX	daily maximum air temperature	(°C)
TMIN	daily minimum air temperature	(°C)

8.3.3 WAT.COM: VARIABLES USED IN THE WATER BALANCE MODULE

AKC	Actual Kc factor	(-)
AREL	arel factor in the flux / ground water level relationship ($Q = arel * \exp(brel * gwl)$)	(mm day ⁻¹)
ARER	root water uptake rate at the surface; intercept of the linear relationship between uptake rate and depth, $S_{max} = arer + brer * depth$	(day ⁻¹)
BREL	brel coefficient in the flux / ground water level relationship ($Q = arel * \exp(brel * gwl)$)	(mm ⁻¹)
BRER	slope of the linear relationship between uptake rate and depth, $S_{max} = arer + brer * depth$	(mm ⁻¹ day ⁻¹)
CBERR_WAT	cumulative error on the water balance for the whole soil profile	(mm)
CBERR_WAT_ISD	cumulative error on the water balance for the layer 1..ISD	(mm)
CEV_INTC	cumulative evaporated interception	(mm)
CFLBU	cumulative flux at the bottom of the profile	(mm)
CFLBUP	cumulative positive flux at the bottom of the profile	(mm)
CFLSD	cumulative flux at the bottom of compartment ISD	(mm)
CFLSDP	cumulative positive flux at the bottom of compartment ISD	(mm)
CINF	cumulative infiltration	(mm)
CIRR	cumulative irrigation water	(mm)
CONDUC	conductivity on the nodes of the compartments	(mm day ⁻¹)
CONIN	conductivity between the nodes of the compartments	(mm day ⁻¹)
CPREC	cumulative precipitation	(mm)
CPSEV	cumulative potential soil evaporation	(mm)
CPTRA	cumulative potential transpiration	(mm)
CRTEX	cumulative root extraction of water for each compartment	(mm)
CSEV	cumulative actual soil evaporation	(mm)
CTRA	cumulative actual transpiration	(mm)
CTRA1	cumulative actual transpiration on the previous time step	(mm)
CWATUPT_ISD	cumulative plant water uptake for the layer 1..ISD	(mm)
CUM_INTC	cumulative interception	(mm)
DMCAP	differential moisture capacity for each node	(mm ⁻¹)
DRZ	rooting depth	(mm)
DSTOR	actual amount of water intercepted	(mm)



DVS1	development stage at the end of the crop initial stage	(-)
DVS2	development stage at the end of the crop development stage	(-)
DVS3	development stage at the end of mid season	(-)
DVS4	development stage at the end of the season	(-)
DXN	depth of the first saturated node	(mm)
EPA	potential transpiration	(mm day ⁻¹)
EPA_MIN_INTC	potential transpiration without accounting the evaporation of intercepted water	(mm day ⁻¹)
EQ_GRWT	switch for calculating the initial soil moisture content and pressure head profile profile in equilibrium with the groundwater table	(-)
ESA	potential soil evaporation	(mm day ⁻¹)
EV_INTC	actual evaporation of intercepted water	(mm day ⁻¹)
FLXA	potential flux at the surface of the soil profile	(mm day ⁻¹)
FLXS	water flux on each node	(mm day ⁻¹)
GPRH	pressure head at the bottom of the soil profile	(mm)
GWL	daily ground water table level	(mm)
HISTOR_FILE file	handle (unit) for the file with the iteration history information	(-)
HYSTLIM	relative pressure head change used to detect a turn point if a hysteresis model is used for the MRC	(mm mm ⁻¹)
IBBCCT	switch for a constant bottom boundary condition	(-)
IBBOCO	code for the type of bottom boundary condition	(-)
IDVS	switch for calculating the Kc values in function of the development stage	(-)
IGIVEPH	switch for the type of initial profile: moisture content or pressure head	(-)
IHIST	switch for recording the iteration history for the water transport calculations	(-)
ILINR	switch for the type of relationship between the reduction of the root water uptake and pressure head (linear = true)	(-)
IRZ	compartment number at the bottom of the rooting zone	(-)
ISMXNL	switch for using a linear relationship to describe the maximal root water uptake in function of depth	(-)
ITER	number of iterations used to calculate the new values of the pressure head for one time step	(-)
ITERTOT	total number of iterations since the beginning of the simulation	(-)



KHYS	kind of moisture retention curve used to calculate the moisture content in case a hysteresis model is used for the moisture retention characteristic	(-)
LAICT	switch for a constant daily LAI value	(-)
MODELK	model number used for the hydraulic conductivity curve	(-)
MODELPF	model number used for the moisture retention characteristic	(-)
NCOMP	number of the bottom compartment of the unsaturated zone	(-)
NPARKON	number of parameters for the conductivity model	(-)
NPARPF	number of parameters for the moisture retention characteristic model	(-)
NR_NO_CONV	number of times there was no convergence during the calculation of the water transport	(-)
NREPEAT	number of times the calculations are repeated in the same time step because of an incorrect upper boundary condition	(-)
P0	pressure head value below which water uptake starts	(mm)
P1	pressure head value below which water uptake is optimal	(mm)
P2H	pressure head value below which water uptake is reduced at high evaporative demand	(mm)
P2L	pressure head value below which water uptake is reduced at low evaporative demand	(mm)
P3	pressure head value below which water uptake stops (wilting point)	(mm)
PARAKON	parameters for the hydraulic conductivity model for each soil layer	(*)
PARAPF	parameters for the moisture retention characteristic model for each soil layer	(*)
PH	most recently calculated pressure head profile	(mm)
PH1	previous value for PH	(mm)
PHSA	pressure head below which evaporation is reduced also called air dry value	(mm)
PHSURF	pressure head at the top of the soil profile	(mm)
PR_WAT_CUM	switch for creation of the file 'WAT_CUM.OUT'	(-)
PR_WAT_ET	switch for creation of the file 'WAT_ET.OUT'	(-)
PR_WAT_HISTOR	switch for creation of the file 'WAT_HIST.OUT'	(-)
PR_WAT_SUM	switch for creation of the file 'WAT_SUM.OUT'	(-)
PR_WAT_TSERIES	array with switches for creation of the time series files	(-)
QDEEP	daily flux at the bottom of the soil profile	(mm day ⁻¹)
RINF	potential infiltration	(mm day ⁻¹)
RLAI	daily value of the leaf area index (LAI)	(m ² m ⁻²)



RNAM	depth above which there is no root water uptake due to senescence (for T > TE)	(mm)
ROOTCT	switch for constant rooting depth	(-)
RTEX	root extraction rate in each compartment	(day ⁻¹)
SMX	maximal root extraction rate for each compartment	(day ⁻¹)
STOR	actual amount of intercepted water	(mm)
SUCRETURN	pressure head for the most recent turn point	(cm)
TB	time when reduction of root extraction near the surface due to senescence starts	(day)
TE	time when reduction of root extraction near the surface due to senescence reaches its maximum value	(day)
TRANSP_ACT	actual crop transpiration on this time step	(mm)
TX1	date at the end of the initial stage	(day)
TX2	date at the end of the crop development stage	(day)
TX3	date at the end of the mid season stage	(day)
VISD	actual water content for the soil profile layer 1..ISD	(mm)
VISDI	initial water content for the soil profile layer 1..ISD	(mm)
VOL	actual water content for the complete soil profile	(mm)
VOLI	initial water content of the soil profile	(mm)
WC	most recently calculated moisture content profile	(cm ³ cm ⁻³)
WC1	previous value for WC	(cm ³ cm ⁻³)
WCRETURN	moisture content for the most recent turn point	(cm ³ cm ⁻³)

8.3.4 SOL.COM: VARIABLES USED IN THE SOLUTE TRANSPORT MODULE

ACSOLIB	adsorbed solute concentration in the immobile zone for the previous time step for each compartment and each solute species	(mg kg ⁻¹)
ACSOLO	adsorbed solute concentration in the immobile zone for the actual time step for each compartment and each solute species	(mg kg ⁻¹)
ACSOLMB	adsorbed solute concentration in the mobile zone for the previous time step for each compartment and each solute species	(mg kg ⁻¹)
ACSOLMO	adsorbed solute concentration in the mobile zone for the actual time step for each compartment and each solute species	(mg kg ⁻¹)
ACSOLO	total adsorbed solute concentration for the actual time step for each compartment and each solute species	(mg kg ⁻¹)
CBERR_SOL	mass balance error for each solute species for the whole soil profile	(mg m ⁻²)
CBERR_SOL_ISD	mass balance error for each solute for the layer 1..ISD	(mg m ⁻²)



CONIRSOL	solute load of the irrigation water for each fertigation and each solute species	(mg m ⁻²)
CSOLB	total solute concentration for the previous time step for each compartment and each solute species	(mg l ⁻¹)
CSOLIB	solute concentration in the immobile zone for the previous time step for each compartment and each solute species	(mg l ⁻¹)
CSOLIO	solute concentration in the immobile zone for the actual time step for each compartment and each solute species	(mg l ⁻¹)
CSOLMB	solute concentration in the mobile zone for the previous time step for each compartment and each solute species	(mg l ⁻¹)
CSOLMO	solute concentration in the mobile zone for the actual time step for each compartment and each solute species	(mg l ⁻¹)
CSOLO	total solute concentration for the actual time step for each compartment for each solute species	(mg l ⁻¹)
DDEPSOL	daily dry deposition for each solute species	(mg m ⁻²)
DECSOLI	solute sink term for each compartment in the immobile region excluding the mobile immobile transfer	(mg l ⁻¹ day ⁻¹)
DECSOLM	solute sink term for each compartment in the mobile region without accounting the mobile immobile transfer	(mg l ⁻¹ day ⁻¹)
DIFFUS	effective diffusion coefficient, corrected for numerical dispersion	(mm ² day ⁻¹)
DLEASA	cumulative downward solute flux at the bottom of the profile	(mg m ⁻²)
DLEASA_ISD	cumulative downward solute flux at the bottom of the layer 1..ISD	(mg m ⁻²)
DSOL	change in solute concentration for the complete profile	(mg m ⁻²)
DSOL_ISD	change in solute concentration for the layer 1..ISD	(mg m ⁻²)
FLXSA	water flux between the nodes	(mm day ⁻¹)
FLXSAH	water flux between the nodes halfway the previous and the actual time step	(mm day ⁻¹)
FSOL	solute load of the inorganic fertiliser applications for each solute species	(mg m ⁻²)
IDINOF	inorganic fertilisation dates	(day)
IDIRR	fertigation dates	(day)
IDPLOW	plowing dates	(day)
IMOBSW	switch for the mobile/immobile concept	(-)
NCSPLLOW	number of compartments affected by the plowing	(-)
NINOF	number of inorganic fertilisations	(-)
NIRR	number of fertigations	(-)



NPLO	number of times the field is plowed	(-)
NR_OF_SOL	number of solutes	(-)
OUT_SOL	array of switches for the solutes for which the programme should create output	(-)
PARASOL	solute transport parameters for each soil layer	(*)
PLEASA	cumulative positive solute flux at the bottom of the soil profile	
PLEASA_ISD	cumulative positive solute flux at the bottom of the layer 1..ISD	(mg m ⁻²)
PR_SOL_CUM	switch for the files with cumulative values	(-)
PR_SOL_SUM	switch for the files with summary information	(-)
PR_SOL_TSERIES	switches for the files with time series	(-)
PTSINK	profile total solute sink over the most recent time step for each solute species	(mg m ⁻²)
PVELA	actual pore velocity between the nodes	(mm day ⁻¹)
PVELAH	pore velocity between the nodes half way the actual and the previous time step	(mm day ⁻¹)
PVELOH	pore velocity on the nodes half way the actual and the previous time step	(mm day ⁻¹)
RATES	potential rate constants for the first order degradation of the solutes	(day ⁻¹)
RESSOL	amount of solute in the fictitious reservoir on top of the profile for each solute species	(mg m ⁻²)
RLEASA	cumulative solute flux at the bottom of the soil profile	(mg m ⁻²)
RLEASA_ISD	cumulative solute flux at the bottom of the layer 1..ISD	(mg m ⁻²)
SFLXSA	solute flux in each node	(mg m ⁻²)
SINKI	solute sink term in each compartment for the immobile soil region	(mg l ⁻¹ day ⁻¹)
SINKM	solute sink term in each compartment for the mobile soil region	(mg l ⁻¹ day ⁻¹)
SOLINFL	solute inflow during the actual day	(mg m ⁻²)
SOLSUR	solute concentration at the surface	(mg m ⁻²)
TCSINK	cumulative sink for the whole profile	(mg m ⁻²)
TCSINK_ISD	cumulative sink for the layer 1..ISD	(mg m ⁻²)
TCSOLIO	solute mass for each compartment for the immobile soil region	(mg m ⁻²)
TCSOLMO	solute mass for each compartment for the mobile soil region	(mg m ⁻²)
TCSOLO	solute mass for each compartment for both soil regions	(mg m ⁻²)
TFLSOL	cumulative solute inflow since the beginning of the simulation	(mg m ⁻²)
TSINKI	cumulative sink for each compartment for the immobile soil region	(mg m ⁻²)



TSINKM	cumulative sink for each compartment for the mobile soil region	(mg m ⁻²)
TSOLI	initial profile total concentrations	(mg m ⁻²)
TSOLI_ISD	initial total concentrations for the layer 1..ISD	(mg m ⁻²)
WCIO	moisture content for the immobile zone on the nodes for each compartment for the actual time step	(cm ³ cm ⁻³)
WCIOB	moisture content for the immobile zone on the nodes for each compartment for the previous time step	(cm ³ cm ⁻³)
WCMA	moisture content for the immobile zone between the nodes for each compartment for the actual time step	(cm ³ cm ⁻³)
WCMAH	moisture content for the immobile zone between the nodes for each compartment between the actual and the previous time step	(cm ³ cm ⁻³)
WCMO	moisture content for the mobile zone on the nodes for each compartment for the actual time step	(cm ³ cm ⁻³)
WCMOB	moisture content for the mobile zone on the nodes for each compartment for the previous time step	(cm ³ cm ⁻³)
WCO	moisture content on the nodes for each compartment for the actual time step	(cm ³ cm ⁻³)
WCOP	moisture content on the nodes for each compartment for the previous time step	(cm ³ cm ⁻³)
WDEPSOL	daily wet deposition for each solute	(mg l ⁻¹)

8.3.5 NIT.COM: VARIABLES USED IN THE NITROGEN BALANCE MODULE

ALFA_RDENS	factor in the exponent of the relationship between the root density and depth	(mm ⁻¹)
CARBLIT	fraction of the organic carbon arriving in the intermediate pool (the litter pool = 0.7*CARBORG)	(mg m ⁻²)
CARBMAN	fraction of the organic carbon arriving in the fast cycling pool (the manure pool = 0.3*CARBORG)	(mg m ⁻²)
CARBORG	organic carbon content for each organic fertilisation dose	(mg m ⁻²)
CCHUMO	carbon content in the humus pool for each compartment	(mg m ⁻²)
CCLITO	carbon content in the litter pool for each compartment	(mg m ⁻²)
CCMANO:	carbon content in the manure pool for each compartment	(mg m ⁻²)
CDEN	cumulative denitrification in each compartment	(mg m ⁻²)
CBERR_CORG	mass balance error for the organic carbon for the whole soil profile	(mg m ⁻²)
CBERR_CORG_ISD	mass balance error for the organic C for the layer 1..ISD	(mg m ⁻²)



CBERR_NORG	mass balance error for the organic N for the whole soil profile	(mg m ⁻²)
CBERR_NORG_ISD	mass balance error for the organic nitrogen for the layer 1..ISD	(mg m ⁻²)
CHYD	cumulative hydrolysis in each compartment	(mg m ⁻²)
CMIN	cumulative mineralisation of nitrogen in each compartment	(mg m ⁻²)
CNHUMO	nitrogen content in the humus pool for each compartment	(mg m ⁻²)
CNIT	cumulative nitrification for each compartment	(mg m ⁻²)
CNLITO	nitrogen content in the litter pool for each compartment	(mg m ⁻²)
CNMANO	nitrogen content in the manure pool for each compartment	(mg m ⁻²)
CUPT	cumulative plant uptake in each compartment	(mg m ⁻²)
CVOL	cumulative volatilisation in each compartment	(mg m ⁻²)
DCORG	change in organic carbon for the complete profile	(mg m ⁻²)
DCORG_ISD	change in organic carbon for the layer 1..ISD	(mg m ⁻²)
DECCORG	organic carbon sink for each compartment	(mg l ⁻¹ day ⁻¹)
DECNORG	organic nitrogen sink for each compartment	(mg l ⁻¹ day ⁻¹)
DNORG	change in organic nitrogen content for the complete profile	(mg m ⁻²)
DNORG_ISD	change in organic nitrogen content for the layer 1..ISD	(mg m ⁻²)
FAG	fraction of plant nitrogen in crop residue at harvest	(-)
FE	carbon turn over efficiency	(-)
FH	carbon humification fraction	(-)
FHP	fraction of nitrogen removed with harvest products	(-)
FLR	fraction of plant nitrogen in living roots at harvest	(-)
G	fraction of the growing season nitrogen uptake occurring	(-)
IDMAN	organic fertilisation dates	(day)
NOF	number of organic fertilisations	(-)
PR_NIT_CUM	switch for the file with cumulative values	(-)
PR_NIT_SUM	switch for the file with summary information	(-)
PR_NIT_TSERIES	array of switches for the files with time series	(-)
PR_TEMP_FOR_NIT	switch for the TEMP.OUT file	(-)
PTCARBORG	total profile carbon content	(mg m ⁻²)
PTCARBORG_ISD	total carbon content for the layer 1..ISD	(mg m ⁻²)
PTCHUM	profile total carbon content in the humus pool	(mg m ⁻²)
PTCHUM_ISD	total carbon content in the humus pool for the layer 1..ISD	(mg m ⁻²)
PTCLIT	profile total carbon in the litter pool	(mg m ⁻²)
PTCLIT_ISD	total carbon in the litter pool for the layer 1..ISD	(mg m ⁻²)
PTCMAN	profile total carbon in the manure pool	(mg m ⁻²)
PTCMAN_ISD	total carbon in the manure pool for the layer 1..ISD	(mg m ⁻²)
PTDEN	profile total denitrification	(mg m ⁻²)



PTDEN_ISD	total denitrification for the layer 1..ISD	(mg m ⁻²)
PTHYD	profile total hydrolysis	(mg m ⁻²)
PTHYD_ISD	total hydrolysis for the layer 1..ISD	(mg m ⁻²)
PTMIN	profile total mineralisation	(mg m ⁻²)
PTMIN_ISD	total mineralisation for the layer 1..ISD	(mg m ⁻²)
PTNHUM	profile total organic nitrogen in the humus pool	(mg m ⁻²)
PTNHUM_ISD	total organic nitrogen in the humus pool for the layer 1..ISD	(mg m ⁻²)
PTNIT	profile total nitrification	(mg m ⁻²)
PTNIT_ISD	total nitrification for the layer 1..ISD	(mg m ⁻²)
PTNITORG	profile total organic nitrogen	(mg m ⁻²)
PTNITORG_ISD	total organic nitrogen for the layer 1..ISD	(mg m ⁻²)
PTNLIT	profile total organic nitrogen in the litter pool	(mg m ⁻²)
PTNLIT_ISD	total organic nitrogen in the litter pool for the layer 1..ISD	(mg m ⁻²)
PTNMAN	profile total organic nitrogen in the manure pool	(mg m ⁻²)
PTNMAN_ISD	total organic nitrogen in the manure pool for the layer 1..ISD	(mg m ⁻²)
PTSCORG	cumulative organic carbon sink for the whole profile	(mg m ⁻²)
PTSCORG_ISD	cumulative organic carbon sink for the layer 1..ISD	(mg m ⁻²)
PTSNORG	cumulative organic nitrogen sink for the whole profile	(mg m ⁻²)
PTSNORG_ISD	cumulative organic nitrogen sink for the layer 1..ISD	(mg m ⁻²)
PTUP	profile total solute uptake	(mg m ⁻²)
PTUP_ISD	total solute uptake for the layer 1..ISD	(mg m ⁻²)
PTVOL	profile total volatilisation	(mg m ⁻²)
PTVOL_ISD	total volatilisation for the layer 1..ISD	(mg m ⁻²)
RCARBMIN	carbon mineralisation for each compartment	(mg l ⁻¹ day ⁻¹)
RDENITI	denitrification in the immobile region for each compartment	(mg l ⁻¹ day ⁻¹)
RDENITM	denitrification in the mobile region for each compartment	(mg l ⁻¹ day ⁻¹)
RDENS	root density in each compartment	(cm l ⁻¹)
RDENS_LEFT	root density in each compartment left at harvest	(cm l ⁻¹)
RDO	distance between the root surface and the soil solution	(mm)
RFRACT_TOT	sum of the root densities in each compartment at harvest	(cm cm ⁻³)
RHUREAI	hydrolysis in the immobile region for each compartment	(mg l ⁻¹ day ⁻¹)
RHUREAM	hydrolysis in the mobile region for each compartment	(mg l ⁻¹ day ⁻¹)
RKDENIT	potential denitrification rate for each compartment	(day ⁻¹)



RKHUM	potential nitrogen mineralisation rate of the humus fraction for each compartment	(day ⁻¹)
RKHYD	potential hydrolysis rate for each compartment	(day ⁻¹)
RKLIT	potential nitrogen mineralisation rate of the litter fraction for each compartment	(day ⁻¹)
RKMAN	potential nitrogen mineralisation rate of the manure fraction for each compartment	(day ⁻¹)
RKNITRI	potential nitrification rate for each compartment	(day ⁻¹)
RKVOL	potential volatilisation rate for each compartment	(day ⁻¹)
RMINI	mineralisation of organic nitrogen in the immobile soil region for each compartment	(mg l ⁻¹ day ⁻¹)
RMINM	mineralisation of organic nitrogen in the mobile soil region for each compartment	(mg l ⁻¹ day ⁻¹)
RNITORG	amount of nitrogen added with last organic fertilisation	(mg m ⁻²)
RNITRII	nitrification in each compartment in the immobile soil region	(mg l ⁻¹ day ⁻¹)
RNITRIM	nitrification in each compartment in the mobile soil region	(mg l ⁻¹ day ⁻¹)
RNMAXP	maximum amount of nitrogen accumulated in the plants at harvest	(mg m ⁻²)
RO	C/N ratio for the microorganisms and humified products	(-)
RORAD	average root radius	(mm)
RVOLI	volatilisation in the immobile region for each compartment	(mg l ⁻¹ day ⁻¹)
RVOLM	volatilisation in the mobile region for each compartment	(mg l ⁻¹ day ⁻¹)
SUNI	plant uptake in the immobile region for each compartment	(mg l ⁻¹ day ⁻¹)
SUNM	plant uptake in the mobile region for each compartment	(mg l ⁻¹ day ⁻¹)
TCORGS	initial organic carbon profile total	(mg m ⁻²)
TCORGS_ISD	initial organic carbon total for the layer 1..ISD	(mg m ⁻²)
TFLCORG	cumulative amount of C added with organic fertilisation	(mg m ⁻²)
TFLNORG	cumulative amount of N added with organic fertilisation	(mg m ⁻²)
TNORGS	initial organic nitrogen profile total	(mg m ⁻²)
TNORGS_ISD	initial organic nitrogen total for the layer 1..ISD	(mg m ⁻²)
W0_RDENS	root density at the surface; a factor in the exponential relationship between root density and depth	(cm l ⁻¹)



8.3.6 TEMP.COM: VARIABLES USED IN THE HEAT BALANCE MODULE

PARATEMP	parameters for describing heat transport in each layer	(*)
PR_TEMP	switch for the file 'TEMP.OUT'	(-)
TEMP	temperature for each compartment	(°C)
WCTO	water content for each compartment	(cm ³ cm ⁻³)
WCTOB	water content for each compartment for previous time step	(cm ³ cm ⁻³)

8.3.7 CROP.COM: VARIABLES USED IN THE CROP GROWTH MODULE

AMX	maximum CO ₂ assimilation rate	(kg(CO ₂)ha ⁻¹ (leaf) hr ⁻¹)
ASRQSO	assimilate requirement for dry matter	(-)
DVS	conversion into storage organs	(kg(C) kg ⁻¹ (DM))
EAI	development stage	(°C) or (-)
EAR	ear weight per unit of leaf weight	(kg(ear) kg ⁻¹ (leaf))
EFF	ear development rate per unit of total above ground biomass	(ha(ear) d ⁻¹ kg ⁻¹ (DM))
NCROP	efficiency of use of absorbed visible radiation for CO ₂ assimilation at low light levels	(kg ha ⁻¹ hr ⁻¹)/(J m ⁻² s ⁻¹)
NR_OF_TABLES	crop number	(-)
NSL	number of tables with input	(-)
NTABEL	number of seedlings	(-)
PR_CROP	number of observations in each table	(-)
RGR	switch for the file 'CROP.OUT'	(-)
RKDF	exponential factor in the LAI development rate, effective temperature relationship	(m ² m ⁻² °C ⁻¹ d ⁻¹)
RLAICR	light extinction coefficient	(m ⁻¹)
RLAT	critical value of the LAI for self shading	(m ² m ⁻²)
RLDF	latitudinal location of the site	(degrees)
RMAINSO	root density for each compartment	(cm cm ⁻³)
RMATR	daily maintenance respiration per unit storage organ weight	(kg kg ⁻¹ d ⁻¹)
RMRD	initial value of the maturity class for potatoes	(-)
RTDEP	maximal rooting depth	(mm)
RW	rooting depth	(cm)
SCP	fraction of the root density in each compartment	(-)
SLA	leaf scattering coefficient	(-)
	specific leaf area	(ha(leaf) kg ⁻¹ (leaf))



SLAI	total leaf area (dead and green leaves)	
	per unit soil surface	(m ² m ⁻²)
SLAIG	the leaf area index	(m ² m ⁻²)
SPECWEIG	specific weight of the roots	(cm g ⁻¹)
SSL	leaf area of one seedling	(m ² seedling ⁻¹)
TABLE	the matrix with the input tables	(*)
TBASE	base temperature	(°C)
WCRN	weight of the crown (sugar beets)	(kg ha ⁻¹)
WKOB	weight of the cob (corn)	(kg ha ⁻¹)
WLV	weight of the leaves	(kg ha ⁻¹)
WRT	weight of the root	(kg ha ⁻¹)
WSO	weight of the storage organs	(kg ha ⁻¹)
WST	weight of the stems	(kg ha ⁻¹)